GENOMIC CHARACTERIZATION OF NECROTROPHIC EFFECTOR SENSITIVITY GENES IN WHEAT

A Dissertation
Submitted to the Graduate Faculty
of the
North Dakota State University
of Agriculture and Applied Science

By

Katherine Lauren Delaney Running

In Partial Fulfillment of the Requirements
for the Degree of
DOCTOR OF PHILOSOPHY

Major Program:
Genomics, Phenomics, and Bioinformatics

June 2022

Fargo, North Dakota

North Dakota State University
Graduate School

Title
GENOMIC CHARACTERIZATION OF NECROTROPHIC EFFECTOR SENSITIVITY GENES IN WHEAT

By

Katherine Lauren Delaney Running

The Supervisory Committee certifies that this ***disquisition*** complies with North Dakota State University's regulations and meets the accepted standards for the degree of

DOCTOR OF PHILOSOPHY

SUPERVISORY COMMITTEE:

Phillip McClean
Chair

Justin Faris

Timothy Friesen

Shaobin Zhong

Approved:

August 1st, 2022
Date

Richard Horsley
Department Chair

ABSTRACT

The necrotrophic fungal pathogens *Parastagonospora nodorum* and *Pyrenophora tritici-repentis* cause the diseases septoria nodorum blotch (SNB) and tan spot, respectively, reducing yield by decreasing the photosynthetic area of the plant. The pathogens produce necrotrophic effectors (NEs) that target host genes to induce cell death. The *Tsc1*-Ptr ToxC and *Tsn1*-Ptr ToxA interactions contribute to plant susceptibility to tan spot, while the *Tsn1*-SnToxA and *Snn5-B1*-SnTox5 interactions contribute to SNB susceptibility. The three main goals of this dissertation were to clone susceptibility genes *Tsc1* and *Snn5* and develop robust genetic markers for use in marker-assisted elimination of *Tsn1*. A genetic linkage map was developed delineating the *Tsc1* region to 184 kb. Structural and gene content comparisons of the identified *Tsc1* and *Tsn1* regions in using the sequenced wheat genomes revealed gene content variation correlating with host phenotypes, reducing the *Tsc1* candidate gene list to just two genes. Comparative sequence analysis in two generated mutant populations revealed the identity of *Tsc1*, which has protein kinase and leucine-rich repeat domains. The structural and gene content comparison of the sequenced genomes in the *Tsn1* region identified two conserved haplotypes in accessions with presence/absence variation corresponding with ToxA sensitivity. Genetic markers flanking *Tsn1* were designed in segments syntenic between *Tsn1*+ and *Tsn1*- accessions, allowing the codominant detection of *Tsn1*. The *Tsn1* markers were validated on over 1,500 wheat accessions, demonstrating a near perfect ability to determine if an accession would be insensitive to ToxA. The application of these markers in wheat breeding programs can effectively reduce susceptibility to ToxA-producing pathogens. *Snn5-B1* candidates were identified in the Chinese Spring genome and validated using random mutagenesis, targeted mutagenesis, and the Cadenza TILLING mutants. *Snn5-B1* contains protein kinase and major sperm protein domains.

Furthermore, a second SnTox5 sensitivity locus, designated *Snn5-B2*, was mapped to the short arm of chromosome 2B in durum wheat. The cloning of susceptibility genes *Tsc1* and *Snn5-B1* allows for the development of molecular markers based on causal polymorphisms and for gene-disruption though gene-editing methods for the selection or creation of nonfunctional alleles that cannot be targeted by NE to induce cell death and disease.

ACKNOWLEDGMENTS

Countless people have supported my efforts in my educational studies and research. First, I am grateful to my advisor, Dr. Justin Faris, for giving me the opportunity to join his lab. He's taught me to ask better questions and balance wonder with purposeful direction. I thank him for the captivating projects. His valuable insight has guided my research provided me opportunities to grow professionally.

I thank my committee members Dr. Phillip McClean, Dr. Timothy Friesen and Dr. Shaobin Zhong for their valuable suggestions and insightful comments. I would like to express my gratitude to my instructors at NDSU for their thoughtful tutledge. Thank you for sharing your knowledge and passion. And I must thank Shannon Ueker for her enthusiastic support of all the graduate students under her guidance.

I am thankful for my wonderful current and former lab mates, Dr. Zengcui Zhang, Dr. Sudeshi Seneviratne, Dr. Amanda Peters Haugrud, Sapna Sharma, Dr. Aliya Momotaz, Dr. Agnes Szabo-Hever, Gurminder Singh, Megan Overlander, Caylee Steen, and Stephanie McCoy for their encouragement, advice, and time. I thank Erika Shay Bauer, Brianna Robinson, Libby Bateman, Molly Holt, Jonathan Schwartz, Marissa Condron, Brandon Rasmusson, and Lydia Lyons for supporting my research.

Thank you to my friends, anyone who ever attended Weekly Pint after work, or played on the Angiosperms trivia team. Thank you for the conversation, moral support, and knowing when I needed to hear advice or to vent about struggles with research.

Thanks to my family. I thank you for your endless support and for pushing me to be my best, in all my endeavors. Immense gratitude to my husband, Colton, for his patience and support. He has encouraged me when I felt frustrated and celebrated every success with me.

DEDICATION

To my family. They made me who I am.

And to the wonderfully kind educators who've nurtured my curiosity.

Thank you for your advice, patience, and faith.

TABLE OF CONTENTS

LIST OF TABLES

LIST OF FIGURES

LIST OF ABBREVIATIONS

BLAST.....basic local alignment search tool

Bp.....basepair

CF.....culture filtrate

DNA.....deoxyribonucleic acid

GWAS.....genome-wide association study

MTA.....marker trait association

NE.....Necrotrophic effector

PCR.....polymerase chain reaction

QTL.....quantitative trait loci

RIL.....recombinant inbred line

RNA.....ribonucleic acid

SNB.....Septoria nodorum blotch

SSR.....simple sequence repeat

STARP.....semi-thermal asymmetric reverse PCR

TILLING.....targeting induced local lesions in genomes

TS.....tan spot

1. GENERAL INTRODUCTION

Today, durum wheat and bread wheat provide about 20% of the calories consumed by humans (reviewed by Faris 2014). As the world population grows, the demand for wheat will also increase. *Parastagonospora nodorum* and *Pyrenophora tritici-repentis*, the causal agents of septoria nodorum blotch (SNB) and tan spot (TS), respectively, reduce the photosynthetic area of the plant, which in turn reduces yield (Eyal 1987; Shabeer and Bockus 1988). An estimated 16.0 and 8.8 million tons of wheat were lost globally in 2019 due to TS and SNB, respectively (Savary et al. 2019; Wulf and Krattinger 2022). The yield loss from just these two pathogens would have been enough grain to produce 34.7 billion loaves of bread. An effective way to combat potential yield loss is by planting cultivars with genetic resistance to the prevalent pathogens, but this is contingent on identifying cultivars with resistance.

Both SNB and TS are necrotrophic pathogens that interact in an inverse gene-for-gene manner with the host (Friesen and Faris 2010). In this case, susceptibility is conferred by dominant host genes that interact with necrotrophic effectors produced by the pathogen, resulting in a compatible interaction leading to cell death. For SNB and TS, resistance is primarily conferred by the lack of susceptibility genes. So far nine host-sensitivity gene-necrotrophic effector interactions have been characterized in the *P. nodorum* pathosystem: *Tsn1*-SnToxA, *Snn1*-SnTox1, *Snn2*-SnTox267, *Snn3-B1*-SnTox3, *Snn3-D1*-SnTox3, *Snn4*-SnTox4, *Snn5*-SnTox5, *Snn6*-SnTox267, and *Snn7*-SnTox267 (reviewed by Peters Haugrud et al. 2022). In the *P. tritici-repentis* pathosystem three main host-sensitivity gene-necrotrophic effector gene interactions have been characterized: *Tsn1*-Ptr ToxA, *Tsc1*-Ptr ToxC, and *Tsc2*-Ptr ToxB (reviewed by Faris et al. 2013). Four of the host sensitivity genes have been cloned: *Snn1*, *Snn3-D1*, and *Tsn1*, which acts as a multi-pathogen sensitivity gene (Shi et al. 2016; Zhang et al. 2021;

Faris et al. 2010). Despite the cloning of *Tsn1*, diagnostic high-throughput markers have not been developed. Chapter 6 of this dissertation addresses this issue, developing markers that can be used to select cultivars that are insensitive to ToxA. The two other research chapters focus on the cloning of *Tsc1* and *Snn5* and characterizing a new host-sensitivity gene-necrotrophic effector interaction in the *P. nodorum* pathosystem. Together, the three research chapters add to the growing body of research dedicated to identifying and charactering host-sensitivity genes towards the goal of selectively removing them from breeding lines by marker-assisted elimination or gene editing, increasing wheat yield and quality.

1.1. Literature cited

Eyal Z, International Maize and Wheat Improvement Center (eds) (1987) The Septoria diseases of wheat: concepts and methods of disease management. CIMMYT, Mexico, D.F

Faris JD (2014) Wheat domestication: Key to agricultural revolutions past and future. In: Tuberosa R, Graner A, Frison E (eds) Genomics of plant genetic resources. Springer Netherlands, Dordrecht, pp 439–464

Faris JD, Liu Z, Xu SS (2013) Genetics of tan spot resistance in wheat. Theor Appl Genetic 126:2197–2217. https://doi.org/10.1007/s00122-013-2157-y

Faris JD, Zhang Z, Lu H, et al (2010) A unique wheat disease resistance-like gene governs effector-triggered susceptibility to necrotrophic pathogens. Proc Natl Acad Sci USA 107:13544–13549. https://doi.org/10.1073/pnas.1004090107

Friesen TL, Faris JD (2010) Characterization of the wheat- Stagonospora nodorum disease system: what is the molecular basis of this quantitative necrotrophic disease interaction? Can J Plant Pathol 32:20–28. https://doi.org/10.1080/07060661003620896

Peters Haugrud AR, Zhang Z, Friesen TL, Faris JD (2022) Genetics of resistance to septoria nodorum blotch in wheat. Theor Appl Genet. https://doi.org/10.1007/s00122-022-04036-9

Savary S, Willocquet L, Pethybridge SJ, et al (2019) The global burden of pathogens and pests on major food crops. Nat Ecol Evol 3:430–439. https://doi.org/10.1038/s41559-018-0793-y

Shabeer A, Bockus WW (1988) Tan spot effects on yield and yield components relative to growth stage in winter wheat. Plant Dis 72:599–602. https://doi.org/10.1094/PD-72-0599

Shi G, Zhang Z, Friesen TL, et al (2016) The hijacking of a receptor kinase-driven pathway by a wheat fungal pathogen leads to disease. Sci Adv 2:e1600822–e1600822. https://doi.org/10.1126/sciadv.1600822

Wulff BB, Krattinger SG (2022) The long road to engineering durable disease resistance in wheat. Curr Opin Biotechnol 73:270–275. https://doi.org/10.1016/j.copbio.2021.09.002

Zhang Z, Running KLD, Seneviratne S, et al (2021) A protein kinase–major sperm protein gene hijacked by a necrotrophic fungal pathogen triggers disease susceptibility in wheat. Plant J 106:720–732. https://doi.org/10.1111/tpj.15194

2. LITERATURE REVIEW

2.1. Necrotrophic plant pathogens

Plant pathogens are classified as biotrophs, hemibiotrophs, and necrotrophs based on their lifestyle. Biotrophic pathogens require living cells to feed and complete their lifestyle. Typically, biotrophs produce effectors to suppress the host immune system (Horbach et al. 2011). Gene-for-gene interactions between host resistance genes and the biotrophic pathogen produced effectors result in effector-triggered immunity (ETI, reviewed by Naveed et al. 2020) Hemi-biotrophs have an initial biotrophic phase followed by a necrotrophic phase (Horbach et al. 2011). Necrotrophic pathogens complete their lifecycle on dead and dying tissue, necrotizing host tissue by secreting cell wall degrading enzymes and effectors. Necrotrophs generally fall into two classes, those with broad-host ranges, such as *Sclerotinia sclereotiorum*, *Botrytis cinera*, and *Rhizoctonia solani*, are termed generalists, while necrotrophic specialists have a narrow host range, sometimes being host-specific (reviewed by Lorang et al. 2019). *Parastagonospora nodorum* and *Pyrenophora tritici-repentis*, the causal agents of septoria nodorum blotch (SNB) and tan spot (TS), respectively, are considered necrotrophic specialists.

Necrotrophs interact with the host according to the inverse gene-for-gene model (Friesen and Faris 2010), where recognition of pathogen proteins or secondary metabolites, termed necrotrophic effectors (NEs), ultimately results in programmed cell death (PCD). Like in gene-for-gene interactions, the recognition of NEs by host gene products results in a typical host defense response characterized by reactive oxygen burst, MAP kinase signaling, and the upregulation of defense response genes (reviewed by Ngou et al. 2022 and Friesen and Faris 2021). In the gene-for-gene interaction of a biotroph, these defense responses limit the growth of the pathogen by triggering a hypersensitive response, ultimately leading to effector-triggered

immunity. In the inverse gene-for-gene model, the same defense responses also lead to PCD. However, this is beneficial to necrotrophic pathogens. Therefore, the result is susceptibility rather than resistance.

2.2. *Parastagonospora nodorum* susceptibility in wheat

The wheat disease septoria nodorum blotch (SNB) is a foliar and glume blotch disease caused by the necrotrophic fungal pathogen *Parastagonospora nodorum*. Susceptibility to *P. nodorum* is controlled by multiple interactions between the host and pathogen that genetically follow the inverse gene-for-gene model (Friesen and Faris 2010). *P. nodorum* produces NEs that target dominant host susceptibility genes, hijacking typical defense pathways to induce cell death. The pathogen can acquire nutrients from the dead and dying tissues. The loss of photosynthetic capacity in necrotic leaves translates to yield losses up to 50% (Eyal 1987).

P. nodorum is a heterothallic filamentous asocomycete in the Dothideomycetes class of fungi (reviewed by Oliver et al. 2012). Although, *P. nodorum* was originally classified under the *Stagonospora* genus as *Stagonospora nodorum* (Goodwin and Zismann 2001), later evaluation of ribosomal RNA sequences and the morphology of sexual and asexual stages of *P. nodorum* isolates revealed differences between *P. nodorum* isolates and *Stagonospora* isolates (Quaedvlieg et al. 2013). The *Parastagonospora* genus, meaning "resembling the genus *Stagonospora*", was created to accommodate species phylogenetically distinct from *Stagonospora* and *Phaeosphaeria.* Other synonyms for *P. nodorum* encountered in literature include *Septoria nodorum*, *Phaeosphaeria nodorum* and *Leptosphaeria nodorum*.

During the parasitic phase of the *P. nodorum* life cycle, ascospores are released from the sexual reproductive structures, pseudothecia, infecting the lower leaves of wheat plants (Oliver et al. 2012). Initial infections are characterized by small, water-soaked chlorotic lesions that

become necrotic. The necrotic lesions are lens-shaped and red-brown with a gray-brown center (Friesen and Faris 2010). Pycnidia develop on the necrotic lesions and spread through splash dispersal to the upper leaves and glumes. Brown-purple blotches form on glumes, hence the name glume blotch (Weber 1922). Severe infections can result in discolored and shriveled seeds, decreasing both yield and quality (McMullen and Adhikari 2009). *P. nodorum* overwinters on infected wheat residue left in the field in its saprotrophic phase, acting as the primary inoculum the following season (Reviewed by Ficke et al. 2018). Infected seeds can also act as primary inoculum.

2.2.1. Host-NE interactions in the wheat-*P. nodorum* pathosystem

Nine host-sensitivity gene-NE interactions have been characterized in the *P. nodorum* pathosystem: *Tsn1*-SnToxA, *Snn1*-SnTox1, *Snn2*-SnTox267, *Snn3-B1*-SnTox3, *Snn3-D1*-SnTox3, *Snn4*-SnTox4, *Snn5*-SnTox5, *Snn6*-SnTox267, and *Snn7*-SnTox267 (reviewed by Peters Haugrud et al. 2022). Three host sensitivity genes (*Tsn1*, *Snn1*, *Snn3-D1*) has been cloned and published (Faris et al. 2010; Shi et al. 2016; Zhang et al. 2021). *Snn3-B1* and an additional SnTox3-sensitivity gene, *Snn3-B2*, have also been cloned and their characterization is underway (Zhang et al. unpublished). In general, wheat genotypes with multiple NE susceptibility genes are more susceptible to isolates producing more than one NE (reviewed by Peters Haugrud et al. 2022). Disease reactions tend to be additive. However, disease severity is controlled by not just the host sensitivity gene-NE interactions, but also the pathogen and host genetic background and regulation of NE expression. All characterized NE genes, besides SnTox4, have been cloned.

2.2.1.1. Tsn1-ToxA

The *Tsn1*-ToxA interaction was first found to contribute to susceptibility to tan spot, caused by the pathogen *Pyrenophora tritici-repentis*. Ptr ToxA was cloned first from *P. tritici-repentis* (Tomás and Bockus 1987; Ballance et al. 1989). Ptr ToxA homologs were subsequently identified in *P. nodorum* (Friesen et al. 2006), *Phaeosphaeria avenaria* f. *tritici 1* (*Pat1*, McDonald et al. 2013), and *Bipolaris sorokiniana* (McDonald et al. 2018). The Ptr ToxA homolog in *P. nodorum*, SnToxA, has 99.7% similarity (Friesen et al. 2006). SnToxA has a higher level of nucleotide diversity than Ptr ToxA, indicating that ToxA was likely horizontally transferred from *P. nodorum* to *P. tritici-repentis*.

SnToxA and Ptr ToxA target *Tsn1* (tan spot necrosis 1), located on the long arm of chromosome 5BL (Faris et al. 1996; Faris et al 2010). The *Tsn1*-SnToxA interaction can explain up to 95% of the variation in disease in wheat infected with SnToxA-producing isolates (Faris and Friesen 2009). *Tsn1* was cloned via positional cloning and contains nucleotide binding, leucine-rich repeat, and serine/threonine protein kinase domains (Faris et al. 2010). *Tsn1* is 10,581 bp, but encodes a protein of only 1490 amino acids. Yeast-two-hybrid experiments indicate that *Tsn1* does not interact with ToxA directly. Recently, ToxA was found to interact with the C-terminal LEA2 extracellular domain of the wheat transmembrane NDR/Hin1-like protein TaNHL10 (Dagvadorj et al. 2022). Importation of ToxA into the cell is dependent on the presence of *Tsn1* (Manning and Ciuffetti 2005), but *Tsn1* has no transmembrane domains. Therefore, it has been postulated that *Tsn1* may act as a guard (Faris et al. 2010). While the interaction between TaNHL10 and *Tsn1* is not yet characterized, TaNHL10 is certainly a promising target for future *Tsn1* interaction studies.

2.2.1.2. Snn1-SnTox1

The *Snn1*-SnTox1 interaction was the first host NE-sensitivity gene interaction identified in the wheat *P. nodorum* pathosystem (Liu et al. 2004a). Using the International Triticeae Mapping Initiative (ITMI) population, Liu et al. (2004a) mapped sensitivity to SnTox1, partially purified from culture filtrates of isolate Sn2000. Both *Snn1* and SnTox1 have been cloned (Liu et al. 2012; Shi et al. 2016b). SnTox1 candidates were identified in the *P. nodorum* reference genome using previously identified characteristics of SnTox1, SnToxA, and SnTox3 (Liu et al. 2012). The identified gene SNOG_20078, was confirmed to encode SnTox1 based on evaluation of sensitivity reactions after the infiltration of cultures expressing SNOG_20078 in *Pichia pastoria*. SnTox1 is 117 amino acids long and contains a signal peptide and chitin binding domain. The chitin binding domain was later proven to bind *P. nodorum* chitin, protecting the fungus from plant chitinases (Liu et al. 2016). Expression of SnTox1 is upregulating during the early stages of infection, peaking at 72 hours post inoculation (Liu et al. 2012). A compatible *Snn1*-SnTox1 interaction triggers an oxidative burst, upregulates defense related genes, and leads to DNA laddering.

Snn1 was mapped to the short arm of chromosome 1B using an F_2 population derived from a cross between Chinese Spring and a Chinse Spring-*T. dicoccoides* 1B disomic chromosome substitution line (Reddy et al. 2008). *Snn1* was delineated to .46 cM. In a new population derived from a cross between Chinese Spring and a Chinese Spring-Hope 1B disomic substitution line, Shi et al. (2016b) delineated the *Snn1* locus to a single gene. *Snn1* is 3045 bp long and consists of 3 exons. It encodes a protein containing a signal sequence and wall-associated receptor kinase galacturonan binding (GUB_WAK), epidermal growth factor-calcium

binding (EGF_CA), transmembrane, and S/TPK domains. *Snn1* was validated via mutagenesis and found to interact directly with SnTox1.

2.2.1.3. Snn2, Snn6, and Snn7 interactions with SnTox267

The interactions *Snn2*-SnTox2, *Snn6*-SnTox6, *Snn7*-SnTox7 were originally thought to be separate interactions between independent host sensitivity genes and NEs (Friesen et al 2007; Gao et al 2015; Shi et al. 2015). However, Richards et al. (2021) recently demonstrated that NEs SnTox2, SnTox6, and SnTox7 are a single protein (SnTox267). Although the original papers describing the interactions used the gene designations *SnTox2*, *SnTox6*, and *SnTox7*, we now know that the gene designation *SnTox267* is more accurate as they are not independent NEs. Therefore, the gene name *SnTox267* will be used here.

The *Snn2*-SnTox267 interaction was first identified in a recombinant inbred population (BG) derived from a cross between two hard red spring wheat cultivars, BR34 and Grandin (Friesen et al. 2007). When BG lines were infiltrated with culture filtrates of *P. nodorum* isolate Sn6, the *Snn2*-SnTox267 interaction accounted for 47% of the variation in disease reactions. *Snn2* was mapped to the short arm of chromosome 2D and delineated to an interval of 4.0 cM (Zhang et al. 2009). Seneviratne (2019) developed a high-resolution map of the *Snn2* region using a cross between BR34 and BG301, a recombinant line selected from the BG population that carries *Snn2*, but no other sensitivity loci. Screening of over 10,000 gametes reduced the *Snn2* locus to an interval of 0.10 cM, corresponding to 0.53 Mb in the Chinese Spring RefSeq1.0 assembly (IWGSC 2018). Thirteen candidate genes were identified in the *Snn2* region with NB-ARC or PK domains. Analysis of these candidate genes is ongoing (Seneviratne and Faris personal communication).

The *Snn6*-SnTox267 interaction was identified in the ITMI population, which was known to segregate for *Snn1* and *Snn3-B1* sensitivity genes (Gao et al. 2015). When inoculated with the isolate Sn6, which has *SnTox1* and *SnTox3* genes, a single QTL was identified on the long arm of chromosome 6A which was not due to *Snn1*-SnTox1 or *Snn3-B1*-SnTox3 interactions. The interaction between the new sensitivity gene, *Snn6*, and it's corresponding NE, now known to be SnTox267, explained 27% of the disease variation. To investigate why the *Snn1*-SnTox1 and *Snn3-B1*-SnTox3 interactions were not additive to the *Snn6*-SnTox267 interaction, Gao et al. (2015) evaluated the expression of *SnTox1* and *SnTox3* in isolate Sn6. *SnTox1* was not expressed, explaining why no *Snn1*-SnTox1 QTL was identified, but *SnTox3* was expressed.

The *SnTox7*-SnTox267 interaction explained 33% of the disease variation in a population derived from a cross between Chinese Spring and a Chinese Spring-Timstein 2D disomic chromosome substitution line when inoculated with Sn6 (Shi et al. 2015). Sensitivity mapped to the long arm of chromosome 2D. Sn6 produces multiple effectors, but sensitivity to them had not yet mapped to chromosome 2D. As such, the new interaction was designated *Snn7*-SnTox7, later updated to *Snn7*-SnTox267 (Richards et al. 2021).

All evidence suggested that the *Snn2*-SnTox2, *Snn6*-SnTox6, and *Snn7*-SnTox7 interactions were independent, and so it was logically presumed that SnTox2, SnTox6, and SnTox7 were independent NE (Friesen et al 2007; Gao et al 2015; Shi et al. 2015). Two GWAS using 197 diverse *P. nodorum* isolates inoculated on BG223 (*Snn2*+) and ITMI37 (*Snn6*+) detected the same genomic locus on *P. nodorum* chromosome 14. The most significant marker in each GWAS was less than 1 kb upstream of candidate gene *CJJ_13380*. SnTox7, SnTox2, and SnTox6 were previously partially purified and found to have similar characteristics (Shi et al. 2015; Friesen et al 2007; Gao et al. 2015). Therefore, Richards et al. (2021) postulated that

CJJ_13380 may also target *Snn7*. QTL mapping of sensitivity to CJJ_13380 in the *Snn7* mapping population (Chinese Spring × Chinese Spring-Timstein 2D) indicated that CJJ_13380 interacts with *Snn7*. CJJ_13380 was functionally validated and proven to interact with *Snn2*, *Snn6*, and *Snn7*. Consequently, the nomenclature SnTox267 was proposed. *Snn2* and *Snn6* were also found to be complementary, where the *Snn7*-SnTox267 interaction was independent.

2.2.1.4. Snn3-D1, Snn3-B1, and *Snn3-B2* interactions with SnTox3

The *Snn3*-SnTox3 interaction was first identified in the BG population (Friesen et al. 2008). *Snn3* was mapped to the short arm of chromosome 5B. In 2011, Zhang et al. identified a SnTox3-sensitivity locus on the short arm of chromosome 5D. Comparative mapping of the SnTox3-sensitivity loci on 5B and 5D indicated that the loci were likely homoeologous. Therefore, the nomenclature *Snn3-B1* and *Snn3-D1* was adopted, referring to the first *Snn3* genes identified in the B and D subgenomes, respectively. Individuals with the *Snn3-B1* allele had less severe reactions than lines with the *Snn3-D1* allele. Shi et al. (2016a) conducted saturation and fine mapping of SnTox3-sensitivity on chromosome 5B, delineating the locus to a 1.5 cM interval in a population derived from a cross between BR34 and Sumai3. Fine mapping of the *Snn3-D1* locus was conducted in a population developed using a cross between *Aegilops tauschii* accessions TA2377 and AL8/78 (Zhang et al. 2021). The *Snn3-D1* region was delineated to a 1.38 cM interval. High resolution mapping was conducted in the same population and an additional F_2 population derived from a cross between BR34 and a synthetic hexaploid carrying the D subgenome from TA2377 in the background of the durum cultivar Langdon (LDN2377). Using a map-based approach the *Snn3-D1* candidate gene region was narrowed to a 362 kb segment on a TA2377 BAC clone that contained 10 putative genes. Comparative sequence

analysis of SnTox3-insensitive mutants confirmed a gene containing PK and major sperm protein (MSP) domains as *Snn3-D1*. Both domains were required for *Snn3-D1* functionality.

In the process of characterizing SnTox3 sensitivity on chromosome 5B, an *Snn3-D1* homoeolog was identified in the genomic region associated with SnTox3-sensitivity (Zhang et al. upublished). This homoeolog, *Snn3-B1*, was functionally validated. Comparative sequence analysis of the *Snn3-B1* sequence in SnTox3-insensitive Sumai3 mutants revealed that sensitivity in Sumai3 was not conferred by *Snn3-B1*. The SnTox3-sensitivity gene on chromosome 5B of Sumai3, referred to as *Snn3-B2*, was ultimately cloned using a MutChromSeq approach. Both *Snn3-B1* and *Snn3-B2* contain PK and MSP domains, like *Snn3-D1*. Preliminary results indicate there may be additional SnTox3 sensitivity genes on chromosome 5B and work is under way to further characterize SnTox3-sensitivity. In general, SnTox3-sensitivity conferred by *Snn3-B2* is stronger than that of *Snn3-B1*.

2.2.1.5. Snn4-SnTox4

The *Snn4*-SnTox4 interaction was identified in a RIL population (Abeysekara et al 2009) derived from a cross between cultivars Arina and Forno (Paillard et al. 2003). *Snn4* was mapped to a 2.5 cM interval on the short arm of chromosome 1A. The contribution of the *Snn4*-SnTox4 interaction to variation in disease when infiltrated with Sn99 depends on the wheat background. In the Arina × Forno population, The *Snn4*-SnTox4 interaction explained 41% of the disease variation, but when the same isolate was used to evaluate susceptibility in a population derived from Katepwa × Salamouni, the *Snn4*-SnTox4 interaction explained just 23% of the variation in disease (Abeysekara et al. 2009; Abeysekara et al. 2012). SnTox4 was partially purified from the Swiss isolate Sn99CH1A7a (Sn99) and found to be 10-30 kDa.

2.2.1.6. Snn5-SnTox5

A population derived from a cross between North Dakota durum wheat variety Lebsock and *T. turgidum* ssp. *carthlicum* accession PI 94749 (LP749) was infiltrated with culture filtrates of *P. nodorum* isolate Sn2000 (Friesen et al. 2012). Sensitivity mapped to the long arm of chromosome 4B, indicating the presence of a new host-NE interaction, *Snn5*-SnTox5. Sharma (2019) conducted saturation mapping in the LP749 population, delineating the *Snn5* region to a 2.8 cM interval corresponding to a 1.38 Mb physical region. Depending on the other NEs produced, the *Snn5*-SnTox5 interaction explained up to 63% of the disease variation in the LP749 population.

SnTox5 was identified in a GWAS and validated using CRISPR/Cas9-mediationg gene disruption and gain-of function transformation methods (Kariyawasam et al. 2022). SnTox5 encodes a small 16.25 k DA protein with a signal peptide and pro-sequence. SnTox5 was found to have a second function facilitating colonization of the mesophyll, even in the absence of a functional *Snn5* allele.

2.3. *Pyrenophora tritici-repentis* susceptibility in wheat

Tan spot is caused by the ascomycete *Pyrenophora tritici-repentis*. *P. tritici-repentis* infects all types of wheat, causing major disease around the world (reviewed by Faris et al. 2013). *P. tritici-repentis* is a necrotrophic fungal pathogen that induces cell death in susceptible wheat genotypes and then feeds on the released nutrients. When wheat is infected necrotic or chlorotic lesions form on the leaves. The dead tissue has lower photosynthetic capabilities, leading to lower energy production, and ultimately, lower yields. In the United States, annual yield losses are estimated at 2-15% however, in favorable conditions yield losses of around 50% have been reported (Bhathal et al. 2003; Evans et al. 1999; Hosford et al. 1982; Rees et al. 1982;

Wegulo et al. 2009). An estimated 16 billion tons of wheat were lost due to tan spot infections in 2019 (Savary et al. 2019; FAOStat http://www.fao.org/faostat/en/#home)

Reductions in yield are typically observed through reduced kernel weight, grain number per head (Shabeer and Bockus 1988), and grain quality due to red or pink smudge (Fernandez et al. 1994) Tan spot infections can also reduce yield through reductions in tillage number, dry matter production, and leaf area index (Rees and Platz 1983) and total biomass (Kremer and Hoffman 1992).

P. tritici-repentis was first described in 1823, where it was found growing on dead rye stalks (Fries 1823). Although *P. tritici-repentis* was first described in 1823, reports of yield losses due to tan spot did not begin until the 1970's, seemingly coinciding with the adaptation of minimum tillage practices. While minimum tillage reduces soil erosion, it increases the disease pressure of *P. tritici-repentis* that survives saprophytically on the dead stalks of the previous crop, providing primary inoculum the following growing season. Tan spot disease management practices combine cultural practices such as crop rotations, tillage treatments, and burning crop residue, with fungicide treatments, and the selection of resistant cultivars (Wegulo 2011).

Although *P. tritici-repentis* is primarily associated with tan spot of wheat, it has a wide host range. *P. tritici-repentis* overwinters, obtaining nutrients from wheat stubble left in the field after harvest. Pseudothecia develop on the wheat stalks, appearing as black pinhead sized fruiting bodies (Wegulo 2011). Asci mature in the pseudothecia and release ascopores in the spring, serving as the primary inoculum. Ascospores are relatively large and are only ejected an average distance of 3-4 cm (Friesen et al. 2003). Dispersal of ascospores relies on wind and therefore initial infections are often in the leaves closest to the primary inoculum (Ciuffetti et al. 2014).

Three host sensitivity gene-*Ptr* interactions have been characterized so far: *Tsn1*-Ptr ToxA, *Tsc2*-Ptr ToxB, and *Tsc1*-Ptr ToxC (Faris et al. 2013). *Tsn1* (Faris et al. 2010), *PtrToxA* (Ciuffetti et al. 1997), and *PtrToxB* (Martinez et al. 2001) have been cloned. In addition to these three characterized interactions with host sensitivity genes, multiple qualitative and quantitative resistance loci have been reported. Most resistance loci have been found to confer recessive resistance and therefore are likely susceptibility loci. However, the *Tsr7* locus confers dominant race-nonspecific resistance (Faris et al. 2020). The *Tsn1*-Ptr ToxA interaction induces necrosis while the *Tsc1*-Ptr ToxC and *Tsc2*-Ptr ToxB interactions induce chlorosis (reviewed by Faris et al. 2013). *Ptr* isolates are classified into races depending on which host differential the isolate is virulent on. Races 2, 3, and 5 produce NEs Ptr ToxA, Ptr ToxC, and Ptr ToxB, respectively. Race 1 isolates produce Ptr ToxA and Ptr ToxC. Race 6 produces Ptr ToxB and Ptr ToxC. Race 7 produces Ptr ToxA and Ptr ToxB. Race 8 produces all three NEs.

2.3.1. *Tsn1*-Ptr ToxA

ToxA was first identified in *P. tritici-repentis* (Lamari and Bernier 1989). Lamari and Bernier (1989) conducted infiltrations with Ptr ToxA and inoculation with Ptr ToxA-producing isolates on a set of F_2 populations. They found that plants sensitive to Ptr ToxA were also susceptible to Ptr ToxA-producing isolates, indicating that a single gene was responsible for both sensitivity and susceptibility. Additionally, segregation ratios among the F_2 progeny and F_1 phenotypes indicated that sensitivity to Ptr ToxA was conferred by a dominant gene. These conclusions were further validated by Faris et al. (1996).

Concurrent studies in 1996 determined that the Ptr ToxA sensitivity gene, named *Tsn1* for “tan spot necrosis”, was located on chromosome 5B. Faris et al. (1996) conducted molecular mapping in a population of 58 F_3 families derived from a cross between resistant synthetic

hexaploid W-7976 and susceptible cultivar 'Kulm'. Sixteen plants per F_3 family were infiltrated with culture filtrate of Race 2 isolate 82-124 (Ptr ToxA +, Ptr ToxC-, Ptr ToxB-) and plants were scored on a binary scale three days after infiltration. DNA from each F_3 family was bulked and subjected to restriction fragment length polymorphism (RFLP) analysis. The RFLP based molecular map placed *Tsn1* on a 10.8 cM interval on the long arm of chromosome 5B. Stock et al. (1996) evaluated a set of Chinese Spring (Kenya Farmer) substitution lines with the same Race 2 isolate, 86-124, and found that Chinese Spring 5B carries a Ptr ToxA resistance gene, *tsn1*. Evaluation of F_2 segregation ratios in both studies determined that resistance was recessive.

In 1999, Anderson and colleagues evaluated Ptr ToxA sensitivity in the set of Chinese Spring nullisomic-tetrasomic stocks (Sears 1954) and chromosome deletion lines (Endo and Gill 1996). Chinese Spring N5BT5D and all 5BL deletion lines were insensitive, but when the 5B chromosome from a sensitive cultivar was substituted into the Chinese Spring 5B chromosome, the line gained sensitivity demonstrating that Chinese Spring didn't carry a tan spot resistance gene on 5BL, rather it lacked the tan spot susceptibility gene *Tsn1* carried in the sensitive cultivars.

A single copy of Ptr ToxA encodes a 13.2 kDa protein with pre- and pro- domains that is imported into the cells (reviewed by Ciuffetti et al. 2010). Recently analysis of Ptr ToxA interactions determined that Ptr ToxA binds to the wheat transmembrane NDR/Hin1-like protein TaNHL10 (Dagvadorj et al. 2022). While it is not yet known how Ptr ToxA gains entry into the cell, perhaps TaNHL10 plays a role. Inside the cell, Ptr ToxA is localized to the chloroplasts.

As previously mentioned, ToxA has been horizontally transferred to four pathogens, *Pyrenophora tritici-repentis* (Tomas and Bockus 1987; Ballance et al. 1989), *Parastagonospora nodorum* (Friesen et al. 2006), *Phaeosphaeria avenaria* f. *tritici 1* (*Pat1*, McDonald et al. 2013),

and *Bipolaris sorokiniana* (McDonald et al. 2018). The presence of *Tsn1* confers susceptibility to isolates producing ToxA. Tsn1 contains nucleotide binding, leucine-rich repeat, and serine/threonine protein kinase domains (Faris et al. 2010). The combination of protein domains is unique and likely arose through a gene fusion event.

2.3.2. *Tsc1*-Ptr ToxC

QTL analysis in the ITMI population identified the QTL *QTsc.ndsu-1A*, later designated *tsc1,* associated with resistance to chlorosis induced by Ptr ToxC-producing isolates (Faris et al. 1997; Effertz et al. 2002). An overlapping QTL associated with chlorosis production, *QTs.zhl-1A*, was identified in RIL populations derived from crosses between bread wheats Louise and Penawawa (LouPen) and LMPG-6 and PI 626573 (LP) (Kariyawasam et al. 2016; Liu et al. 2017). In the LP and LouPen populations, *QTs.zhl-1A* explained 22 and 27% of the variation in disease, respectively.

Neither *Tsc1* or *PtrToxC* have been cloned, but Ptr ToxC is predicted to be a non-ionic, polar, low molecular mass molecule (Effertz et a. 2002). Recently, a gene required for Ptr ToxC production was identified in a population segregating to Ptr ToxC production (Shi et al. 2022). Isolates that did not produce Ptr ToxC were transformed with the gene, PtrM_13157, but were still unable to produce chlorosis on *Tsc1*+ lines. As PtrM_13157 is required for Ptr ToxC production, it is not sufficient, the gene designation *ToxC1* was given.

2.3.3. *Tsc2*-Ptr ToxB

Ptr ToxB is a small-secreted protein cloned from race 5 isolates (Martinez et al. 2001). Ptr ToxB encodes an 87-aa pre-protein with a 23-aa signal peptide (Martinez et al. 2001; Strelkov and Lamari 2003). ToxB encodes no known functional domains. Multiple Ptr ToxB copies are present in Ptr ToxB producing isolates (Martinez et al. 2004; Amaike et al. 2008). Ptr

ToxB copy number is associated with higher Ptr ToxB expression and a greater impact on tan spot susceptibility (Strelkov et al. 2002; Stelkov and Lamari 2003; Martinez et al. 2004).

Tsc2 was mapping to the short arm of chromosome 2B by Friesen and Faris (2004) using the ITMI population. Abeysekara et al (2010) delineated the *Tsc2* locus to a 3.3 cM region in a RIL population derived from a cross between Salamouni and Katepwa. A GWAS using durum wheats evaluated for sensitivity to Ptr ToxB, expressed in *P. pastoris* (Galagedara et al. 2020). Nine markers in the *Tsc2* region were significantly associated with Ptr ToxB sensitivity, with the most significant marker explaining 41.2% of the phenotypic variation. The physical positions of the markers place *Tsc2* between 23.9 and 24.5 Mb in the Chinese Spring RefSeq1.0 assembly (IWGSC 2018). Using association mapping panels and a MAGIC population, Corsi et al. (2020) mapped *Tsc2* to a 1.9 Mb region containing 104 genes in Chinese Spring.

2.4. Literature cited

Abeysekara NS, Faris JD, Chao S, McClean PE, Friesen TL (2012) Whole-genome analysis of Stagonospora nodorum blotch resistance and validation of the SnTox4-*Snn4* interaction in hexaploid wheat. Phytopathology 102:94–104

Abeysekara NS, Friesen TL, Keller B, Faris JD (2009) Identification and characterization of a novel host-toxin interaction in the wheat-Stagonospora nodorum pathosystem. Theor Appl Genet 120:117–126

Abeysekara NS, Friesen TL, Liu ZH, McClean PE, Faris JD (2010) Marker development and saturation mapping of the tan spot Ptr ToxB sensitivity locus *Tsc2* in hexaploid wheat. Plant Genome 3:179-189

Amaike S, Ozga JA, Basu U, Strelkov SE (2008) Quantification of *ToxB* gene expression and formation of appressoria by isolates of *Pyrenophora tritici-repentis* differing in

pathogenicity. Plant Pathol 57:623–633. https://doi.org/10.1111/j.1365-3059.2007.01821.x

Anderson JA, Effertz RJ, Faris JD, Francl LJ, Meinhardt SW, Gill BS (1999) Genetic analysis of sensitivity to a *Pyrenophora tritici-repentis* necrosis-inducing toxin in durum and common wheat. Phytopathology 89:293–297

Ballance GM, Lamari L, Bernier CC (1989) Purification and characterization of a host selective toxin from *Pyrenophora tritici-repentis*. Physiol Mol Plant P 35:203–213

Bhathal JS, Loughman R, Speijers J (2003) Yield reduction in wheat in relation to leaf disease from yellow (tan) spot and septoria nodorum blotch. Eur. J Plant Pathol109:435–443.

Ciuffetti LM, Manning VA, Pandelova I, Betts MF, Martinez JP (2010) Host-selective toxins, Ptr ToxA and Ptr ToxB, as necrotrophic effectors in the *Pyrenophora tritici-repentis*—wheat interaction. New Phytol 187:911–919

Ciuffetti LM, Manning VA, Pandelova I, et al (2014) *Pyrenophora tritici-repentis*: A plant pathogenic fungus with global impact. In: Dean RA, Lichens-Park A, Kole C (eds) Genomics of plant-associated fungi: Monocot pathogens. Springer Berlin Heidelberg, Berlin, Heidelberg, 1–39

Ciuffetti LM, Tuori RP, Gaventa JM (1997) A single gene encodes a selective toxin causal to the development of tan spot of wheat. Plant Cell 9:135-144

Corsi B, Percival-Alwyn L, Downie RC, Venturini L, Iagallo EM, Mantello CC, McCormick-Barnes C, See PT, Oliver RP, Moffat CS, and Cockram J (2020) Genetic analysis of wheat sensitivity to the ToxB fungal effector from *Pyrenophora tritici-repentis*, the causal agent of tan spot. Theor Appl Genet 133:935-950. https://doi.org/10.1007/s00122-019-03517-8

Dagvadorj B, Outram MA, Williams SJ, Solomon PS (2022) The necrotrophic effector ToxA from *Parastagonospora nodorum* interacts with wheat NHL proteins to facilitate *Tsn1* -mediated necrosis. Plant J 110:407–418. https://doi.org/10.1111/tpj.15677

Effertz RJ, Meinhardt SW, Anderson JA, Jordahl JG, Francl LJ (2002) Identification of a chlorosis-inducing toxin from *Pyrenophora tritici-repentis* and the chromosomal location of an insensitivity locus in wheat. Phytopathology 92:527-533

Evans CK, Hunger RM, Siegerist WC (1999) Comparison of greenhouse and field testing to identify wheat resistant to tan spot. Plant Dis 83:269–273.

Eyal Z (1987) The Septoria diseases of wheat: concepts and methods of disease management. CIMMYT, Mexico

Faris JD, Anderson JA, Francl LJ, Jordahl JG (1996) Chromosomal location of a gene conditioning insensitivity in wheat to a necrosis-inducing culture filtrate from *Pyrenophora tritici-repentis*. Phytopathology 86:459–463

Faris JD, Anderson JA, Francl LJ, Jordahl JG (1997) RFLP mapping of resistance to chlorosis induction by *Pyrenophora tritici-repentis* in wheat. Theor Appl Genet 94:98-103

Faris JD, Friesen TL (2009) Reevaluation of a tetraploid wheat population indicates that the *Tsn1*-ToxA interaction is the only factor governing Stagonospora nodorum blotch susceptibility. Phytopathology 99:906–912

Faris JD, Liu Z, Xu SS (2013) Genetics of tan spot resistance in wheat. Theor Appl Genet 126:2197-2217. doi: 10.1007/s00122-013-2157-y

Faris JD, Overlander ME, Kariyawasam GK, et al (2020) Identification of a major dominant gene for race-nonspecific tan spot resistance in wild emmer wheat. Theor Appl Genet 133:829–841. https://doi.org/10.1007/s00122-019-03509-8

Faris JD, Zhang Z, Lu H et al. (2010) A unique wheat disease resistance-like gene governs effector-triggered susceptibility to necrotrophic pathogens. Proc Natl Acad Sci USA 107:13544–13549

Fernandez MR, Clarke JM, DePauw RM, et al (1994) Black point and red smudge in irrigated durum wheat in southern Saskatchewan in 1990-1992. Can J Plant Pathol 16:221–227

Ficke A, Cowger C, Bergstrom G, Brodal G (2018) Understanding yield loss and pathogen biology to improve disease management: septoria nodorum blotch - A case study in wheat. Plant Dis 102:696–707. https://doi.org/10.1094/PDIS-09-17-1375-FE

Fries EM (1823) Systema mycologicum. Vol. 2. *Lundæ*. (In Latin)

Friesen TL, Ali S, Stack RW, et al (2003) Rapid and efficient production of the *Pyrenophora tritici-repentis* teleomorph. Can J Bot 81:890–895.

Friesen TL, Chu C, Xu SS, Faris JD (2012) SnTox5-*Snn5*: a novel Stagonospora nodorum effector-wheat gene interaction and its relationship with the SnToxA-*Tsn1* and SnTox3-*Snn3-B1* interactions. Mol Plant Pathol 13:1101–1109

Friesen TL, Faris JD (2010) Characterization of the wheat-Stagonospora nodorum system: what is the molecular basis of this quantitative necrotrophic disease interaction? Can J Plant Pathol 32:20–28

Friesen TL, Faris JD (2021) Characterization of effector-target interactions in necrotrophic pathosystems reveals trends and variation in host manipulation. Ann Rev Phytopathol 59:77–98

Friesen TL, Meinhardt SW, Faris JD (2007) The *Stagonospora nodorum*-wheat pathosystem involves multiple proteinaceous host-selective toxins and corresponding host sensitivity genes that interact in an inverse gene-for-gene manner. Plant J 51:681–692

Friesen TL, Stukenbrock EH, Liu Z, Meinhardt S, Ling H, Faris JD, Rasmussen JB, Solomon PS, McDonald BA, Oliver RP (2006) Emergence of a new disease as a result of interspecific virulence gene transfer. Nat Genet 38:953–956

Friesen TL, Zhang Z, Solomon PS, Oliver RP, Faris JD (2008) Characterization of the interaction of a novel *Stagonospora nodorum* host-selective toxin with a wheat susceptibility gene. Plant Physiol 146:682–693

Galagedara N, Liu Y, Fiedler J, Shi G, Chiao S, Xu SS, Faris JD, Li X, and Liu Z (2020) Genome-wide association mapping of tan spot resistance in a worldwide collection of durum wheat. Theor Appl Genet 133:2227-2237. https://doi.org/10.1007/s00122-020-03593-1

Gao Y, Faris JD, Liu Z, Kim YM, Syme RA, Oliver RP, Xu SS, Friesen TL (2015) Identification and characterization of the SnTox6-*Snn6* interaction in the *Parastagonospora nodorum*-wheat pathosystem. Mol Plant Microbe Interac 28:615–625

Goodwin SB, Zismann VL (2001) Phylogenetic analyses of the ITS region of ribosomal DNA reveal that *Septoria passerinii* from barley is closely related to the wheat pathogen *Mycosphaerella graminicola*. Mycologia 93:934–946. doi: 10.1080/00275514.2001.12063227

Horbach R, Navarro-Quesada AR, Knogge W, Deising HB (2011) When and how to kill a plant cell: infection strategies of plant pathogenic fungi. J Plant Physiol 168:51–62. doi: 10.1016/j.jplph.2010.06.014

Hosford RM, Jr (1982) Tan spot-developing knowledge 1902-1981, virulent races and wheat differentials, methodology, rating systems, other leaf diseases, literature. In: Tan Spot of

Wheat and Related Diseases Workshop, Fargo, North Dakota, Agricultural Experiment Station, North Dakota State University 1-24

International Wheat Genome Sequencing Consortium (IWGSC), IWGSC RefSeq principal investigators, Appels Ret al. (2018). Shifting the limits in wheat research and breeding using a fully annotated reference genome. Science 361, eaar7191. doi: 10.1126/science.aar7191

Kariyawasam GK, Carter AH, Rasmussen JB, et al (2016) Genetic relationships between race-nonspecific and race-specific interactions in the wheat–*Pyrenophora tritici-repentis* pathosystem. Theor Appl Genet 129:897–908. https://doi.org/10.1007/s00122-016-2670-x

Kariyawasam GK, Richards JK, Wyatt NA, et al (2022) The *Parastagonospora nodorum* necrotrophic effector SnTox5 targets the wheat gene *Snn5* and facilitates entry into the leaf mesophyll. New Phytol 233:409–426. https://doi.org/10.1111/nph.17602

Kremer M, Hoffmann GM (1992) Effect to *Drechslera tritici-repentis* as the cause of wheat yellow leaf spot disease on kernel yield and dry matter production. J Phytopathol 99: 509-605

Lamari L, Bernier CC (1989) Evaluation of wheat lines and cultivars to tan spot *Pyrenophora tritici-repentis* based on lesion type. Can J Plant Pathol 11:49–56

Liu Z, Gao Y, Kim YM, Faris JD, Shelver WL, de Wit PJGM, Xu SS, Friesen TL (2016) SnTox1, a *Parastagonospora nodorum* necrotrophic effector, is a dual-function protein that facilitates infection while protecting from wheat-produced chitinases. New Phytol 211:1052–1064

Liu Z, Zhang Z, Faris JD, Oliver RP, Syme R, McDonald MC, McDonald BA, Solomon PS, Lu S, Shelver WL, Xu S, Friesen TL (2012) The cysteine rich necrotrophic effector SnTox1 produced by *Stagonospora nodorum* triggers susceptibility of wheat lines harboring *Snn1*. PLoS Pathog 8:e1002467

Liu Z, Zurn JD, Kariyawasam G, et al (2017) Inverse gene-for-gene interactions contribute additively to tan spot susceptibility in wheat. Theor Appl Genet 130:1267–1276. https://doi.org/10.1007/s00122-017-2886-4

Liu ZH, Faris JD, Meinhardt SW, Ali S, Rasmussen JB, Friesen TL (2004a) Genetic and physical mapping of a gene conditioning sensitivity in wheat to a partially purified host-selective toxin produced by *Stagonospora nodorum*. Phytopathology 94:1056–1060

Lorang J (2019) Necrotrophic exploitation and subversion of plant defense: A lifestyle or just a phase, and implications in breeding resistance. Phytopathology 109:332–346. https://doi.org/10.1094/PHYTO-09-18-0334-IA

Manning VA, Ciufetti LM (2005) Localization of Ptr ToxA produced by *Pyrenophora tritici-repentis* reveals protein import into wheat mesophyll cells. Plant Cell 17:3203–3212

Martinez JP, Oesch NW, Ciuffetti LM (2004) Characterization of the multiple copy host selective toxin gene, *ToxB*, in pathogenic and nonpathogenic isolates of *Pyrenophora tritici-repentis*. Mol Plant-Microbe Interact 22:665-676

Martinez JP, Ottum SA, Ali S, Francl LJ, Ciuffetti, LM (2001) Characterization of the ToxB gene from *Pyrenophora tritici-repentis*. Mol Plant-Microbe Interact 14:675-677

McMullen M, Adhikari T (2009) Fungal leaf spot diseases of wheat: Tan spot, Stagonospora nodorum blotch and Septoria tritici blotch. NDSU extension service

Naveed ZA, Wei X, Chen J, et al (2020) The PTI to ETI Continuum in Phytophthora-Plant Interactions. Front Plant Sci 11:593905. https://doi.org/10.3389/fpls.2020.593905

Ngou BPM, Ding P, Jones JDG (2022) Thirty years of resistance: Zig-zag through the plant immune system. Plant Cell 34:1447–1478. https://doi.org/10.1093/plcell/koac041

Oliver RP, Friesen TL, Faris JD, Solomon PS (2012) *Stagonospora nodorum*: from pathology to genomics and host resistance. Ann Rev Phytopathol 50:23–43

Peters Haugrud AR, Zhang Z, Friesen TL, Faris JD (2022) Genetics of resistance to septoria nodorum blotch in wheat. Theor Appl Genet. https://doi.org/10.1007/s00122-022-04036-9

Quaedvlieg W, Verkley GJM, Shin H-D, et al (2013) Sizing up septoria. Studies in mycology 75:307–390. https://doi.org/10.3114/sim0017

Reddy L, Friesen TL, Meinhardt SW, Chao S, Faris JD (2008) Genomic analysis of the *Snn1* locus on wheat chromosome arm 1BS and the identification of candidate genes. Plant Genome 1:55–66

Rees R, Platz G (1983) Effects of yellow spot on wheat: comparison of epidemics at different stages of crop development. Aust J Agric Res 34:39

Rees R, Platz G, Mayer R (1982) Yield losses in wheat from yellow spot: comparison of estimates derived from single tillers and plots. Aust J Agric Res 33:899-908

Richards JK, Kariyawasam G, Seneviratne S, Wyatt NA, Xu SS, Liu Z, Faris JD, Friesen TL (2021) A triple threat: the *Parastagonospora nodorum* SnTox267 effector exploits three distinct host genetic factors to cause disease in wheat. New Phytol. https://doi.org/10.1111/nph.17601

Savary S, Willocquet L, Pethybridge SJ, et al (2019) The global burden of pathogens and pests on major food crops. Nat Ecol Evol 3:430–439. https://doi.org/10.1038/s41559-018-0793-y

Seneviratne, S (2019). Genomic analysis of septoria nodorum blotch susceptibility genes *Snn1* and *Snn2* in wheat. North Dakota State University

Shabeer A, Bockus WW (1988) Tan Spot effects on yield and yield components relative to growth stage in winter wheat. Plant Dis 72:599–602.

Sharma, S (2019) Genetics of wheat domestication and septoria nodorum blotch susceptibility in wheat. North Dakota State University

Shi G, Friesen TL, Saini J, Xu SS, Rasmussen JB, Faris JD (2015) The wheat *Snn7* gene confers susceptibility on recognition of the *Parastagonospora nodorum* necrotrophic effector SnTox7. Plant Genome. https://doi.org/10.3835/plantgenome2015.02.0007

Shi G, Kariyawasam G, Liu S, et al (2022) A conserved hypothetical gene is required but not sufficient for Ptr ToxC production in *Pyrenophora tritici-repentis*. Mol Plant-Microbe Interact 35:336–348. https://doi.org/10.1094/MPMI-12-21-0299-R

Shi G, Zhang Z, Friesen TL, Bansal U, Cloutier S, Wicker T, Rasmussen JB, Faris JD (2016a) Marker development, saturation mapping, and high-resolution mapping of the Septoria nodorum blotch susceptibility gene *Snn3-B1* in wheat. Mole Genet Genom 291:107–119

Shi G, Zhang Z, Friesen TL, Raats D, Fahima T, Brueggeman RS, Lu S, Trick HN, Liu Z, Chao W, Frenkel Z, Xu SS, Rasmussen JB, Faris JD (2016b) The hijacking of a receptor kinase-driven pathway by a wheat fungal pathogen leads to disease. Sci Adv 2:e1600822

Strelkov SE, Lamari L (2003) Host-parasite interactions in tan spot (*Pyrenophora tritici-repentis*) of wheat. Can J Plant Pathol 25:339-349

Strelkov SE, Lamari L, Sayoud R, Smith RB (2002) Comparative virulence of chlorosis-inducing races of *Pyrenophora tritici-repentis*. Can J Plant Pathol 24:29-35

Tomás A, Bockus WW (1987) Cultivar specific toxicity of culture filtrate of *Pyrenophora tritici-repentis*. Phytopathology 77:1337–1366

Wegulo SN (2011) Tan spot of cereals. *The Plant Health Instructor*. DOI: 10.1094/PHI-I-2011-0426-01

Zhang Z, Friesen TL, Simons KJ, Xu SS, Faris JD (2009) Development, identification, and validation of markers for marker-assisted selection against the *Stagonospora nodorum* toxin sensitivity genes *Tsn1* and *Snn2* in wheat. Mol Breed 23:35–49

Zhang Z, Friesen TL, Xu SS, Shi G, Liu Z, Rasmussen JB, Faris JD (2011) Two putatively homoeologous wheat genes mediate recognition of SnTox3 to confer effector-triggered susceptibility to *Stagnonospora nodorum*. Plant J 65:27–38

Zhang Z, Running KLD, Seneviratne S, Peters Haugrud AR, Szabo-Hever A, Shi G, Brueggeman R, Xu SS, Friesen TL, Faris JD (2021) A protein kinase-major sperm protein gene hijacked by a necrotrophic fungal pathogen triggers disease susceptibility in wheat. Plant J. https://doi.org/10.1111/tpj.15194

3. RAPID CLONING OF DISEASE RESISTANCE GENES IN WHEAT

3.1. Abstract

Wheat is challenged by pathogen pressures, resulting in yield losses. Plants use genes to respond to pathogen pressures, upregulating defense responses. Making sure that wheat cultivars have the best genes or alleles to respond to variable pathogen pressures starts with identifying the resistance and susceptibility genes. Subsequent gene-editing or marker selection methods can be used to create or select favorable alleles, increasing resistance to pathogens and pests. The wheat genome is large and highly repetitive, hindering gene cloning efforts. Recent advances in gene cloning methods often use reduced representation sequencing methods such as transcriptome sequencing, exome capture, or chromosome flow sorting, to reduce genome complexity, quickly filtering analysis to regions more likely to contain the causal gene. The rapid cloning methods MutRenSeq, AgRenSeq, K-mer GWAS, and MutChromSeq identify candidate genes without the development and screening of high-resolution mapping populations, which is often required in positional cloning. With an explosion of genome assemblies, genomic resources, and rapid cloning methods, researchers have tackled the complex wheat genome and identified 49 resistance and susceptibility genes.

3.2. Introduction

Pathogens and pests pose a significant threat to global food security, affecting not just primary yields, but also the stability and distribution of production and the quality of food (Savary et al. 2017). An estimated 21.47% of global wheat yields are lost annually due to pathogens and pests (Savary et al. 2019), equating to ~210 million metric tons of grain per year, enough to bake 290 billion loaves of bread (Wulff and Krattinger 2022). Wheat pathogens and pests are not just responsible for the loss of grain yield but also all the resource inputs required to

grow wheat. Effective crop disease management strategies combine agronomic practices that reduce the initial disease inoculum and infection rate, in part by selecting varieties with genetic resistance. To develop genetically resistant wheat, resistance (R) genes need to be identified, characterized, and deployed. In some diseases, like tan spot or septoria nodorum blotch, susceptibility is conferred by dominant genes. In these cases, susceptibility (S) genes need to be removed or disrupted rather than deployed.

Gene cloning is crucial to the efficient deployment of R genes and removal of S genes. Cloning a gene requires identifying the nucleotide sequence of a gene and functionally validating the gene. Diversity and functional studies can assess the effects of genetic variation within an R or S gene on resistance/susceptibility, allowing researchers to develop molecular markers targeting the variants, which can be used to select breeding lines with the most beneficial alleles. Cloned R genes can also be introduced into modern cultivars via gene complementation, introgressions, or crossing, and S genes can be removed through marker-assisted elimination or gene editing. The methods and resources used to clone R and S genes are shared, and as such R/S genes will refer to resistance or susceptibility genes in this chapter.

While over 460 R/S genes in wheat have been described, only 49 have been cloned (Hafeez et al. 2021; Table 3.1). The genome of hexaploid bread wheat is large and repetitive due, in part, to its hybridization history, making it challenging to clone R/S genes. The basic seven-chromosome Triticeae progenitor split into the *Triticum* and *Aegilops* branches about 3 million years ago (MYA) (reviewed by Faris 2014). Modern day bread wheat (*Triticum aestivum* ssp. *aestivum* L., $2n = 6x = 42$, AABBDD) is an allohexaploid that evolved as a result of two amphiploidization events involving the hybridization of two different species followed by spontaneous chromosome doubling through meiotic restitution division, several mutations, and

interspecific gene flow. Around 0.5 MYA the wild diploid species *T. urartu* Tumanian ex Gandylian ($2n = 2x = 14$, AA) hybridized with a species similar to *Aegilops speltoides* Tausch ($2n = 2x = 14$, SS) to form tetraploid wheat *Triticum turgidum* ssp. *dicoccoides* Thell ($2n = 4x = 28$, AABB), also known as wild emmer. *T. turgidum* ssp. *durum* ($2n = 4x = 28$, AABB), durum wheat, is a free-threshing derivative of *T. turgidum* ssp. *dicoccoides*, and it is today widely cultivated and used to make pasta and other semolina-based products. The second amphiploidization event occurred around 8,000 years ago. A *T. turgidum* ssp. and the diploid wild goat grass *Aegilops tauschii* Coss. ($2n = 2x = 14$, DD) hybridized to form hexaploid wheat *T. aestivum* ($2n = 6x = 42$, AABBDD), which today provides about 20% of the caloric intake of humans.

Despite their polyploid nature, bread and durum wheat behave like diploid plants genetically, with homologous chromosomes pairing and segregating during meiosis. The pairing of homoeologous chromosomes is prevented by genes *Ph1* and *Ph2* (Riley and Chapman 1958; Sears and Okamoto 1959; Mello-Sampayo and Lorente 1968). The diploid-like pairing of wheat chromosomes in meiosis simplifies segregation studies and genetic mapping of traits.

Due to their hybridization history, hexaploid and tetraploid wheat often have three or two copies of each gene, respectively, called homoeologous genes. Homoeologous genes are often highly conserved, with ~97% identity across their coding regions (Schreiber et al. 2012). The high sequence conservation among homoeologous genes hinders the development of homoeolog-specific molecular markers. Additionally, around 85% of the wheat genome is repetitive elements (Wicker et al. 2018), making it difficult to design molecular markers that only target one locus for use in molecular mapping or marker-assisted selection.

Bread and durum wheat genomes are large, 12 and 16 Gb respectively. The sequencing and assembly of such large genomes is computationally challenging, further complicated by the highly repetitive nature of wheat genomes and interchromosomal gene duplications (IWGSC et al. 2014). The complexity of the wheat genome has hampered the generation of genomic data and bioinformatic analysis. Despite the challenges, multiple high quality genome assemblies have been constructed (Table 3.2). Genome assemblies are essential for genomic studies. Wheat genome assemblies are used to design molecular markers and bait libraries, assess candidate genes, and evaluate structural variation. The assemblies act as a foundation for developing genomic resources and tools that aid in the cloning of R/S genes.

The first cloned R gene in wheat, *Lr10*, was published in 2003 (Feuillet et al. 2003) and since then 40 more R/S genes have been cloned from *Triticum* or *Aegilops* species, and an additional eight R/S genes have been cloned from related species and been shown to be functional in wheat (Table 3.1, current as of 6/1/2022). Between 2003 and 2013, ten R/S genes were cloned. The next ten R/S genes were published in just three years. In 2020, 10 R/S genes were published in a single year. Here, I will review the surge of genomic resources and gene cloning methods that have contributed to the acceleration of R/S gene cloning in wheat.

Table 3.1. Cloned resistance and susceptibility genes effective in wheat.

Gene	Gene function	Class	Cloning method	Validation method	Origin	Year	Reference
Lr10	Leaf rust resistance	NLR	Mapping	mutagenesis (EMS), gene complementation	*T. aestivum*	2003	Feuillet et al. 2003
Lr21	Leaf rust resistance	NLR	Mapping	gene complementation	*T. aestivum*	2003	Huang et al 2003
Pm3 (alleles a, b, d, & f)	Powdery mildew resistance	NLR	Mapping	transient expression, mutagenesis (1 mutant γ-rays)	*T. aestivum*	2005/03	Srichumpa et al. 2005/ Yahiaoui et al. 2003
Lr1	Leaf rust resistance	NLR	Mapping	virus-induced gene silencing, gene complementation	*T. aestivum*	2007	Cloutier et al. 2007
Lr34/Yr18/Sr57/Pm38/Ltn1	Leaf rust, Stripe rust, Stem rust, Powdery mildew and Leaf tip necrosis resistance	Abscisic acid transporter	Mapping	mutagenesis (γ-irradiation, sodium azide)	*T. aestivum*	2009	Krattinger et al. 2009
Yr36 (*WKS1*)	Stripe rust resistance	START Kinase	Mapping	mutagenesis (EMS), gene complementation	*T. turgidum* ssp. *dicoccoides*	2009	Fu et al. 2009
Tsn1	Stagonospora nodorum blotch and tan spot resistance	Serine/threonine protein kinase-NLR	Mapping	mutagenesis (EMS)	*T. turgidum* ssp. *durum*	2010	Faris et al. 2010
Sr33	Stem rust resistance	NLR	Mapping	mutagenesis (EMS), gene complementation	*Ae. tauschii*	2013	Periyannan et al. 2013
Sr35	Stem rust resistance	NLR	Mapping	mutagenesis (EMS), gene complementation	*T. monoccocum*	2013	Seintenac et al. 2013
Pm8	Powdery mildew resistance	NLR	Homology-based	transient expression, gene complementation	*Secale cereale*	2013	Hurni et al. 2013
*Yr10 (Yr10cg)**	Stripe rust resistance	NLR	Mapping	gene complementation	*T. aestivum*	2014	Liu et al. 2014
Lr67/Yr46/Sr55/Pm46/Ltn3	Leaf rust, Stripe rust, Stem rust, Powdery mildew resistance, and Leaf tip necrosis resistance	Hexose transporter	Mapping	mutagenesis (EMS), gene complementation	*T. aestivum*	2015	Moore et al. 2015
Sr50	Stem rust resistance	NLR	Mapping	mutagenesis (EMS), gene complementation	*Secale cereale*	2015	Mago et al. 2015
*Fhb1***	Fusarium head blight resistance	Pore-forming toxin-like gene	Mapping	mutagenesis (EMS), RNAi-induced gene silencing, gene complementation	*T. aestivum*	2016	Rawat et al. 2016
Snn1	Septoria nodorum blotch	Wall-associated receptor kinase (WAK)	Mapping	mutagenesis (EMS), gene complementation	*T. aestivum*	2016	Shi et al. 2016

Table 3.1. Cloned resistance and susceptibility genes effective in wheat (continued).

Gene	Gene function	Class	Cloning method	Validation method	Origin	Year	Reference
Pm2a	Powdery mildew resistance	NLR	MutChromSeq	mutagenesis (EMS)	*T. aestivum*	2016	Sánchez-Martín et al. 2016
Sr22 (alleles a and b)	Stem rust resistance	NLR	MutRenSeq	mutagenesis (EMS), gene complementation	*T. boeoticum* /*T. monococcum*	2016	Steuernagel et al. 2016
Sr45	Stem rust resistance	NLR	MutRenSeq	mutagenesis (EMS), gene complementation (dif paper)	*Ae. tauschii*	2016	Steuernagel et al. 2016
Pm60	Powdery mildew resistance	NLR	Mapping	virus-induced gene silencing, gene complementation, transient expression	*T. urartu*	2017	Zou et al. 2017
Sr13	Stem rust resistance	NLR	Mapping	mutagenesis (TILLING), gene complementation	*T. durum*	2017	Zhang et al. 2017
Lr22a	Leaf rust resistance	NLR	Mapping and TACCA	mutagenesis (EMS)	*Ae. tauschii*	2017	Thind et al. 2017
*Pm21***	Powdery mildew resistance	NLR**	Mapping, MutRenSeq	EMS, gene complementation	*Dasypyrum villosum*	2017/18	He et al. 2017/Xing et al. 2018
Stb6	Septoria tritici blotch resistance	Wall-associated receptor kinase (WAK)-like protein	Mapping	gene-complementation, virus-induced gene silencing, TILLING	*T. aestivum*	2018	Saintenac et al. 2018
Sr21	Stem rust resistance	NLR	Mapping	mutagenesis (EMS), gene complementation	*T. monoccocum*	2018	Chen et al. 2018
Yr15	Stripe rust resistance	Tandem kinase-pseudokinase	Mapping	mutagenesis (EMS), gene complementation	*T. dicoccoides*	2018	Klymiuk et al. 2018
Yr5a (*Yr5*), *Yr5b* (*YrSP*)****	Stripe rust resistance	BED-NLR	MutRenSeq	mutagenesis (EMS)	*T. aestivum*	2018	Marchal et al. 2018
Yr7	Stripe rust resistance	BED-NLR	MutRenSeq	mutagenesis (EMS)	*T. aestivum*	2018	Marchal et al. 2018
Pm17	Powdery mildew resistance	NLR	Homology-based	transient expression, gene complementation	*Secale cereale*	2018	Singh et al. 2018
Sr46	Stem rust resistance	NLR	AgRenSeq	mutagenesis (EMS), gene complementation	*Ae. tauschii*	2019	Arora et al. 2019
YrAS2388R	Stripe rust resistance	NLR	Mapping	mutagenesis (EMS), gene complementation	*Ae. tauschii*	2019	Zhang et al. 2019
Sr60 (*WKS2*)	Stem rust resistance	Tandem kinase	Mapping	gene complementation	*T. monoccocum*	2020	Chen et al. 2019

Table 3.1. Cloned resistance and susceptibility genes effective in wheat (continued).

Gene	Gene function	Class	Cloning method	Validation method	Origin	Year	Reference
Pm5e	Powdery mildew resistance	NLR	Mapping	mutagenesis (EMS), gene complementation	*T. aestivum*	2020	Xie et al. 2020
Pm24	Powdery mildew resistance	Tandem kinase	Mapping	mutagenesis (EMS), gene complementation	*T. aestivum*	2020	Lu et al. 2020
Pm41	Powdery mildew resistance	NLR	Mapping	mutagenesis (EMS), gene complementation	*T. turgidum* ssp. *dicoccoides*	2020	Li et al. 2020
YrU1	Stripe rust resistance	ANK-NLR-WRKY	Mapping	gene complementation	*T. urartu*	2020	Wang et al. 2020a
Sm1	Orange wheat blossom midge resistance	NLR-Kinase-MSP domains	Mapping and haplotype analysis	mutagenesis (EMS)	*T. aestivum*	2020	Walkowiak et al. 2020
Pm1a	Powdery mildew resistance	NLR	Mapping, MutChromSeq	mutagenesis (EMS), gene complementation	*T. aestivum*	2020	Hewitt et al. 2020
Fhb7	Fusarium head blight resistance	Glutathione S-transferase	Mapping	mutagenesis (EMS), virus-induced gene silencing, gene complementation	*Thinopyrum elongatum*	2020	Wang et al. 2020b
Sr26	Stem rust resistance	NLR	MutRenSeq	mutagenesis (EMS), gene complementation	*Thinopyrum ponticum*	2020	Zhang et al. 2020
Sr61	Stem rust resistance	NLR	MutRenSeq	mutagenesis (EMS), gene complementation	*Thinopyrum ponticum*	2020	Zhang et al. 2020
Lr14a	Leaf rust resistance	Ankyrin transmembrane domain protein	MutChromSeq	mutagenesis (EMS), virus-induced gene silencing	*T. aestivum*	2021	Kolodziej et al. 2020
Snn3-D1	Septoria nodorum blotch	Protein kinase major sperm protein	Mapping	mutagenesis (EMS)	*Ae. tauschii*	2021	Zhang et al. 2021
Stb16q	Septoria tritici blotch resistance	Cysteine-rich receptor-like kinase (CRK)	Mapping	Ems (1 mutant), gene complementation (1 transformant)	*Ae. tauschii*	2021	Saintenac et al. 2021
Pm4a,b	Powdery mildew resistance	MCTP-kinase	MutChromSeq	mutagenesis (EMS), gene complementation, virus-induced gene silencing	*T. aestivum*	2021	Sánchez-Martín et al. 2021
*Lr13/Ne2/Yr27******	Leaf rust resistance	NLR	MutRenSeq/Mapping	mutagenesis (EMS), virus-induced gene silencing, gene complementation gene complementation (Mutageneis, VIGs)	*T. aestivum*	2021/2022	Hewitt et al. 2021; Yan et al. 2021; Athiyannan et al. 2022

Table 3.1. Cloned resistance and susceptibility genes effective in wheat (continued).

Gene	Gene function	Class	Cloning method	Validation method	Origin	Year	Reference
Sr27	Stem rust resistance	NLR	MutRenSeq	mutagenesis (EMS), transient expression,	*Triticale*	2021	Upadhyaya et al. 2021
SrTA1662	Stem rust resistance	NLR	K-mer GWAS	gene complementation	*Ae. tauschii*	2022	Gaurav et al. 2022
Sr62	Stem rust resistance	tandem kinase	Mapping	mutagenesis (EMS), gene complementation	*Ae. sharonensis*	2022	Yu et al. 2022
Lr42	Leaf rust resistance	NLR	BSR-Seq	Mutagenesis (EMS), gene complementation, viris-induced gene silencing	*Ae. tauschii*	2022	Lin et al. 2022

* *Yr10* provides race specific resistance to yellow rust. A later analysis determine that *Yr10* does not provide race-specific resistance in the manner expected, and therefore may not be *Yr10*. Instead, the authors refer to the cloned *Yr10* as *Yr10 candidate gene* or *Yr10cg* (Yuan et al 2018)

** Two later studies identified *Fhb1* as a histidine-rich calcium-binding protein (Li et al. 2019; Su et al. 2019).

****Pm21* was initially reported as a Sr/Thr kinase (Cao et al. 2011)

*****Yr5a* and *Yr5b* are alleles

******Yr27* is a distinct allele of *Lr13/Ne2*

3.3. Advances in wheat sequencing

High quality genomic sequences and assemblies act as the basis for gene cloning efforts in wheat. Several hexaploid, tetraploid, and diploid *Triticum* full genome assemblies have been released in the last five years (Table 3.2). The International Wheat Genome Sequencing Consortium (IWGSC) was formed in 2005 with the goal of producing a high quality reference genome assembly of hexaploid bread wheat.

The bread wheat variety Chinese Spring was selected for sequencing due to the extensive genetic and molecular resources developed using Chinese Spring (Gill et al. 2004). Sears developed aneuploid stocks that could be used to physically map genes and markers to specific chromosomes (Sears 1954; Sears 1966; Sears and Sears 1978). Segmental deletion lines (Endo and Gill 1996) further specified physical regions within chromosomal arms and were used to map 16,000 expressed sequence tag (EST) loci (Qi et al. 2004).

Hexaploid wheat was estimated to be 16 Gb and highly repetitive. A reduced-representation sequencing approach was used to reduce the genome complexity and size (IWGSC 2014). Individual telosomic chromosomes developed by Sears and Sears 1978 were separated by flow cytometry and BAC libraries were constructed for each chromosome arm. The bin-mapped ESTs were used to assess the purity of the sorted fractions (Qi et al. 2004). Short read paired-end sequences of each BAC library were assembled resulting in a 10.2 Gb draft assembly. The assembly, called the Chinese Spring Survey Sequences (CSS) represented 61% of the genome sequence (IWGSC 2014).

Table 3.2. *Triticum* and *Aegilops* assemblies.

Species	Genotype	year	genomes	type	reference	doi or link
Ae. tauschii	AL8/78	2013	D	scaffold	Jai et al. 2013	10.1038/nature12028
T. urartu	G1812/PI428198	2013	A	scaffold	Ling et al. 2013	10.1038/nature11997
T. turgidum ssp. *durum*	Cappelli	2014	AB	scaffold	IWGSC 2014	10.1126/science.1251788
T. aestivum	Chinese Spring	2014	B	pseudomolecule	Choulet et al. 2014	10.1126/science.1249721
T. aestivum	Chinese Spring	2014	ABD	scaffold	IWGSC 2014	10.1126/science.1251788
Ae. speltoides	ERX391140	2014	SS	scaffold	IWGSC 2014	10.1126/science.1251788
T. turgidum ssp. *durum*	Strongfield	2014	AB	scaffold	IWGSC 2014	10.1126/science.1251788
Synthetic hexaploid	W7984	2015	ABD	scaffold	Chapman et al. 2015	10.1186/s13059-015-0582-8
T. aestivum	Chinese Spring doubled haploid (Dv418)	2017	ABD	scaffold	Zimin et al. 2017a	10.1093/gigascience/gix097
Ae. tauschii	AL8/78	2017	D	pseudomolecule	Luo et al. 2017	10.1038/nature24486
Ae. tauschii	AL8/78	2017	D	pseudomolecule	Zhao et al. 2017	10.1038/s41477-017-0067-8
Ae. tauschii	AL8.78	2017	D	Scaffold	Zimin et al. 2017b	10.1101/gr.213405.116.
T. aestivum	Chinese Spring	2017	ABD	scaffold	Clavijo et al. 2017	10.1101/gr.217117.116
T. turgidum ssp. *durum*	Kronos	2017	AB	scaffold	N/A	http://opendata.earlham.ac.uk/Triticum_turgidum/
T. aestivum ssp. *dicoccoides*	Zavitan	2017	AB	pseudomolecule	Avni et al. 2017	10.1126/science.aan0032
T. aestivum	Chinese Spring	2018	ABD	pseudomolecule	IWGSC et al. 2018	10.1126/science.aar7191
T. urartu	G1812/PI428198	2018	A	pseudomolecule	Ling et al. 2018	10.1038/s41586-018-0108-0
T. turgidum ssp. *durum*	Svevo	2019	AB	pseudomolecule	Maccaferri et al. 2019	10.1038/s41588-019-0381-3
T. aestivum ssp. *dicoccoides*	Zavitan	2019	AB	pseudomolecule	Zhu et al. 2019	10.1534/g3.118.200902
T. aestivum	2670/PI 190962	2020	ABD	pseudomolecule	Walkowiak et al. 2020	10.1038/s41586-020-2961-x
T. aestivum	ArinaLrFor	2020	ABD	pseudomolecule	Walkowiak et al. 2020	10.1038/s41586-020-2961-x
T. aestivum	Cadenza	2020	ABD	scaffold	Walkowiak et al. 2020	10.1038/s41586-020-2961-x
T. aestivum	CDC Landmark	2020	ABD	pseudomolecule	Walkowiak et al. 2020	10.1038/s41586-020-2961-x
T. aestivum	CDC Stanley	2020	ABD	pseudomolecule	Walkowiak et al. 2020	10.1038/s41586-020-2961-x
T. aestivum	Claire	2020	ABD	scaffold	Walkowiak et al. 2020	10.1038/s41586-020-2961-x
T. aestivum	Jagger	2020	ABD	pseudomolecule	Walkowiak et al. 2020	10.1038/s41586-020-2961-x
T. aestivum	Julius	2020	ABD	pseudomolecule	Walkowiak et al. 2020	10.1038/s41586-020-2961-x
T. aestivum	LongReach Lancer	2020	ABD	pseudomolecule	Walkowiak et al. 2020	10.1038/s41586-020-2961-x
T. aestivum	Mace	2020	ABD	pseudomolecule	Walkowiak et al. 2020	10.1038/s41586-020-2961-x
T. aestivum	Norin 61	2020	ABD	pseudomolecule	Walkowiak et al. 2020	10.1038/s41586-020-2961-x
T. aestivum	Paragon	2020	ABD	scaffold	Walkowiak et al. 2020	10.1038/s41586-020-2961-x
T. aestivum	Robigus	2020	ABD	scaffold	Walkowiak et al. 2020	10.1038/s41586-020-2961-x
T. aestivum	SY Mattis	2020	ABD	pseudomolecule	Walkowiak et al. 2020	10.1038/s41586-020-2961-x

Table 3.2. *Triticum* and *Aegilops* assemblies (continued).

Species	Genotype	year	genomes	type	reference	doi or link
T. aestivum	Weebill 1	2020	ABD	scaffold	Walkowiak et al. 2020	10.1038/s41586-020-2961-x
T. aestivum ssp *tibetanum* Shao	Zang1817	2020	ABD	pseudomolecule	Guo et al. 2021	10.1038/s41467-020-18738-5
Ae. Tauschii	AL8/78	2021	D	pseudomolecule	Wang et al. 2021	10.1093/g3journal/jkab325
Ae. tauschii (AY17)	AY17	2021	D	pseudomolecule	Zhou et al. 2021	10.1038/s41477-021-00934-w
Ae. tauschii (AY61)	AY61	2021	D	pseudomolecule	Zhou et al. 2021	10.1038/s41477-021-00934-w
T. aestivum	Chinese Spring (RefSeq v2.1)	2021	ABD	pseudomolecule	Zhu et al. 2021	10.1111/tpj.15289
T. aestivum	Fielder	2021	ABD	pseudomolecule	Sato et al. 2021	10.1093/dnares/dsab008
T. aestivum	Renan	2021	ABD	pseudomolecule	Aury et al. 2022	10.1093/gigascience/giac034
Ae. tauschii (T093)	T093	2021	D	pseudomolecule	Zhou et al. 2021	10.1038/s41477-021-00934-w
Ae. tauschii (XJ02)	XJ02	2021	D	pseudomolecule	Zhou et al. 2021	10.1038/s41477-021-00934-w
Ae. Longissima	AEG-6782-2	2022	S^{l}	pseudomolecule	Avni et al. 2022	10.1111/tpj.15664
Ae. speltoides	AEG-9674-1	2022	S	pseudomolecule	Avni et al. 2022	10.1111/tpj.15664
Ae. Sharonensis	AS_1644	2022	S^{sh}	pseudomolecule	Yu et al. 2022	10.1038/s41467-022-29132-8
T. aestivum	Kariega	2022	ABD	pseudomolecule	Athiyannan et al. 2022	10.1038/s41588-022-01022-1
T. aestivum	Sonmez	2022	ABD	pseudomolecule	Akpinar et al. 2022	10.21203/rs.3.rs-1095548/v1
T. aestivum	Attraktion	2022	ABD	pseudomolecule	Kale et al. 2022	10.1111/pbi.13843
Ae. Bicornis	TB01	2022	S^{b}	pseudomolecule	Li et al. 2022	10.1016/j.molp.2021.12.019
Ae. Searsii	TE01	2022	S^{s}	pseudomolecule	Li et al. 2022	10.1016/j.molp.2021.12.019
Ae. sharonensis	TH02	2022	S^{sh}	pseudomolecule	Li et al. 2022	10.1016/j.molp.2021.12.019
Ae. Longissima	TL05	2022	S^{l}	pseudomolecule	Li et al. 2022	10.1016/j.molp.2021.12.019
Ae. speltoides	TS01	2022	S	pseudomolecule	Li et al. 2022	10.1016/j.molp.2021.12.019

A pseudomolecule level assembly of chromosome 3B was produced separately (Choulet et al. 2014). A minimum tiling path of 8452 BACs was sequenced with Roche/454 paired end reads and after scaffold assembly, Illumina reads from flow sorted chromosome 3B were used to fill gaps. A detailed SNP based genetic map from the CS × Renan population was used to orient and order scaffolds. Ultimately, the pseudomolecule level assembly represented 93% of chromosome 3B. 124, 201 high confidence gene loci were annotated in the CSS and chromosome 3B assembly (IWGSC 2014).

In 2014 and 2015, multiple scaffold level assemblies of *Triticum* and *Aegilops* species were published. Whole genome shotgun (WGS) assemblies of the *Triticum turgidum* sp. *durum* cultivars 'Cappelli' and 'Strongfield' were released in 2014 alongside an assembly of *Aegilops speltoides* accession ERX391140 (SS) (IWGSC 2014). These assemblies consisted of numerous small contigs with unknown order, orientation, and space between contigs. WGS assemblies often result in piling of repetitive elements, but offer a draft assembly of low copy DNA, and such can be used to identify alleles, design gene specific markers, or compare genes and gene families among assemblies. In 2015, Chapman et al. integrated WGS and genetic mapping to assemble and order contigs of the synthetic hexaploid W7984. Despite the WGS method and lack of chromosome isolation via flow sorting, the assembly was 9.1 Gb, just 1.1 Gb smaller than the CSS assembly.

With the growth of sequencing and assembly methods, more wheat scaffold and pseudomolecule level assemblies became available (Figure 3.1, Figure 3.1). As of June 2022, 43 unique accessions have scaffold and/or pseudomolecule level assemblies (Table 3.2). In 2020, there was a significant increase in the number of hexaploid accessions with pseudomolecule or scaffold level assemblies. Through a large international collaborative effort, Walkowiak et al.

(2020) published the 10+ Wheat Genomes paper, including pseudomolecule assemblies of nine bread wheats and one *T. aestivum* ssp. *spelta* accession and the scaffold level assemblies of five additional bread wheats. Prior to this, Chinese Spring and the synthetic hexaploid W7984 were the only hexaploids with either a pseudomolecule or scaffold level assembly. Principal component analysis of exome sequence capture alleles in ~1,200 hexaploid accessions revealed that Chinese Spring was genetically distant from other hexaploids (Walkowiak et al. 2020). The accessions included in the 10+ wheat genomes paper were selected to more accurately represent the full diversity of hexaploid wheat, allowing analysis of intergenome variability. The genome of the Tibetan semi-wild wheat (*T. aestivum* ssp. *tibetanum* Shao) accession Zang1817 was also published the same year (Guo et al. 2020)

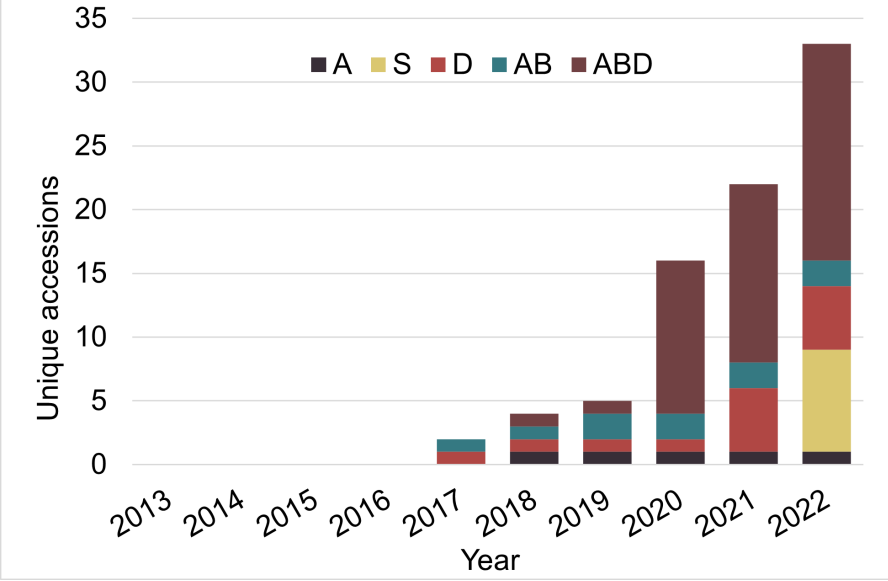

Figure 3.1. Cumulative accessions with pseudomolecule level assemblies.
Color corresponds to the subgenome of the accession.

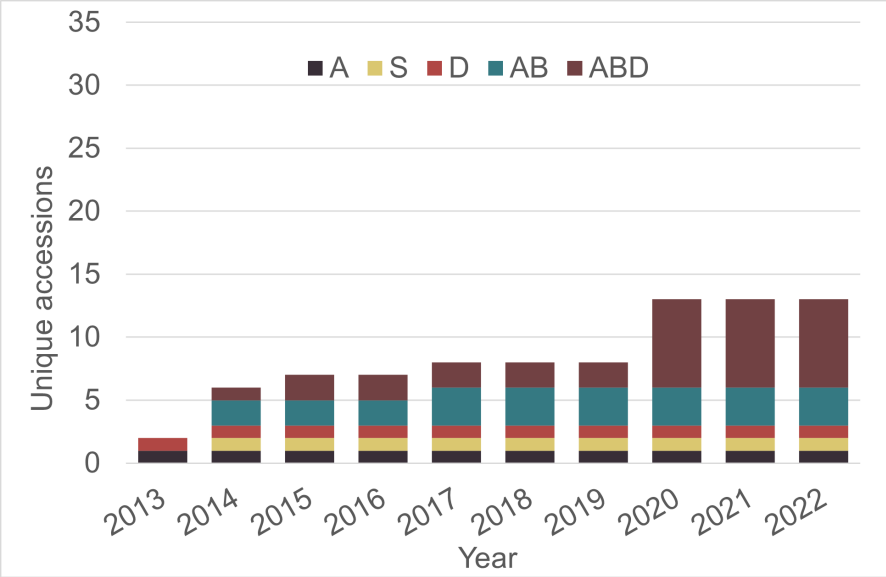

Figure 3.2. Cumulative accessions with scaffold level assemblies.
Color corresponds to the subgenome of the accession.

Most of the *Triticum* and *Aegilops* assemblies and genome browsers are hosted on websites. Although, not all are hosted on a single website and different assembly and annotation versions are available on different websites, so care should be taken when comparing assemblies or annotations from different sources. Many of these websites host additional resources that may be useful in the gene cloning and characterization process, such as molecular markers, exome capture data, varietal SNPs, and TILLING mutants.

The following are useful websites for accessing the genome assemblies:

- GrainGenes (Yao et al. 2022) - https://wheat.pw.usda.gov
- Ensembl Plants-http://plants.ensembl.org/Triticum_aestivum
- URGI-https://urgi.versailles.inrae.fr/blast/
- Grassroots Infrastructure-https://grassroots.tools/service/blast-blastn
- CerealsDB -https://www.cerealsdb.uk.net/cerealgenomics/CerealsDB/blast_WGS.php

3.4. Map-based cloning

Map-based cloning was used to clone the first wheat R gene, *Lr10*, in 2003 (Feuillet et al. 2003). Since then, map-based cloning has been the most frequently used method to clone R/S genes in wheat (around 75%, Table 3.1). Map-based cloning uses the genetic relationship between a gene and molecular markers to place a gene on a genetic map. Originally, an iterative approach termed chromosome walking was used to narrow down the candidate gene region. The two closest molecular markers were used to screen libraries of genomic clones (yeast artificial chromosomes or bacterial artificial clones, YACs or BACs) to identify overlapping clones, "walking" closer to the gene of interest until you identified a clone containing the gene. Sequencing of the clone would reveal the nucleotide sequence of the R/S gene. While we still use the term "cloning", the screening of genetic clones is no longer necessary to clone a gene.

Map-based cloning has largely been replaced with high density mapping, which still takes advantage of the genetic recombination between molecular markers and the R/S gene in a population segregating for resistance or susceptibility. High-throughput genotyping technologies like the Illumina or Affimetrix DNA microarrays, custom Kompetative allele specific PCR (KASP) arrays, or genotyping by sequencing offer high-density genotyping at affordable costs.

The size of the candidate gene region, the genetic region between the closest markers flanking the R/S gene, is dependent on both the marker density and the recombination rate. In a population of fixed size, like a recombinant inbred or doubled haploid population, there is a finite number of recombination events. Sometimes there are not enough recombination events in a population to reduce the candidate gene region to a reasonable size. If the marker density is too low, recombination events can go undetected, resulting in a larger candidate gene region. Even in

cases where marker density and recombination rate are high, a candidate gene region may be gene rich, making it hard to determine which gene is causal.

Additional molecular markers in a region cosegregating with the gene will not increase resolution. Map-based cloning also requires access to the DNA sequence between the flanking markers. This need is often met by the multiple sequenced wheat genomes. It's important to remember that even if the sequenced wheat genotypes do not carry a functional allele of the R gene, they may carry a nonfunctional allele. As such, it may be useful to identify candidate genes even in genotypes that do not display the desired resistant or susceptible phenotype.

In the case that the sequenced wheat genotypes do not carry an allele of the R/S gene, or when the R/S gene is in an area of low recombination, like an introgressed region from a wild relative or near a centromere, alternate gene cloning methods may be more appropriate. Map-based cloning can be slow, dependent on the generation of the mapping population, and require screening of 1000's of gametes.

3.5. Reduced representation sequencing methods

Reduced representation sequencing is a key step in rapid cloning methods in wheat. Reduced representation sequencing reduces genome complexity, and therefore the cost and time of sequencing and analysis. The three main methods of reduced representation sequencing are transcriptome or RNA sequencing, exome capture, and chromosome flow sorting (Figure 3.3). These methods allow preferential sequencing of more relevant spaces, either genic regions or promoters, or the specific chromosome containing an R/S gene. In some cases, reduced representation sequencing methods are incorporated into rapid cloning methods.

In target enrichment, the baits or capture probes, hybridize to the targets and then are bound by streptavidin-coated magnetic beads. The magnetic beads are "captured" by a magnet,

unbound DNA is washed away, and the remaining target enriched library is amplified and sequenced. Capture probes assays can target genes, promoters, and even specific types of genes like NLRs. Exome capture assays targeting the genic region of wheat have been designed from the sequenced wheat genomes, each using an increasing design space size as additional wheat genome sequences became available.

In 2015, Jordan et al. designed an exome capture probe assay called the "wheat exome capture" (WEC) using a design space of 110 Mb from a 3.8 Gb low-copy number genome assembly of Chinese Spring (Brenchley et al. 2012). To identify genic regions, they aligned reported wheat cDNA and EST sequences and conducted a BLASTN search using Brachypodium exon sequences. Krasileva et al. (2017) designed *T. turgidum* and *T. aestivum* exome capture probes to target gene annotations from the CSS assembly, transcripts from transcriptome studies, and unannotated homologs of barley in wheat. The exome capture probes targeted 85 Mb. Following the publication of high-quality reference wheat genome assemblies and annotations in 2017 and 2018, Gardiner et al. (2019) discovered that the existing exome capture assay only targeted 32.6% of the high confidence gene set of wheat. Using the high confidence annotated genes in the Chinese Spring TGACv1 and RefSeq.v1 genome assemblies, *Ae. Tauschii* assembly Aet v4.0, and the *T. turgidum* ssp. *dicoccoides* WEWSeq v1.0 assembly, they designed exome capture probe sets targeting genes and putative promoters. Probes of ~75 bp were designed approximately every 120 bp across 786 Mb of design space, of which 509 Mb was gene space, and 277 Mb was putative promoter sequences. The exome capture and promoter capture probe sets designed by Jordan et al. (2012), Krasileva et al. (2017), and Gardiner et al. (2019) were available through NimbleGen (Roche), but have since been discontinued. The most recent exome capture assay, the myBaits® Expert Wheat Exome capture, designed using the

Chinese Spring RefSeq v1.0 assembly, captures over 250 Mb of coding sequence (Daicel Arbor Biosciences).

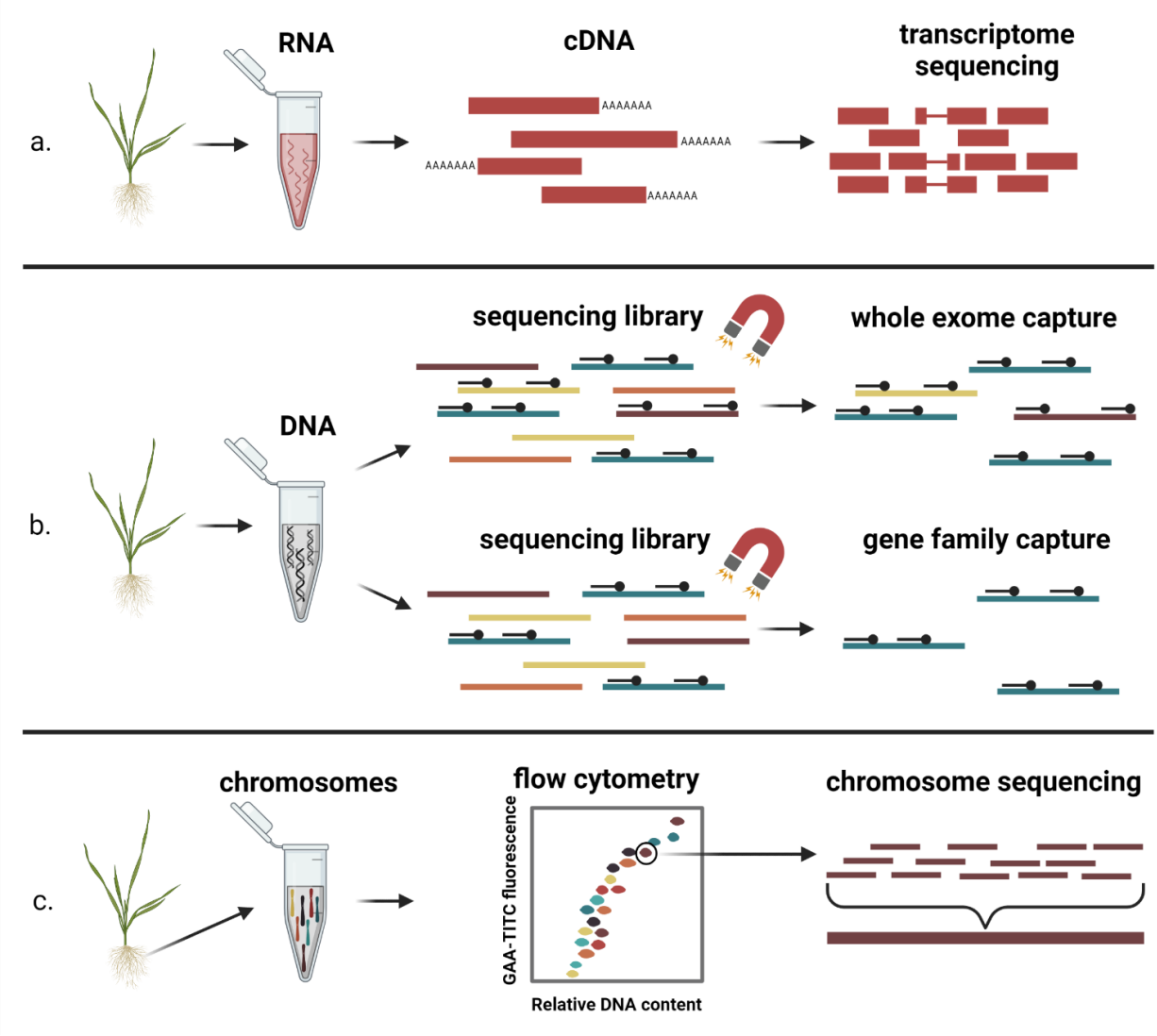

Figure 3.3. Reduced sequencing methods.
A. Transcriptome sequencing. RNA is isolated from tissue and reverse transcribed into cDNA, which is sequenced and mapped to a reference assembly. B. Exome sequencing. DNA is isolated from tissue and a DNA sequencing library is prepared. Short biotintylated baits complementary to the targets hybridize to the DNA, bind to magnetic beads, and are captured by a magnet, yielding a target enriched sequencing library. C. Chromosome flow sorting. Liquid suspensions of mitotic chromosomes collected from dividing root cells are fluorescently labeled and separated using flow cytometry based on the fluorochrome signal and relative DNA content.

Further reducing genome complexity, capture probes assays can be developed targeting a particular gene class, such as NLR genes. NLR genes are the most common class of cloned R/S gene in wheat (Table 3.1) and the wheat pangenome is estimated to contain 6-8 thousand NLR genes (Walkowiak et al. 2020). Exome capture of NLR genes and subsequent sequencing is termed Resistance gene enrichment Sequencing (RenSeq). The first R genes cloned using RenSeq were *Rpi-ber2* and *Rpi-rzc1*, which confer resistance against *Phytothora infestans* infections in potato (Jupe et al. 2013). Bulked segregant analysis (BSA) was applied to two segregating biparental populations. RenSeq was applied to the resistant and susceptible bulks allowing the identification of SNPs in NLRs linked to resistance. RenSeq is a key method in multiple rapid cloning strategies. However. RenSeq-based cloning methods only capture one class of genes and are biased towards those that are already annotated because probes were designed to target annotated NLR genes.

Transcriptome sequencing, or RNA-Seq, is a less biased reduced representation sequencing method as it is not limited to previously annotated genes and/or a gene family. RNA-Seq combined with BSA, BSR-Seq, was applied to two *Ae. tauschii* populations to map *Lr42*, yielding just three candidate genes (Lin et al. 2022). RNA-Seq is limited to detected genes that are expressed at the time of RNA collected in sufficient levels and assembly of transcripts can be challenged by the co-expression of homoeologs. Lin et al. (2022) avoided the latter challenge by conducting RNA-Seq on a diploid.

Another alternative to exome capture is chromosome flow sorting. Chromosome flow sorting separates an individual chromosome via flow cytometry based on the chromosome size and base-pair composition (Dolezel et al. 2011). Following separation, the individual chromosome can be sequenced, as was done to complete the CSS assembly (IWGSC 2014).

Chromosome flow sorting is a highly specialized skill requiring unique equipment available in few labs.

3.6. Rapid cloning methods

RenSeq in coupled with mutational genomics in the MutRenSeq rapid cloning strategy (Steurnagel et al. 2016). In the MutRenSeq method, a mutant population is screened and then RenSeq is conducted on confirmed mutants. Mutations in NLRs are associated with the mutant phenotype, identifying candidate gene(s).

Sr22 and *Sr45* were the first wheat R/S genes cloned in wheat using MutRenSeq (Steurnagel et al. 2016). *Sr22*, which provides stem rust resistance, resided in introgressions from *T. boeoticum* and *T. monococcum,* but had poor agronomic performance due to linkage drag (Olson et al. 2010). Additionally, mapping efforts were hampered by reduced recombination in the *Sr22* region (Steurnagel et al. 2016). To clone stem rust resistance genes *Sr22* and *Sr45*, Steurnagel et al. (2016) developed EMS-mutant populations for each R gene and applied RenSeq to six mutants/population and the wild type. In each mutant population, comparative sequence analysis of the NLRs in the mutants and wild type revealed one gene with mutations in all six mutants. MutRenSeq effectively eliminated the need for high resolution mapping, which is particularly difficult when the R/S gene of interest resides in a low recombination region. MutRenSeq has since been used to clone stem rust resistance genes *Sr26*, *Sr27*, and *Sr61*, stripe rust resistance genes *Yr5* and *Yr7*, leaf rust resistance gene *Lr13/Ne2*, and powdery mildew resistance gene *Pm21* (Xing et al. 2018; Marchal et al. 2018; Zhang et al. 2020, Hewitt et al. 2021; Yan et al. 2021, Upadhyaya et al. 2021).

MutRenSeq is a powerful tool to quickly clone NLR resistance genes and is particularly advantageous when trying to clone a gene in an area of low recombination. However, it is limited

to genotypes that can be easily mutagenized and R genes in the NLR family. In general, higher ploidy levels tend to tolerate higher EMS levels. The lower tolerance of mutagen dose results in lower mutation density, increasing the number of mutants that must be generated and phenotypically evaluated to identify independent lines with mutant alleles. In some cases, mutagenesis of diploids can result in sterile plants, and thus the MutRenSeq method is not usable.

To address the limitations of MutRenSeq, Association Genetics RenSeq (AgRenSeq) was developed (Arora et al. 2019). AgRenSeq combines association genetics and RenSeq. A diversity panel is phenotyped for disease reactions and RenSeq is conducted on the panel. K-mers within the sequenced NLR are identified and mapped to a reference. Then, associations between k-mers and phenotypes are calculated and plotted, similarly to a Manhattan plot As k-mers are identified in genes, the contigs significant k-mers map to represent candidate genes. To test AgRenSeq, a panel of 174 *Ae. tauschii* ssp. *strangulata* was genotyped and evaluated for stripe rust resistance. Two previously cloned genes, *Sr33* and *Sr45*, served as positive controls (Periyannan et al. 2013; Steuernagel et al. 2016). The panel was phenotyped with six races of wheat stem rust pathogen *Puccinia graminis* f. sp. *tritici* (PGT) and k-mers associated with resistance were identified. K-mers associated with resistance to PGT RKQQC, which is avirulent to *Sr33*, resided on the contig containing the previously cloned *Sr33*. *Sr45*, which was previously identified using MutRenSeq (Steuernagel et al. 2016), was also identified via AgRenSeq. Candidate genes for *Sr46* and *SrTA1662* were also identified in this study and the *Sr46* candidate was functionally validated by mutagenesis and gene complementation.

Arora et al. (2019) demonstrated the ability of AgRenSeq to directly identify candidate genes. AgRenSeq requires shot gun sequencing of the entire diversity panel, which can initially

be expensive and laborious. However, once this has been completed, the same panel can be used to clone multiple R/S genes. As with other RenSeq based cloning methods, AgRenSeq is limited to cloning NLR genes.

K-mer based association mapping, or Kmer GWAS, is an extension of AgRenSeq. Kmer GWAS does not include RenSeq, so there is no enriching for NLRs. Instead, k-mers are identified from short Illumina reads and projected onto a reference assembly. The analysis is similar to AgRenSeq, but because k-mers can be anywhere, not just within candidate genes, one must analyze the genes near the k-mers that were significantly associated with the phenotype. Guarav et al. (2022) conducted short-read sequencing on 242 *Ae. tauschii* accessions and used Kmer-GWAS to identify a 50-kb linkage disequilibrium block containing two candidate genes for stem rust resistance gene *SrTA1662*. Subsequent functional validation via gene complementation confirmed that *SrTA1662* is an NLR. The panel sequenced in Guarav et al. (2022) is publicly available and can be used to rapidly clone R/S genes from *Ae. tauschii* accessions. Similar to AgRenSeq, Kmer-GWAS is limited by initial sequencing of a diversity panel.

In 2016, Sanchez-Martin et al. published the rapid cloning method MutChromSeq, cloning the powdering mildew resistance gene *Pm2a*. *Pm2a* had previously mapped to chromosome 6A (Huang and Roder 2004). Using the MutChromSeq method, which applied the reduced representation sequencing method chromosome flow sorting, chromosome 6A was sorted from six confirmed EMS-derived powdery mildew susceptible mutants and wild type genotypes. The separated chromosomes were sequenced and assembled, followed by sequence analysis to identify mutation overlap. Contigs with mutations in all or most of the mutant lines are most likely to contain the candidate gene. Two contigs were identified, although one was

later discarded due to an abnormal SNV frequency, leaving just one contig with a NLR gene. MutChromSeq is similar to MutRenSeq, but it is not limited to NLR genes. MutChromSeq was also used to clone leaf rust resistance gene *Lr14a* with ankyrin transmembrane protein domains and *Pm4b*, which contains kinase, C2, and transmembrane domains (Kolodziej et al. 2021, Sanchez-Martin et al. 2021).

3.7. Literature cited

Akpinar BA, Leroy P, Watson-Haigh NS, et al (2022) Reference genome sequencing of the elite bread wheat cultivar, "Sonmez." In Review. https://doi.org/10.21203/rs.3.rs-1095548/v1

Arora S, Steuernagel B, Gaurav K, et al (2019) Resistance gene cloning from a wild crop relative by sequence capture and association genetics. Nat Biotechnol 37:139–143. https://doi.org/10.1038/s41587-018-0007-9

Athiyannan N, Abrouk M, Boshoff WHP, et al (2022) Long-read genome sequencing of bread wheat facilitates disease resistance gene cloning. Nat Genet 54:227–231. https://doi.org/10.1038/s41588-022-01022-1

Aury J-M, Engelen S, Istace B, et al (2022) Long-read and chromosome-scale assembly of the hexaploid wheat genome achieves high resolution for research and breeding. GigaScience 11:giac034. https://doi.org/10.1093/gigascience/giac034

Avni R, Lux T, Minz-Dub A, et al (2022) Genome sequences of three *Aegilops* species of the section *Sitopsis* reveal phylogenetic relationships and provide resources for wheat improvement. Plant J 110:179–192. https://doi.org/10.1111/tpj.15664

Avni R, Nave M, Barad O, et al (2017) Wild emmer genome architecture and diversity elucidate wheat evolution and domestication. Science 357:93–97. https://doi.org/10.1126/science.aan0032

Brenchley R, Spannagl M, Pfeifer M, et al (2012) Analysis of the bread wheat genome using whole-genome shotgun sequencing. Nature 491:705–710. https://doi.org/10.1038/nature11650

Cao A, Xing L, Wang X, et al (2011) Serine/threonine kinase gene *Stpk-V*, a key member of powdery mildew resistance gene *Pm21*, confers powdery mildew resistance in wheat. Proc Natl Acad Sci USA 108:7727–7732. https://doi.org/10.1073/pnas.1016981108

Chapman JA, Mascher M, Buluç A, et al (2015) A whole-genome shotgun approach for assembling and anchoring the hexaploid bread wheat genome. Genome Biol 16:26. https://doi.org/10.1186/s13059-015-0582-8

Chen S, Rouse MN, Zhang W, et al (2020) Wheat gene *Sr60* encodes a protein with two putative kinase domains that confers resistance to stem rust. New Phytol 225:948–959. https://doi.org/10.1111/nph.16169

Chen S, Zhang W, Bolus S, et al (2018) Identification and characterization of wheat stem rust resistance gene *Sr21* effective against the Ug99 race group at high temperature. PLoS Genet 14:e1007287. https://doi.org/10.1371/journal.pgen.1007287

Choulet F, Alberti A, Theil S, et al (2014) Structural and functional partitioning of bread wheat chromosome 3B. Science 345:1249721. https://doi.org/10.1126/science.1249721

Clavijo BJ, Venturini L, Schudoma C, et al (2017) An improved assembly and annotation of the allohexaploid wheat genome identifies complete families of agronomic genes and provides genomic evidence for chromosomal translocations. Genome Res 27:885–896. https://doi.org/10.1101/gr.217117.116

Cloutier S, McCallum BD, Loutre C, et al (2007) Leaf rust resistance gene *Lr1*, isolated from bread wheat (*Triticum aestivum L.*) is a member of the large *psr567* gene family. Plant Mol Biol 65:93–106. https://doi.org/10.1007/s11103-007-9201-8

Doležel J, Kubaláková M, íhalíková J, et al (2011) Chromosome analysis and sorting using flow cytometry. In: Birchler JA (ed) Plant Chromosome Engineering. Humana Press, Totowa, NJ, pp 221–238

Faris JD (2014) Wheat domestication: Key to agricultural revolutions past and future. In: Tuberosa R, Graner A, Frison E (eds) Genomics of plant genetic resources. Springer Netherlands, Dordrecht, pp 439–464

Faris JD, Zhang Z, Lu H, et al (2010) A unique wheat disease resistance-like gene governs effector-triggered susceptibility to necrotrophic pathogens. Proc Natl Acad Sci USA 107:13544–13549. https://doi.org/10.1073/pnas.1004090107

Feuillet C, Travella S, Stein N, et al (2003) Map-based isolation of the leaf rust disease resistance gene *Lr10* from the hexaploid wheat (*Triticum aestivum* L.) genome. Proc Natl Acad Sci USA 100:15253–15258. https://doi.org/10.1073/pnas.2435133100

Fu D, Uauy C, Distelfeld A, et al (2009) A kinase-START gene confers temperature-dependent resistance to wheat stripe rust. Science 323:1357–1360. https://doi.org/10.1126/science.1166289

Gardiner L-J, Brabbs T, Akhunov A, et al (2019) Integrating genomic resources to present full gene and putative promoter capture probe sets for bread wheat. GigaScience 8:. https://doi.org/10.1093/gigascience/giz018

Gaurav K, Arora S, Silva P, et al (2022) Population genomic analysis of *Aegilops tauschii* identifies targets for bread wheat improvement. Nat Biotechnol 40:422–431. https://doi.org/10.1038/s41587-021-01058-4

Gill BS, Appels R, Botha-Oberholster A-M, et al (2004) A workshop report on wheat genome sequencing. Genetics 168:1087–1096. https://doi.org/10.1534/genetics.104.034769

Guo W, Xin M, Wang Z, et al (2020) Origin and adaptation to high altitude of Tibetan semi-wild wheat. Nat Commun 11:5085. https://doi.org/10.1038/s41467-020-18738-5

Hafeez AN, Arora S, Ghosh S, et al (2021) Creation and judicious application of a wheat resistance gene atlas. Molecular Plant 14:1053–1070. https://doi.org/10.1016/j.molp.2021.05.014

He H, Zhu S, Ji Y, et al (2017) Map-based cloning of the gene *Pm21* that confers broad spectrum resistance to wheat powdery mildew. https://doi.org/10.1101/177857

Hewitt T, Zhang J, Huang L, et al (2021) Wheat leaf rust resistance gene *Lr13* is a specific *Ne2* allele for hybrid necrosis. Molecular Plant 14:1025–1028. https://doi.org/10.1016/j.molp.2021.05.010

Huang L, Brooks SA, Li W, et al (2003) Map-based cloning of leaf rust resistance gene *Lr21* from the large and polyploid genome of bread wheat. Genetics 164:655–664. https://doi.org/10.1093/genetics/164.2.655

Huang X-Q, Röder MS (2004) Molecular mapping of powdery mildew resistance genes in wheat: A review. Euphytica 137:203–223. https://doi.org/10.1023/B:EUPH.0000041576.74566.d7

Hurni S, Brunner S, Buchmann G, et al (2013) Rye *Pm8* and wheat *Pm3* are orthologous genes and show evolutionary conservation of resistance function against powdery mildew. Plant J 76:957–969. https://doi.org/10.1111/tpj.12345

Jia J, Zhao S, Kong X, et al (2013) *Aegilops tauschii* draft genome sequence reveals a gene repertoire for wheat adaptation. Nature 496:91–95. https://doi.org/10.1038/nature12028

Jordan KW, Wang S, Lun Y, et al (2015) A haplotype map of allohexaploid wheat reveals distinct patterns of selection on homoeologous genomes. Genome Biol 16:48. https://doi.org/10.1186/s13059-015-0606-4

Jupe F, Witek K, Verweij W, et al (2013) Resistance gene enrichment sequencing (RenSeq) enables reannotation of the NB-LRR gene family from sequenced plant genomes and rapid mapping of resistance loci in segregating populations. Plant J 76:530–544. https://doi.org/10.1111/tpj.12307

Kale SM, Schulthess AW, Padmarasu S, et al (2022) A catalogue of resistance gene homologs and a chromosome-scale reference sequence support resistance gene mapping in winter wheat. Plant Biotechnol J pbi.13843. https://doi.org/10.1111/pbi.13843

Klymiuk V, Yaniv E, Huang L, et al (2018) Cloning of the wheat *Yr15* resistance gene sheds light on the plant tandem kinase-pseudokinase family. Nat Commun 9:3735. https://doi.org/10.1038/s41467-018-06138-9

Kolodziej MC, Singla J, Sánchez-Martín J, et al (2021) A membrane-bound ankyrin repeat protein confers race-specific leaf rust disease resistance in wheat. Nat Commun 12:956. https://doi.org/10.1038/s41467-020-20777-x

Krasileva KV, Vasquez-Gross HA, Howell T, et al (2017) Uncovering hidden variation in polyploid wheat. Proc Natl Acad Sci USA 114:. https://doi.org/10.1073/pnas.1619268114

Krattinger SG, Lagudah ES, Spielmeyer W, et al (2009) A putative ABC transporter confers durable resistance to multiple fungal pathogens in wheat. Science 323:1360–1363. https://doi.org/10.1126/science.1166453

Li G, Zhou J, Jia H, et al (2019) Mutation of a histidine-rich calcium-binding-protein gene in wheat confers resistance to Fusarium head blight. Nat Genet 51:1106–1112. https://doi.org/10.1038/s41588-019-0426-7

Li L-F, Zhang Z-B, Wang Z-H, et al (2022) Genome sequences of five *Sitopsis* species of *Aegilops* and the origin of polyploid wheat B subgenome. Mol Plant 15:488–503. https://doi.org/10.1016/j.molp.2021.12.019

Li M, Dong L, Li B, et al (2020) A CNL protein in wild emmer wheat confers powdery mildew resistance. New Phytologist 228:1027–1037. https://doi.org/10.1111/nph.16761

Lin G, Chen H, Tian B, et al (2022) Cloning of the broadly effective wheat leaf rust resistance gene *Lr42* transferred from *Aegilops tauschii*. Nat Commun 13:3044. https://doi.org/10.1038/s41467-022-30784-9

Ling H-Q, Ma B, Shi X, et al (2018) Genome sequence of the progenitor of wheat A subgenome *Triticum urartu*. Nature 557:424–428. https://doi.org/10.1038/s41586-018-0108-0

Ling H-Q, Zhao S, Liu D, et al (2013) Draft genome of the wheat A-genome progenitor *Triticum urartu*. Nature 496:87–90. https://doi.org/10.1038/nature11997

Liu W, Frick M, Huel R, et al (2014) The stripe rust resistance gene *Yr10* encodes an evolutionary-conserved and unique CC–NBS–LRR Sequence in wheat. Mol Plant 7:1740–1755. https://doi.org/10.1093/mp/ssu112

Lu P, Guo L, Wang Z, et al (2020) A rare gain of function mutation in a wheat tandem kinase confers resistance to powdery mildew. Nat Commun 11:680. https://doi.org/10.1038/s41467-020-14294-0

Luo M, Xie L, Chakraborty S, et al (2021) A five-transgene cassette confers broad-spectrum resistance to a fungal rust pathogen in wheat. Nat Biotechnol 39:561–566. https://doi.org/10.1038/s41587-020-00770-x

Luo M-C, Gu YQ, Puiu D, et al (2017) Genome sequence of the progenitor of the wheat D genome *Aegilops tauschii*. Nature 551:498–502. https://doi.org/10.1038/nature24486

Maccaferri M, Harris NS, Twardziok SO, et al (2019) Durum wheat genome highlights past domestication signatures and future improvement targets. Nat Genet 51:885–895. https://doi.org/10.1038/s41588-019-0381-3

Mago R, Zhang P, Vautrin S, et al (2015) The wheat *Sr50* gene reveals rich diversity at a cereal disease resistance locus. Nature Plants 1:15186. https://doi.org/10.1038/nplants.2015.186

Marchal C, Zhang J, Zhang P, et al (2018) BED-domain-containing immune receptors confer diverse resistance spectra to yellow rust. Nature Plants 4:662–668. https://doi.org/10.1038/s41477-018-0236-4

Moore JW, Herrera-Foessel S, Lan C, et al (2015) A recently evolved hexose transporter variant confers resistance to multiple pathogens in wheat. Nat Genet 47:1494–1498. https://doi.org/10.1038/ng.3439

Olson EL, Brown-Guedira G, Marshall D, et al (2010a) Development of wheat lines having a small introgressed segment carrying stem rust resistance gene *Sr22*. Crop Sci 50:1823–1830. https://doi.org/10.2135/cropsci2009.11.0652

Olson EL, Brown-Guedira G, Marshall D, et al (2010b) Development of wheat lines having a small introgressed segment carrying stem rust resistance gene *Sr22*. Crop Sci 50:1823–1830. https://doi.org/10.2135/cropsci2009.11.0652

Periyannan S, Moore J, Ayliffe M, et al (2013) The gene *Sr33,* an ortholog of barley *Mla* genes, encodes resistance to wheat stem rust race Ug99. Science 341:786–788. https://doi.org/10.1126/science.1239028

Qi LL, Echalier B, Chao S, et al (2004) A chromosome bin map of 16,000 expressed sequence tag loci and distribution of genes among the three genomes of polyploid wheat. Genetics 168:701–712. https://doi.org/10.1534/genetics.104.034868

Rawat N, Pumphrey MO, Liu S, et al (2016) Wheat *Fhb1* encodes a chimeric lectin with agglutinin domains and a pore-forming toxin-like domain conferring resistance to Fusarium head blight. Nat Genet 48:1576–1580. https://doi.org/10.1038/ng.3706

Saintenac C, Cambon F, Aouini L, et al (2021) A wheat cysteine-rich receptor-like kinase confers broad-spectrum resistance against *Septoria tritici* blotch. Nat Commun 12:433. https://doi.org/10.1038/s41467-020-20685-0

Saintenac C, Lee W-S, Cambon F, et al (2018) Wheat receptor-kinase-like protein *Stb6* controls gene-for-gene resistance to fungal pathogen *Zymoseptoria tritici*. Nat Genet 50:368–374. https://doi.org/10.1038/s41588-018-0051-x

Saintenac C, Zhang W, Salcedo A, et al (2013) Identification of wheat gene *Sr35* that confers resistance to Ug99 stem rust race group. Science 341:783–786. https://doi.org/10.1126/science.1239022

Sánchez-Martín J, Steuernagel B, Ghosh S, et al (2016) Rapid gene isolation in barley and wheat by mutant chromosome sequencing. Genome Biol 17:221. https://doi.org/10.1186/s13059-016-1082-1

Sánchez-Martín J, Widrig V, Herren G, et al (2021) Wheat *Pm4* resistance to powdery mildew is controlled by alternative splice variants encoding chimeric proteins. Nat Plants 7:327–341. https://doi.org/10.1038/s41477-021-00869-2

Sato K, Abe F, Mascher M, et al (2021) Chromosome-scale genome assembly of the transformation-amenable common wheat cultivar 'Fielder.' DNA Research 28:dsab008. https://doi.org/10.1093/dnares/dsab008

Savary S, Bregaglio S, Willocquet L, et al (2017) Crop health and its global impacts on the components of food security. Food Sec 9:311–327. https://doi.org/10.1007/s12571-017-0659-1

Savary S, Willocquet L, Pethybridge SJ, et al (2019) The global burden of pathogens and pests on major food crops. Nat Ecol Evol 3:430–439. https://doi.org/10.1038/s41559-018-0793-y

Schreiber AW, Hayden MJ, Forrest KL, et al (2012) Transcriptome-scale homoeolog-specific transcript assemblies of bread wheat. BMC Genomics 13:492. https://doi.org/10.1186/1471-2164-13-492

Sears ER (1953) Nullisomic analysis in common wheat. Am Nat 87:245–252. https://doi.org/10.1086/281780

Shi G, Zhang Z, Friesen TL, et al (2016) The hijacking of a receptor kinase–driven pathway by a wheat fungal pathogen leads to disease. Sci Adv 2:e1600822. https://doi.org/10.1126/sciadv.1600822

Singh SP, Hurni S, Ruinelli M, et al (2018) Evolutionary divergence of the rye *Pm17* and *Pm8* resistance genes reveals ancient diversity. Plant Mol Biol 98:249–260. https://doi.org/10.1007/s11103-018-0780-3

Srichumpa P, Brunner S, Keller B, Yahiaoui N (2005) Allelic series of four powdery mildew resistance genes at the *Pm3* locus in hexaploid bread wheat. Plant Physiol. 139:885–895. https://doi.org/10.1104/pp.105.062406

Steuernagel B, Periyannan SK, Hernández-Pinzón I, et al (2016) Rapid cloning of disease-resistance genes in plants using mutagenesis and sequence capture. Nat Biotechnol 34:652–655. https://doi.org/10.1038/nbt.3543

Su Z, Bernardo A, Tian B, et al (2019) A deletion mutation in TaHRC confers Fhb1 resistance to Fusarium head blight in wheat. Nat Genet 51:1099–1105. https://doi.org/10.1038/s41588-019-0425-8

The International Wheat Genome Sequencing Consortium (IWGSC), Appels R, Eversole K, et al (2018) Shifting the limits in wheat research and breeding using a fully annotated reference genome. Science 361:eaar7191. https://doi.org/10.1126/science.aar7191

The International Wheat Genome Sequencing Consortium (IWGSC), Mayer KFX, Rogers J, et al (2014) A chromosome-based draft sequence of the hexaploid bread wheat (*Triticum aestivum*) genome. Science 345:1251788. https://doi.org/10.1126/science.1251788

Thind AK, Wicker T, Šimková H, et al (2017) Rapid cloning of genes in hexaploid wheat using cultivar-specific long-range chromosome assembly. Nat Biotechnol 35:793–796. https://doi.org/10.1038/nbt.3877

Upadhyaya NM, Mago R, Panwar V, et al (2021) Genomics accelerated isolation of a new stem rust avirulence gene–wheat resistance gene pair. Nat Plants 7:1220–1228. https://doi.org/10.1038/s41477-021-00971-5

Vendramin V, Ormanbekova D, Scalabrin S, et al (2019) Genomic tools for durum wheat breeding: de novo assembly of Svevo transcriptome and SNP discovery in elite germplasm. BMC Genomics 20:278. https://doi.org/10.1186/s12864-019-5645-x

Walkowiak S, Gao L, Monat C, et al (2020) Multiple wheat genomes reveal global variation in modern breeding. Nature 588:277–283. https://doi.org/10.1038/s41586-020-2961-x

Wang H, Sun S, Ge W, et al (2020a) Horizontal gene transfer of *Fhb7* from fungus underlies *Fusarium* head blight resistance in wheat. Science 368:eaba5435. https://doi.org/10.1126/science.aba5435

Wang H, Zou S, Li Y, et al (2020b) An ankyrin-repeat and WRKY-domain-containing immune receptor confers stripe rust resistance in wheat. Nat Commun 11:1353. https://doi.org/10.1038/s41467-020-15139-6

Wang L, Zhu T, Rodriguez JC, et al (2021) *Aegilops tauschii* genome assembly Aet v5.0 features greater sequence contiguity and improved annotation. Genes Genom Genet 11:jkab325. https://doi.org/10.1093/g3journal/jkab325

Wicker T, Gundlach H, Spannagl M, et al (2018) Impact of transposable elements on genome structure and evolution in bread wheat. Genome Biol 19:103. https://doi.org/10.1186/s13059-018-1479-0

Wulff BB, Krattinger SG (2022) The long road to engineering durable disease resistance in wheat. Curr Opin Biotechnol 73:270–275. https://doi.org/10.1016/j.copbio.2021.09.002

Xie J, Guo G, Wang Y, et al (2020) A rare single nucleotide variant in *Pm5e* confers powdery mildew resistance in common wheat. New Phytologist 228:1011–1026. https://doi.org/10.1111/nph.16762

Xing L, Hu P, Liu J, et al (2018) *Pm21* from *Haynaldia villosa* encodes a CC-NBS-LRR protein conferring powdery mildew resistance in wheat. Mol Plant 11:874–878. https://doi.org/10.1016/j.molp.2018.02.013

Yahiaoui N, Srichumpa P, Dudler R, Keller B (2004) Genome analysis at different ploidy levels allows cloning of the powdery mildew resistance gene *Pm3b* from hexaploid wheat: Positional cloning of *Pm3* from hexaploid wheat. Plant J37:528–538. https://doi.org/10.1046/j.1365-313X.2003.01977.x

Yan X, Li M, Zhang P, et al (2021) High-temperature wheat leaf rust resistance gene *Lr13* exhibits pleiotropic effects on hybrid necrosis. Mol Plant 14:1029–1032. https://doi.org/10.1016/j.molp.2021.05.009

Yao E, Blake VC, Cooper L, et al (2022) GrainGenes: a data-rich repository for small grains genetics and genomics. Database 2022:baac034. https://doi.org/10.1093/database/baac034

Yu G, Matny O, Champouret N, et al (2022) *Aegilops sharonensis* genome-assisted identification of stem rust resistance gene *Sr62*. Nat Commun 13:1607. https://doi.org/10.1038/s41467-022-29132-8

Yuan C, Wu J, Yan B, et al (2018) Remapping of the stripe rust resistance gene *Yr10* in common wheat. Theor Appl Genet 131:1253–1262. https://doi.org/10.1007/s00122-018-3075-9

Zhang C, Huang L, Zhang H, et al (2019) An ancestral NB-LRR with duplicated 3′UTRs confers stripe rust resistance in wheat and barley. Nat Commun 10:4023. https://doi.org/10.1038/s41467-019-11872-9

Zhang J, Zhang P, Dodds P, Lagudah E (2020) How target-sequence enrichment and sequencing (TEnSeq) pipelines have catalyzed resistance gene cloning in the wheat-rust pathosystem. Front Plant Sci 11:678. https://doi.org/10.3389/fpls.2020.00678

Zhang W, Chen S, Abate Z, et al (2017) Identification and characterization of *Sr13*, a tetraploid wheat gene that confers resistance to the Ug99 stem rust race group. Proc Natl Acad Sci USA 114:. https://doi.org/10.1073/pnas.1706277114

Zhang Z, Running KLD, Seneviratne S, et al (2021) A protein kinase–major sperm protein gene hijacked by a necrotrophic fungal pathogen triggers disease susceptibility in wheat. Plant J 106:720–732. https://doi.org/10.1111/tpj.15194

Zhao G, Zou C, Li K, et al (2017) The *Aegilops tauschii* genome reveals multiple impacts of transposons. Nature Plants 3:946–955. https://doi.org/10.1038/s41477-017-0067-8

Zhou Y, Bai S, Li H, et al (2021) Introgressing the *Aegilops tauschii* genome into wheat as a basis for cereal improvement. Nat Plants 7:774–786. https://doi.org/10.1038/s41477-021-00934-w

Zhu T, Wang L, Rodriguez JC, et al (2019) Improved genome sequence of wild emmer wheat Zavitan with the aid of optical maps. Genes Genom Genet 9:619–624. https://doi.org/10.1534/g3.118.200902

Zimin AV, Puiu D, Hall R, et al (2017a) The first near-complete assembly of the hexaploid bread wheat genome, *Triticum aestivum*. GigaScience 6:. https://doi.org/10.1093/gigascience/gix097

Zimin AV, Puiu D, Luo M-C, et al (2017b) Hybrid assembly of the large and highly repetitive genome of *Aegilops tauschii* , a progenitor of bread wheat, with the MaSuRCA mega-reads algorithm. Genome Res 27:787–792. https://doi.org/10.1101/gr.213405.116

Zou S, Wang H, Li Y, et al (2018) The NB-LRR gene *Pm60* confers powdery mildew resistance in wheat. New Phytol 218:298–309. https://doi.org/10.1111/nph.14964

4. SATURATION MAPPING AND CLONING OF THE TAN SPOT SUSCEPTIBILITY LOCUS *Tsc1* IN WHEAT[1]

4.1. Abstract

The necrotrophic fungal pathogen *Pyrenophora tritici-repentis* (*Ptr*) causes the foliar disease tan spot in both bread wheat and durum wheat. Wheat lines carrying the tan spot susceptibility gene *Tsc1* are susceptible to Ptr ToxC-producing isolates, which cause chlorosis. *Tsc1* was mapped in two low-resolution biparental populations derived from LMPG-6 × PI 626573 and Louise × Penawawa. In total, 58 genetic markers were developed and mapped, delineating the *Tsc1* candidate gene region to a 1.4 cM genetic interval spanning 184 kb on the short arm of chromosome 1A. Inoculations of the sequenced accession CDC Landmark with the Ptr ToxC-producing isolate resulted in the development of chlorosis whereas inoculations with a Ptr ToxC-disrupted strain resulted in no chlorosis, indicating CDC Landmark likely carries *Tsc1*. Therefore, the CDC Landmark genome was used in addition to the Chinese Spring genome to evaluate *Tsc1* candidate genes. Comparative analysis of candidate genes in the Chinese Spring and CDC Landmark genomes reduced the candidates to just two genes. Mutant analysis confirmed one of those two as *Tsc1*. *Tsc1* contains protein kinase and leucine-rich repeat domains, both of which are necessary for function as confirmed by mutagenesis in two

[1] Part of the material in this chapter pertaining to the saturation mapping of the *Tsc1* region was co-authored by Katherine L. D. Running, Aliya Momotaz, Gayan K. Kariyawasam, Jason D. Zurn, Maricelis Acevedo, Arron H. Carter, Zhaohui Liu and Justin D. Faris and published in the following article:
Running KLD, Momotaz A, Kariyawasam GK, Zurn JD, Acevedo M, Carter AH, Liu Z, Faris JD. (2022) Genomic analysis and delineation of the tan spot susceptibility locus *Tsc1* in wheat. Front Plant Sci 13:793925
KR, AM, and JF initiated and planned the study and developed markers. MA and AC developed the mapping populations. GK and JZ performed initial genotyping analyses with SNP arrays. GK and ZL performed tan spot inoculation experiments and analyses. KR performed linkage and genomic analyses. KR and JF interpreted the data and wrote the manuscript. All authors reviewed and edited the manuscript. Additional sections regarding, candidate gene comparison and the generation, phenotyping, sequencing, and sequence analysis of mutants and candidate genes, not previously published, leading to the identification and validation of *Tsc1,* culminating in new results and discussion, were completed by KR.

genotypes. The map-based cloning of *Tsc1* provides a strong foundation for functional characterization of *Tsc1* and the development of diagnostic *Tsc1* markers to aid in the production of *Ptr*-resistant wheat.

4.2. Introduction

Pyrenophora tritici-repentis (Died.) Drechs. (*Ptr*) is a necrotrophic homothallic ascomycete that causes the foliar disease tan spot in cultivated wheat, including common wheat (*Triticum aestivum* L., $2n = 6x = 42$, AABBDD genomes), durum wheat (*T. turgidum* ssp. *durum* (Desf.) Husnot., $2n = 4x = 28$, AABB genomes), and wild relatives (reviewed by Faris et al. 2013). Tan spot, or yellow leaf spot, was first described as a minor pathogen in 1823 (Hosford 1982). Tan spot epidemics began in the 1970s, coinciding with the adoption of minimum tillage practices. Minimum tillage practices are believed to have caused an increase in disease incidence because *Ptr* overwinters on wheat residue, infecting crops the following season. Crop rotations and fungicide applications can reduce disease incidence and severity, but the most effective method for reducing disease incidence is through the development of genetically resistant varieties.

Ptr produces and secretes multiple necrotrophic effectors (NEs). The recognition of NEs by corresponding host sensitivity genes leads to a compatible interaction resulting in the development of necrotic and chlorotic lesions. The NEs and host sensitivity genes interact in an inverse gene-for-gene manner where the pathogen hijacks host defense pathways leading to necrotrophic effector-triggered susceptibility (NETS) (Liu et al. 2009; Friesen and Faris 2010). These necrotic and chlorotic lesions reduce the photosynthetic area of the plant resulting in reduced kernel weight and grain number (Shabeer and Bockus 1988).

Three host sensitivity gene-*Ptr* NE interactions have been characterized so far: *Tsn1*-Ptr ToxA, *Tsc2*-Ptr ToxB, and *Tsc1*-Ptr ToxC (reviewed by Faris et al. 2013). One host sensitivity gene, *Tsn1* (Faris et al. 2010), and two NE genes, *PtrToxA* (Ballance et al. 1996; Ciuffetti et al. 1997) and *PtrToxB* (Martinez et al. 2001), have been cloned. The *Tsn1*-Ptr ToxA interaction produces necrosis, whereas the *Tsc2*-Ptr ToxB and *Tsc1*-Ptr ToxC interactions produce chlorosis. *Ptr* isolates are classified into races depending on their virulence patterns on a set of host differentials (reviewed by Faris et al. 2013).

In addition to the inverse gene-for-gene interactions, five tan spot resistance genes have also been identified (reviewed by Faris et al. 2013) including a major dominant gene, *Tsr7*, that confers race-nonspecific resistance in both tetraploid and hexaploid wheat (Faris et al. 2020). The other tan spot resistance genes, *tsr2* (Singh et al. 2006), *tsr3* (Tadesse et al. 2006a), *tsr4* (Tadesse et al. 2006b) and *tsr5* (Singh et al. 2008), confer recessive resistance. It is therefore possible that they are recessive alleles of host sensitivity genes that interact with yet unidentified NEs (reviewed in Faris et al. 2013).

A quantitative trait locus (QTL, *QTsc.ndsu-1A*) associated with resistance to chlorosis induced by Ptr ToxC-producing isolates was first identified in the International Triticeae Mapping Initiative W-7984 × Opata 85 recombinant inbred line (RIL) population (Faris et al. 1997; Effertz et al. 2002). The same QTL was shown to coincide with Ptr ToxC sensitivity (Effertz et al. 2002), and the gene underlying sensitivity was designated *Tsc1*. Ptr ToxC was predicted to be a small non-ionic polar molecule that induces chlorosis on wheat varieties possessing *Tsc1*.

A QTL designated *QTs.zhl-1A* was mapped to chromosome arm 1AS in two RIL populations (Kariyawasam et al. 2016; Liu et al. 2017) corresponding to the position of

QTsc.ndsu-1A. In a RIL population derived from the cross Louise × Penawawa (LouPen) (Carter et al. 2020), *QTs.zhl-1A* was associated with disease caused by race 1, race 3, and AR CrossB10 *Ptr* isolates and explained up to 22% of the phenotypic variation (Kariyawasam et al. 2016). F_1 plants from the same cross exhibited chlorosis after inoculation with the race 3 isolate 331-9, indicating that the chlorosis was conferred by a dominant susceptibility gene as opposed to the lack of a dominant resistance gene. In the LMPG-6 × PI 626573 (LP) RIL population, *QTs.zhl-1A* was associated with susceptibility explaining up to 27% of the variation in disease.

Additional QTL corresponding to the *Tsc1* region have been identified in many hexaploid populations including, but not limited to, the biparental populations TA161-L1 × TAM105 (Kalia et al. 2018), IGW2547 × Annuello (Shankar et al. 2017), and Ernie × Betavia (Li et al. 2011), and a MAGIC population derived from Event, BAYP4535, Ambition, Firl3565, Format, Potenzial, Bussard, and Julius (Stadlmeier et al. 2019). A meta-QTL analysis identified two meta-QTL in the *Tsc1* region. However, they likely both correspond to *Tsc1* (Liu et al. 2020). QTL in the *Tsc1* region have also been identified in durum wheat. In a worldwide collection of durum wheat, a recent evaluation using a Ptr ToxC-producing isolate revealed a QTL, likely corresponding to *Tsc1*, on the short arm of chromosome 1A (Galagedara et al. 2020).

Ptr ToxC is predicted to be a small non-ionic, polar, molecule (Effertz et al. 2002). Genetic mapping using a *P. tritici-repentis* population segregating for Ptr ToxC production deliminated Ptr ToxC to a 173 kb region (Shi et al. 2022). Subsequent comparative sequence analysis of candidate genes in Ptr ToxC negative and positive sequenced *Ptr* isolates identified four candidates corelating with Ptr ToxC production. Amplification of the four candidates in a larger set of isolates revealed only one candidate gene, PtrM4_13157, corelated with production of Ptr ToxC. PtrM4_13157 was determined to be required for Ptr ToxC production via the

production and evaluation of deletion mutants. Interestingly, the transformation of PtrM4_13157 into isolates that did not producing Ptr ToxC did not result in production of Ptr ToxC, indicating that while PtrM4_13157 is required for Ptr ToxC production, it is not sufficient. Therefore, the authors designated PtrM4_13157 "ToxC1" as additional genes are likely required for the production of Ptr ToxC.

Wheat lines containing the *Tsc1* gene exhibit a large amount of chlorosis resulting in severe tan spot susceptibility when infected with Ptr ToxC-producing isolates (Figure 4.1). Our goal was to clone the *Tsc1* gene using a map-based approach to gain a better understanding of the *Tsc1*-Ptr ToxC interaction at the molecular level. Toward this goal, the objectives of the current research were to: 1) develop molecular markers and saturated genetic linkage maps of the genomic region containing the *Tsc1* gene, 2) define and characterize the genetic and physical interval containing the *Tsc1* locus, 3) identify candidate genes for *Tsc1* in the wheat reference genome sequence, 4) develop *Tsc1* EMS mutants, and 5) validate *Tsc1* candidates. Achievement of these objectives provides a strong foundation for launching the next phase of objectives toward functional characterization of *Tsc1*.

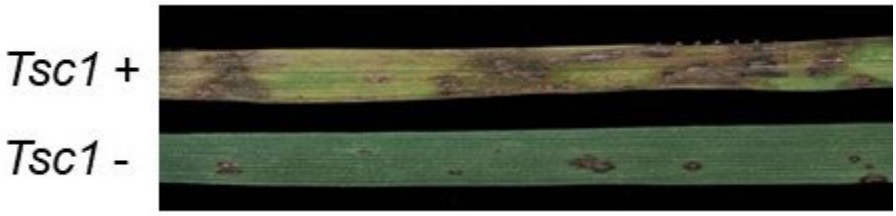

Figure 4.1. Leaves of wheat genotypes with *Tsc1* (top) and without *Tsc1* (bottom) inoculated with a *Pyrenophora tritici-repentis* Ptr ToxC-producing isolate.

4.3. Materials and methods

4.3.1. Plant materials

The LouPen and LP biparental populations were used to map newly developed markers within the *Tsc1* region. Louise and LMPG-6 exhibit extensive chlorosis when inoculated with Ptr

ToxC-producing isolates because they carry the dominant *Tsc1* allele, whereas Penawawa and PI 626573 are free of chlorosis when inoculated with the same isolates because they harbor the recessive *tsc1* allele (Kariyawasam et al. 2016; Liu et al. 2017). The LouPen population consists of 188 RILs and was originally developed to map stripe rust resistance derived from Louise (Carter et al. 2009). The LP population consists of 240 RILs and was originally developed to map stem rust Ug99 resistance in PI 626573 (Zurn et al. 2014). Sixteen hexaploid varieties were genotyped with markers closely linked to *Tsc1* to test the usefulness of markers for marker-assisted selection (MAS) (Table 4.1). Sequenced accessions ArinaLrFor, Cadenza, Chinese Spring, Claire, Jagger, Kronos, Lancer, CDC Landmark, Mace, Norin 61, Paragon, Robigus, CDC Stanley, Svevo, and Weebil were evaluated to determine if they produced chlorosis when inoculated with a Ptr ToxC producing isolate. The North Dakota State University hard red spring wheat cultivar Prosper, which exhibits extensive chlorosis when inoculated with Ptr ToxC-producing isolates, was used for mutagenesis. Three previously identified LMPG-6 EMS mutants, LMPG-6ems752, LMPG-6ems1052, and LMPG-6ems1620, were used to validate the *Tsc1* candidate.

Table 4.1. Allelic state and corresponding references of hexaploid genotypes evaluated with markers developed in this research and tightly linked to *Tsc1*.

Genotype	*Tsc1* allele	Reference
Opata 85	*Tsc1*	Faris et al. 1997
Louise	*Tsc1*	Kariyawasam et al. 2016
LMPG-6	*Tsc1*	Liu et al. 2017
6B365	*Tsc1*	Lamari and Bernier 1989
Kulm	*Tsc1*	Effertz et al. 2002
Trenton	*Tsc1*	Effertz et al. 2001
Ning 7840	*Tsc1*	Sun et al. 2010
W-7984	*tsc1*	Faris et al. 1997
Penawawa	*tsc1*	Kariyawasam et al. 2016
PI 626573	*tsc1*	Liu et al. 2017
Glenlea	*tsc1*	Lamari and Bernier 1989
6B662	*tsc1*	Lamari et al. 1995
Salamouni	*tsc1*	Lamari et al. 1995
Chinese Spring	*tsc1*	Tadesse et al. 2006a
Erik	*tsc1*	Singh and Hughes 2004
Katepwa	*tsc1*	Lamari et al. 1995

4.3.2. Inoculations and disease evaluation

The LouPen and LP populations were inoculated with the Ptr ToxC-producing race 3 isolate 331-9 in Kariyawasam et al. (2016) and Liu et al. (2017), respectively. Although previously unreported, data on the presence and absence of chlorosis induced by isolate 331-9 was collected, and that data was used here to map chlorosis induction as a qualitative trait representing the *Tsc1* locus in both populations.

In this study, I inoculated 15 previously sequenced wheat accessions-with the Ptr ToxC-producing race 1 isolate Pti2 and an engineered strain of Pti2 that had the *PtrToxC* gene disrupted, Pti2Δ13157-1 (Shi et al. 2022) to determine if any of the sequenced wheat lines carried *Tsc1*. Inoculations of the sequenced wheat accessions along with the *Tsc1*- lines 6B662, Glenlea, and Salamouni and the *Tsc1*+ line 6B365were repeated five times.

Three hundred and eighty-six Prosper M_2 families were inoculated with isolate Pti2 with 12 M_2 plants per family being evaluated. Previously, Dr. Aliya Momotaz inoculated 576 LMPG-6 M_2 families, 14 plants/family, with race 1 isolate Asc1 (Ptr ToxA+, Ptr ToxC +) to identify mutants that did not produce chlorosis. All subsequent LMPG-6 mutant inoculations were performed by Dr. Aliya Momotaz. Individual Prosper and LMPG-6 M_2 plants not exhibiting chlorosis were transplanted into pots, grown in the greenhouse, and self-pollinated. Twelve Prosper M_3 and eight LMPG-6 M_3 per transplanted M_2 were inoculated with Pti-2 and Asc1, respectively, to confirm the lack of chlorosis production.

All plants were grown, inoculated, and evaluated as previously described in Liu et al. (2017). Inoculum was prepared according to Lamari and Bernier (1989). Disease reactions were evaluated 7 days post inoculation and plants were scored based on the presence and absence of chlorosis.

4.3.3. Marker development and *Tsc1* mapping

The LouPen and LP populations were previously genotyped with the wheat 9K iSelect Assay BeadChip (Cavanagh et al. 2013) and whole genome maps were assembled (Zurn et al. 2014; Kariyawasam et al. 2016). Several methods were used to develop and/or identify additional markers within the *Tsc1* genomic region of chromosome 1A. First, simple sequence repeat (SSR) markers previously mapped and known to detect loci on chromosome arm 1AS were identified from the Graingenes database (https://wheat.pw.usda.gov/GG3/).

Second, contextual sequences of SNP markers derived from the 9K and 90K arrays known to map to the short arm of chromosome 1A were used as queries in BLASTn searches of either Chinese Spring survey sequences (IWGSC 2014), the Chinese Spring reference genome v1.0 (IWGSC 2018), or the wild emmer wheat genome sequence of Zavitan (Avni et al. 2017).

The corresponding survey sequences and approximately 10 kb segments of the Chinese Spring and Zavitan genome sequences encompassing the SNP BLAST hits were then subjected to searches for SSRs using SSRIT (https://archive.gramene.org/db/markers/ssrtool) and gene-like or low-copy DNA features by using the survey sequence or extracted genome segment sequence as a query in BLASTx searches against the NCBI non-redundant database (https://blast.ncbi.nlm.nih.gov/Blast.cgi). SSRs and gene-like features were used to develop SSR and sequence-tagged site (STS) markers, respectively, and primers were designed using Primer 3 (Rozen and Skaletsky 1999).

Third, a genome-wide association study of tan spot resistance in durum wheat (Galagedara et al. 2020) revealed a genotype-by-sequencing (GBS) marker on chromosome arm 1AS associated with reaction to the Ptr ToxC-producing isolate Pti2 and was therefore likely associated with *Tsc1*. We used the sequence of this GBS marker to develop a semi-thermal asymmetric reverse PCR (STARP) marker (Long et al. 2017) to map the locus in the LouPen and LP populations.

All markers were amplified via polymerase chain reaction (PCR) and electrophoresed on 6% nondenaturing polyacrylamide gels. Gels were stained with Gelred™ nucleic acid stain (Biotium Corporate, Hayward, CA), and scanned with a Typhoon 9410 or FLA 9500 variable mode imager (GE healthcare Biosciences, Waukesha, WI). Genetic linkage maps were constructed in MapDisto v2.1.7 (Heffelfinger et al. 2017) as described in Faris et al. (2014). Maps were visualized in MapChart 2.32 (Voorrips 2002). All PCR primers used for the identification of markers in this research are listed in Supplementary Table 1.

4.3.4. Identification of candidate genes

Candidate genes were first identified in the Chinese Spring v2.1 assembly using the closest flanking markers to *Tsc1* (*fcp730* and *fcp734*) in the LouPen genetic map to identify the candidate region (Zhu et al. 2021). High- and low-confidence annotated genes in the Chinese Spring v2.1 reference assembly were considered for analysis of protein domains (accessed 2021/12/7). Additionally, the candidate gene region of CDC Landmark v1.0 (Walkowiak et al. 2020) was annotated with the TriAnnot pipeline (Leroy et al. 2012). Conserved protein domains of the annotated genes were identified by searching the Pfam database (https://www.ebi.ac.uk/Tools/hmmer/search/hmmscan). Genes less than 500 bp long or those with no Pfam hits more significant than 1×10^{-5} were considered pseudogenes or gene fragments and were excluded from further analysis. Genes with only transposase domains were also excluded. The positions of the annotated genes identified in the Chinese Spring v2.1 annotation were identified in CDC Landmark using BLAST (https://wheat.pw.usda.gov/blast/). In Ensembl plants release 52, the de novo annotation of CDC Landmark completed by Plant Genomes and Systems Biology and the Earlham Institute became available. Therefore, the coding sequences of candidate genes annotated in Chinese Spring v2.1 and CDC Landmark were obtained from GrainGenes and Ensembl plants (http://plants.ensembl.org), respectively. Nucleotide polymorphisms were identified via BLAST alignment and the coding sequences were translated using the Expasy Translate Tool (https://web.expasy.org/translate/). The predicted amino acid sequences of the candidate genes in each genotype were aligned using Clustal Omega (https://www.ebi.ac.uk/Tools/msa/clustalo/). Gene topology was predicted using DEEPTMHMM (Hallgren et al. 2022).

4.3.5. Generation and identification of chlorosis-non-producing mutants

1077 Prosper M_1 were grown in the greenhouse at 21˚C with a 16-hour photoperiod after treatment with 0.30% EMS in 0.05 M phosphate buffer as described in Williams et al. (1992). Seed was bulk harvested from individual plants. 386 M_2 families consisting of twelve plants were evaluated for disease reactions here. Two-week-old M_2 seedlings were inoculated with race 1 isolate Pti2 (Ptr ToxA+, Ptr ToxC +) and scored for the presence of chlorosis seven days post inoculation. Previously, the *Tsc1+* line LMPG-6 was used for mutagenesis using the same procedure as was used for Prosper mutagenesis. Prosper and LMPG-6 M_2 plants that did not produce chlorosis were considered putative *Tsc1* mutants and were self-pollinated to obtain M_3 seed. Twelve to fourteen M_3 plants per putative *Tsc1* mutant were re-evaluated for chlorosis production the same way M_2 plants were evaluated. M_3 families that were homogenous for the lack of chlorosis production were considered true *Tsc1* mutant lines.

4.3.6. DNA extraction

DNA was extracted from LouPen and LP RILs according to Faris et al (2010). DNA was extracted from the sequenced wheat accessions and the EMS mutants in a similar manner, but with minor modifications to the tissue grinding steps as newer equipment was available. Leaf tissue was collected from two-week old plants and placed inside a 2 mL flat bottomed microcentrifuge tube with a 5/32 in. stainless steel bearing ball (Thomson, Radford, VA). Samples were cooled to -80 °C and then ground on a Retsch Mixer Mill MM 400 (Retsch GmbH, Hann, Germany). Tubes were ground for a total of 120 s at 24 Hz with the adapter orientation being changed midway to prevent uneven grinding. After extraction, the DNA concentration was quantified using Nanodrop spectrophotometer ND-8000 (ThermoFisher Scientific, Waltham, MA), and diluted to approximately 100 ng/µL for PCR reactions.

4.3.7. *Tsc1* sequencing

Primers were designed from the CDC Landmark v1.0 genome (Walkowiak et al. 2020) to amplify the candidate gene, using NCBI Primer 3 and CodonCode Aligner 7.1.2 (Rozen and Skaletsky 1999; CodonCode Corporation, Centerville, Massachusetts, USA,http://www.codoncode.com/aligner/). The candidate gene was amplified from chlorosis-resistant mutants and wild type genotypes in four overlapping fragments using the primers in Table 4.2. Twenty-microliter sequencing reactions consisted of 400 ng of template DNA, 1× PCR buffer, 1.5 mM $MgCl_2$, 0.125 mM dNTPs, 8 nmol of each primer, and 2 units of Taq polymerase. PCR cycling conditions included an initial denaturation at 94°C for 5 min, followed by 35 cycles of 94°C for 30 s, an annealing temperature starting at 61°C that decreased by 0.2°C each cycle for 30 seconds, and a 72°C extension for 2 min, followed by a final extension at 72°C for 7 min. Seven microliters of each PCR product were electrophoresed on 1% agarose gels to confirm successful amplification. The remaining PCR product was digested using ExoSAP IT (Thermo Fisher Scientific, Waltham, Massachusetts, USA). Two independent PCR reactions per fragment were sent for Sanger sequencing (Eurofins Genomics, Louisville, KY, USA). Point mutations were identified in the genomic sequences of the candidate genes via sequence comparison of mutant and wild type sequences using Geneious Prime 2021.2.2 (https://www.geneious.com/prime/).

Table 4.2. Primers used for amplification and sequencing of *Tsc1* genomic DNA

Forward	Reverse
Tsc1_gDNA_F1 ATCTCCTCGGGAATGGGACC	Tsc1_gDNA_R1 GGCACCCTTCTATCGCTGTC
Tsc1_gDNA_F2 GAGGGATAGTTGTACTAGCTTGGT	Tsc1_gDNA_R2 AACACACAGCCCTCCTCCAA
Tsc1_gDNA_F3 ACAAGTATCTTTCGTTTATGCTGAC	Tsc1_gDNA_R3 TTGGGCATCTTGCTGAATCTA
Tsc1_gDNA_F4 TACGATAGTCCCTGACGCCT	Tsc1_gDNA_R4 TGGAAGTTTGCCAGGTGTGA

4.4. Results

4.4.1. Disease reactions to Ptr ToxC-producing isolates in mapping populations and sequenced lines

Population parents LMPG-6 and Louise were previously found to exhibit chlorosis in response to Ptr ToxC-producing isolates, whereas PI 626573 and Penawawa were resistant to the same isolates (Kariyawasam et al. 2016; Liu et al. 2017). The disease reaction scores of the sequenced lines inoculated with Pti2 and with the *PtrToxC*-disrupted Pti2 strain Pti2Δ13157-1 were compared to determine if chlorosis production was due to the *Tsc1*-Ptr ToxC interaction. Of the 15 sequenced lines, only CDC Landmark was found to exhibit chlorosis when inoculated with Pti2, but not when inoculated with Pti2Δ13157-1, indicating CDC Landmark carries a functional *Tsc1* allele.

4.4.2. Saturation mapping of the *Tsc1* locus

In the first LouPen genetic map, *Tsc1* mapped distal to the 9K SNP markers *IWA4643*, *IWA414*, *IWA3680*, and *IWA1388*, thus placing *Tsc1* within the first 15.2 Mb of the Chinese Spring v2.1 chromosome 1A short arm. Testing of SSR markers previously mapped to chromosome 1AS in other wheat mapping populations identified six markers polymorphic

between Louise and Penawawa (Supplementary Table 1). Amplicon sequence analysis revealed the SSR markers *gpw7072* and *psp2999* targeted the same locus (data not shown). Once these six SSR markers were added to the genetic linkage map, the *Tsc1* region was narrowed to approximately the first 5 Mb of the physical map. At this point, all markers mapped proximal to *Tsc1,* and more markers needed to be developed, particularly distal to *Tsc1*, to delineate the *Tsc1* region.

Prior to the availability of the whole genome reference sequence of the hexaploid wheat cultivar Chinese Spring, SNPs from the 9K and 90K SNP arrays known to map to chromosome 1AS were used to identify Chinese Spring survey sequences. Twelve STS markers and two SSR markers designed from the survey sequences were polymorphic and mapped in the LouPen population (Supplementary Table 1). An additional three SSR and one STS markers were designed from the Zavitan genome assembly as well as ten SSRs markers from the Chinese Spring reference v1.0. Some of the newly designed markers mapped distal to *Tsc1* and further delineated the *Tsc1* region. *Tsc1* cosegregated with two markers, and the candidate gene region based on the genetic map constructed in the LouPen population was 184 kb. In total, the LouPen genetic map spanned 31.8 cM with 42 loci and had a marker density of 1.32 markers/cM (Figure 4.2).

The initial genetic map of the LP population placed *Tsc1* within a ~7.2 Mb region of the short arm of chromosome 1A between the 9K SNP markers *IWA1376* and *IWA8622*. Seven previously mapped SSR markers were polymorphic between LMPG-6 and PI 626573, including four that were included in the LouPen genetic map. The inclusion of these seven markers on the LP genetic linkage map delineated the *Tsc1* region to 3.9 Mb on the physical map.

To reduce the candidate gene region further, additional markers were designed in the same manner as they were for mapping in the LouPen population. Fourteen STS and five SSR markers designed from the Chinese Spring survey sequences and eight SSR and two STS markers derived from the Zavitan genome assembly were mapped in the LP population (Supplementary Table 1). An additional five SSR markers designed from the Chinese Spring reference v1.0 were added to the LP genetic map. These additional STS and SSR markers reduced the candidate gene region to approximately 1 Mb, an order of magnitude larger than the candidate gene region defined by mapping in the LouPen population. The LP map consisted of 47 loci spanning 36.1 cM, which gives a marker density of 1.30 markers/cM (Figure 4.2).

Recombination rates were compared between the LP and LouPen populations within the mapped regions to determine which population delineated the *Tsc1* locus to the smallest genomic region, or if a composite of the two maps could be used to define the *Tsc1* locus to a smaller region. The most distal and proximal markers in common between the two maps were *fcp683* and *wmc24,* respectively. The region defined by these markers encompassed 26.3 Mb on the Chinese Spring v2.1 reference genome, and it spanned 31.2 and 35.5 cM of genetic distance in the LouPen and LP populations, respectively. Therefore, the recombination rate across this region was higher in the LP population (1.35 cM/Mb) compared to the LouPen population (1.19 cM/Mb).

Comparison of recombination rates in the vicinity of the *Tsc1* locus revealed a different scenario. The markers *fcp704* and *fcp779*, which were the two markers in common to both maps that detect recombination events most closely flanking *Tsc1* on the distal and proximal sides, respectively, were separated by 4.4 cM on the LouPen map and 1.5 cM on the LP map (Figure 4.2). Unfortunately, the amplicon sequence for *fcp704* was not present in the Chinese Spring

v2.1 genome making it impossible to determine the physical distance between these common flanking markers. The next closest marker on the distal side of *Tsc1* common to both maps and present in Chinese Spring was *fcp693*. The genetic distances between *fcp779* and *fcp693* in the LouPen and LP populations was 4.4 and 3.7 cM, respectively. The physical distance between these two markers in the Chinese Spring reference genome was 5.7 Mb, which translates to 0.77 cM/Mb in the LouPen population and 0.64 cM/Mb in the LP population. Therefore, the recombination frequency near the *Tsc1* locus was higher in the LouPen population compared to the LP population.

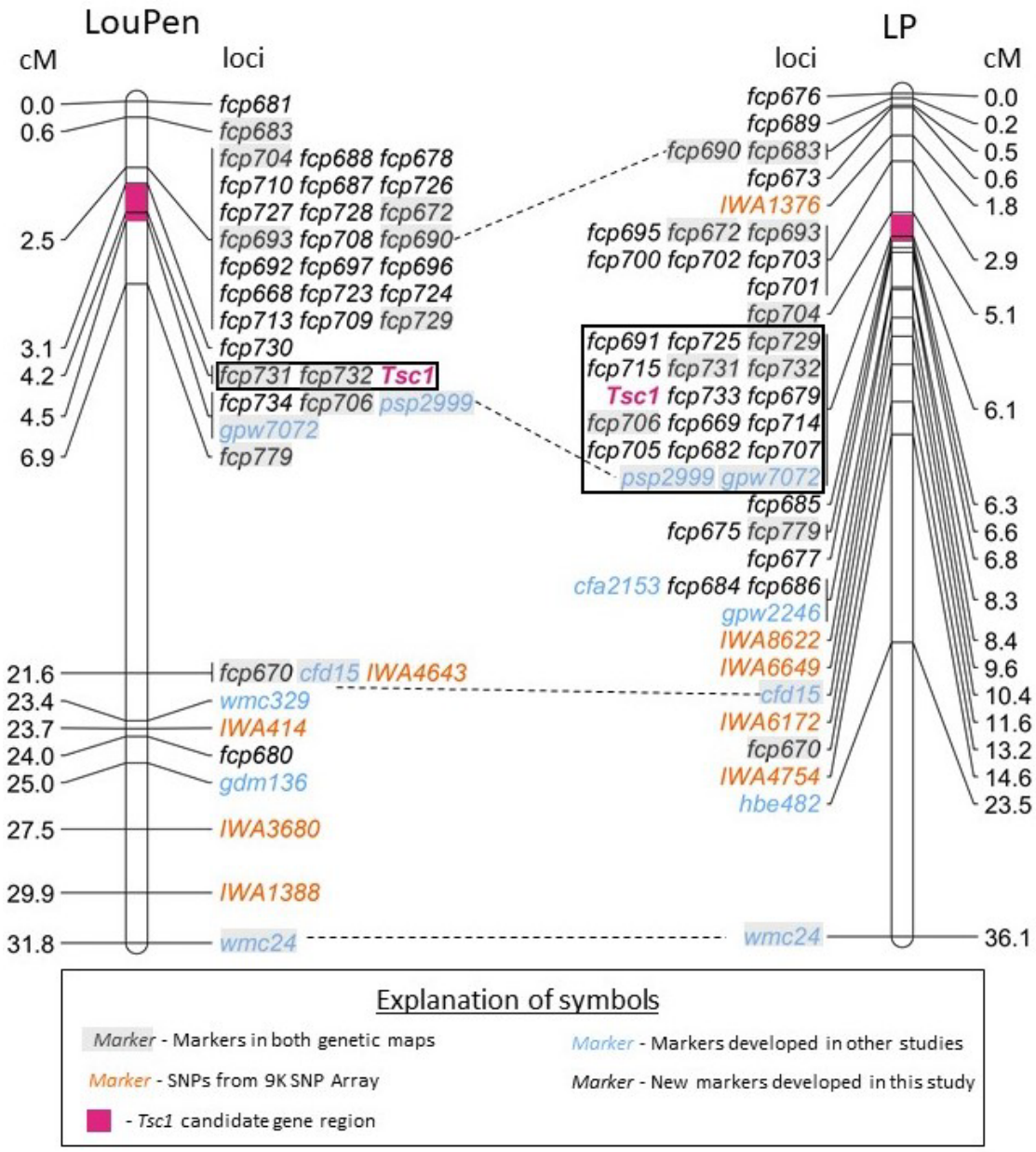

Figure 4.2. Saturation maps of the *Tsc1* region developed in Louise × Penawawa (LouPen) and LMPG-6 × PI 626573 (LP) populations.
The LouPen genetic map is on the left and the LP genetic map is on the right. Loci mapped are listed on the right of the LouPen genetic map and the left of the LP genetic map. Opposite the loci, the genetic distances are displayed in centiMorgans (cM). Markers in orange are SNP markers from the wheat 9 K iSelect Assay BeadChip. Markers in black are simple sequence repeat (SSR) markers designed in this study. Blue markers were designed in other studies. Dashed lines connect markers mapped in both populations. The black outlined rectangle indicates the loci cosegregating with *Tsc1*. The pink shaded portion of the chromosome represents the candidate gene region in each population.

The genetic order of the markers in LouPen was compared to the physical order in the Chinese Spring v2.1 reference genome due to the higher genetic resolution near *Tsc1* (Figure 4.3). There were two instances of non-collinearity. Firstly, marker *fcp683* mapped more distal in LouPen than its physical position, which would place it within the markers cosegregating at 2.5 cM. On the proximal side of *Tsc1*, the markers *IWA414* and *fcp680* were inverted relative to their physical position. These minor inconsistencies between genetic and physical order of the markers are indicative of rearrangements in the Chinese Spring genome relative to Louise and Penawawa. However, the rearrangements do not encompass or alter the candidate gene region.

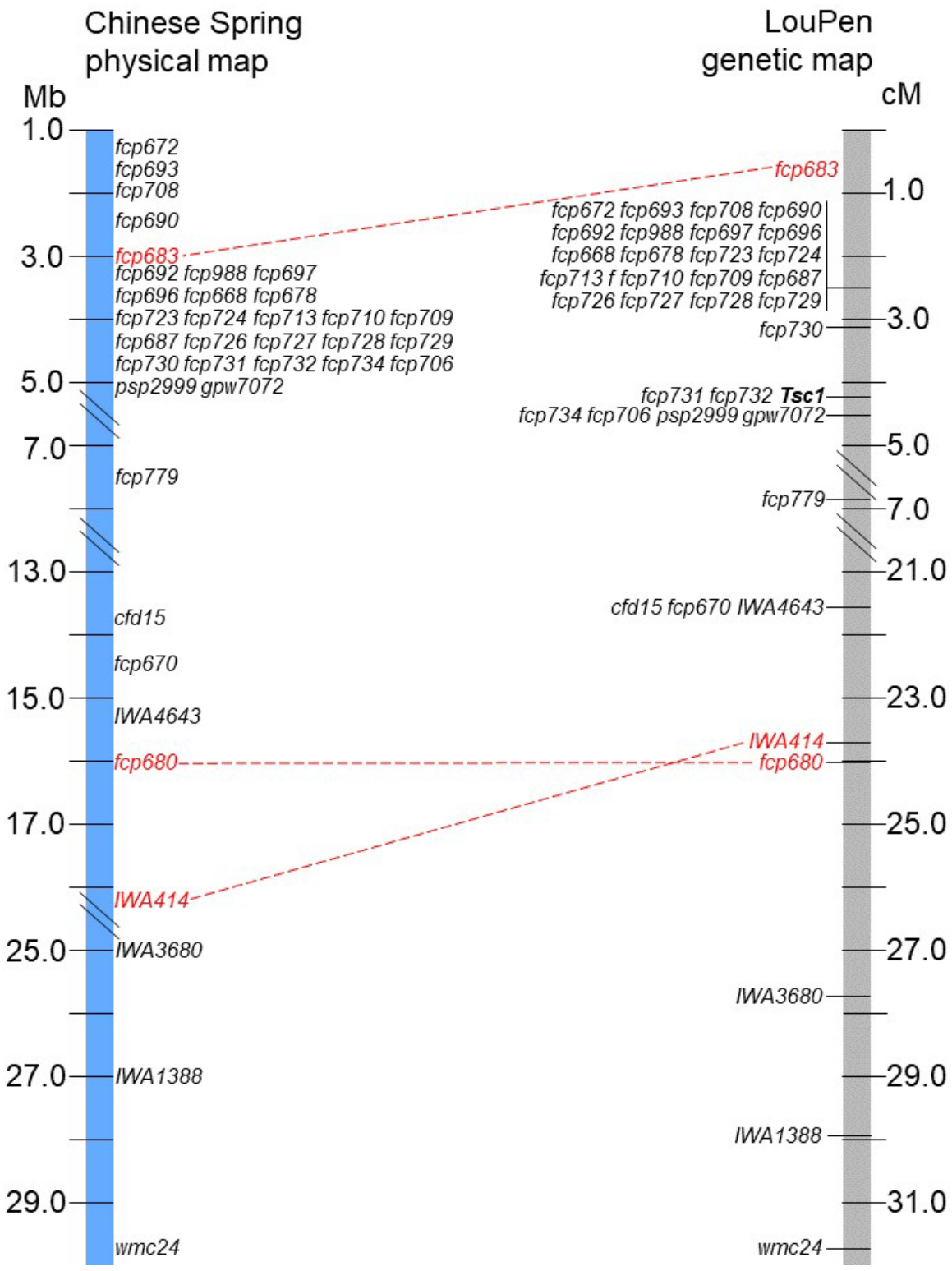

Figure 4.3. Comparison of the physical and genetic order of markers.
The LouPen genetic map is on the right and the Chinese Spring v2.1 physical map is on the left. Markers in red font connected by red dashed lines are not colinear. All other markers are colinear.

4.4.3. Delineation of the candidate gene region and identification of candidate genes

In the LouPen population, the *Tsc1* candidate gene region was delineated by *fcp730* and *fcp734*, which were 1.4 cM apart (Figure 4.2). This region corresponded to approximately 184 kb in the Chinese Spring reference v2.1 genome (Figure 4.4). Two markers, *fcp732* and *fcp731* cosegregated with *Tsc1*, and they spanned just 17 kb.

The candidate gene region, delineated by *fcp704* and *fcp685*, was larger in the LP population. As *fcp704* is not in the Chinese Spring reference genome, the next closest marker, *fcp701*, was selected to delineate the candidate gene region to 3.9 Mb in the LP population. The 16 markers that cosegregated with *Tsc1* spanned a total of 967 kb in the Chinese Spring v2.1 reference genome.

Given this finding, the delineated region on the genetic map developed in the LouPen population was used to define the *Tsc1* candidate region and to identify candidate genes based on the Chinese Spring reference sequence (Figure 4.4). No genes were identified between the distal flanking marker *fcp730* and the markers *fcp731* and *fcp732*, which cosegregated with *Tsc1*. A gene containing nucleotide binding and ARC (NB-ARC) domains was identified between *fcp731* and *fcp732*. Between *fcp732* and the proximal flanking marker, *fcp734*, there were four protein kinase and leucine rich repeat (PK-LRR) domain-containing genes and two genes with only an LRR domain. Two additional genes within this segment included a gene with a retinal pigment epithelial membrane protein domain and a pseudo-gliadin gene. The former was considered a gene fragment as it did not contain a start codon. A large family of gliadins is known to exist on chromosome 1A in wheat, so it is not surprising that a pseudo-gliadin was identified. However, gliadins have not been shown to be involved in disease resistance or susceptibility, and therefore the pseudo-gliadin gene was not considered a candidate. In total, nine genes were identified in

Chinese Spring and seven were considered candidates including one NB-ARC, four PK-LRR, and two LRR domain-containing genes (Figure 4.4).

4.4.4. Evaluation of markers closely linked to *Tsc1*

To identify markers that could be potentially used for MAS of Ptr ToxC-insensitive lines, i.e. elimination of the dominant *Tsc1* allele, markers closely linked to the *Tsc1* locus were evaluated on a panel of hexaploid wheat lines on which phenotypic evaluations with Ptr ToxC-producing isolates has been conducted, and therefore the allelic status at the *Tsc1* locus is known (Table 4.1). The markers *fcp731* and *fcp732*, which cosegregated with *Tsc1* in the LouPen population, were selected for evaluation as well as *fcp729* and flanking markers *fcp730*, *fcp734*, and *psp2999*. Among the hexaploid lines evaluated, seven were resistant to chlorosis induced by Ptr ToxC-producing isolates of *Ptr,* and nine were susceptible and developed extensive chlorosis (Table 4.1).

Analysis of amplified fragments for these six markers revealed that no marker allele was associated with the allelic state of *Tsc1* (Figure 4.5). The best association was with *fcp732* where five out of nine resistant lines had null marker alleles.

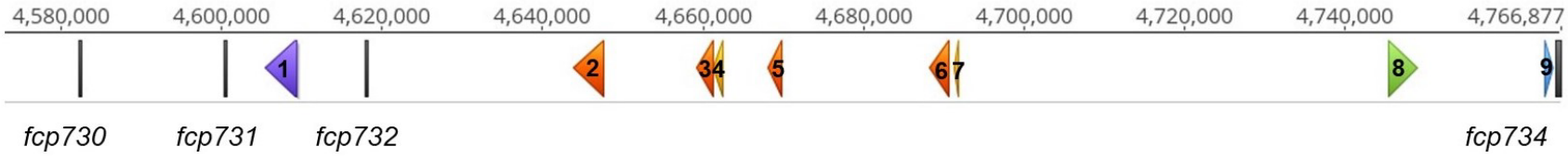

Gene	Gene ID	Protein domains	Pfam IDs	Position
1	TraesCS1A03G0017700	NB-ARC	PF00931.24, PF05729.14	4605426-4609380 (-strand)
2	TraesCS1A03G0018400	Protein kinase, LRR	PF00069.27, PF13855.8, PF12799.9, PF08263.14, PF07714.19	4643782-4647658 (- strand)
3	TraesCS1A03G0018600	Protein kinase, LRR	PF00069.27, PF13855.8, PF00560.35, PF07714.19	4659235-4661188 (- strand)
4	TraesCS1A03G0018700LC	LRR	PF13855.8	4661210-4662412 (- strand)
5	TraesCS1A03G0018800	Protein kinase, LRR	PF00069.27, PF13855.8, PF00560.35, PF07714.19, PF12799.9	4668102-4669750 (- strand)
6	TraesCS1A03G0018900	Protein kinase, LRR	PF00069.27, PF07714.19, PF00560.35	4688180-4690620 (- strand)
7	TraesCS1A03G0019000LC	LRR	PF13855.8	4691237-4691755 (- strand)
8	TraesCS1A03G0019100LC	Retinal pigment epithelial membrane protein	PF03055.17	4745413..4748957 (+ strand)
9	TraesCS1A03G0019200	Pseudo-gliadin	PF13016.8, PF00234.24	4764892-4765791 (+ strand)

Figure 4.4. *Tsc1* candidate gene region in Chinese Spring reference genome v2.1.
The scale on the top represents the physical position in base pairs. Genetic markers are displayed as vertical gray bars. Genes are displayed as arrows, labeled 1–5, corresponding to the genes in the table below. Genes with nucleotide binding and ARC (NB-ARC), protein kinase (PK) and leucine-rich repeat (LRR), LRR, retinal pigment epithelial membrane, and gliadin domains are shown in purple, orange, yellow, green, and blue, respectively. Gene IDs, protein domains, Pfam IDs, and physical positions of each gene are included in the table.

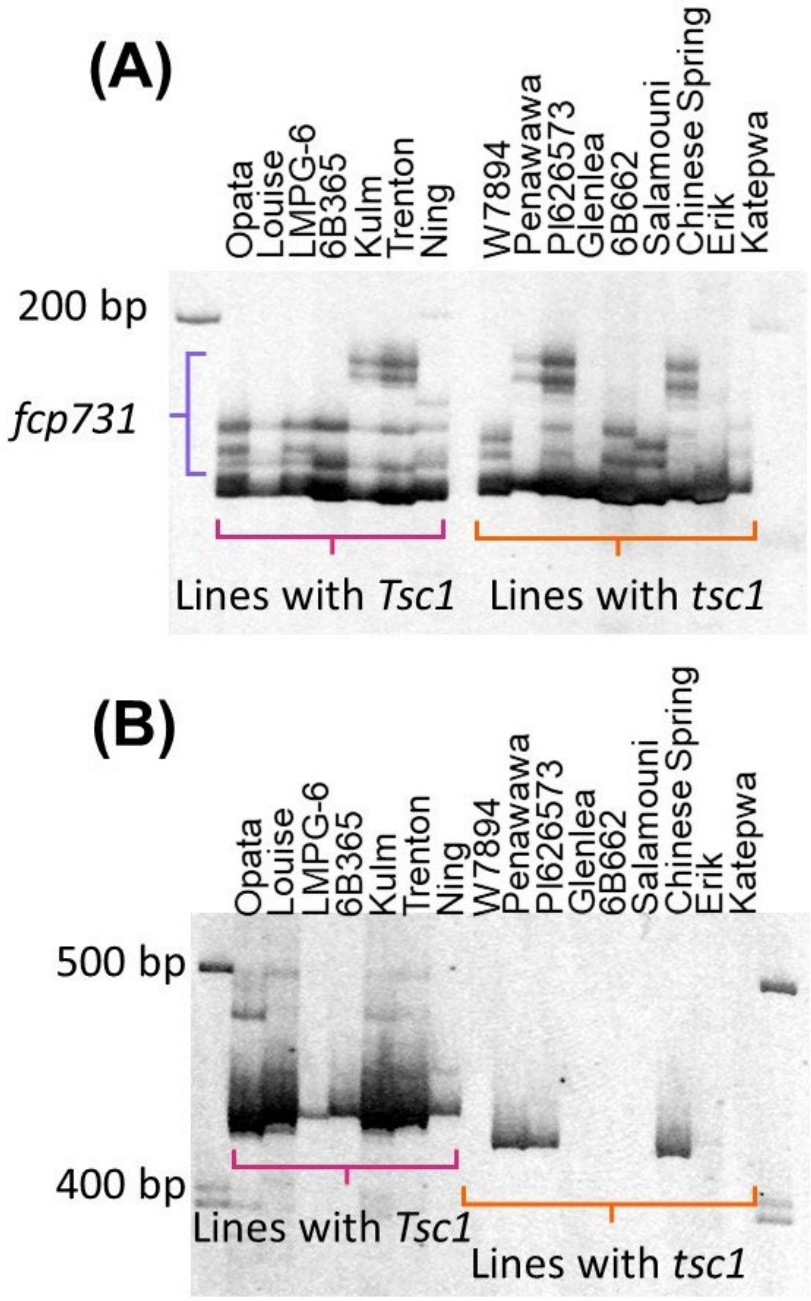

Figure 4.5. Evaluation of markers cosegregating with *Tsc1*.
The polyacrylamide gel images of markers *fcp731* (A) and *fcp732* (B) run on lines with known sensitivity statuses (Table 4.1) are shown. Horizontal brackets in pink and orange denote amplicons in lines with *Tsc1* and *tsc1*, respectively. The primary amplicon was scored for marker *fcp732* (B). The amplicons denoted by the purple bracket were scored for marker *fcp731* (A).

4.4.5. Comparison of the candidate gene regions of Chinese Spring and CDC Landmark

Because Chinese Spring is resistant to chlorosis caused by Ptr ToxC-producing isolates, it was possible that *Tsc1* was absent in Chinese Spring. Consequently, the candidate gene region was annotated in CDC Landmark, as inoculations indicated that it carried a functional *Tsc1* allele. The annotation of CDC Landmark did not reveal any unique candidate genes. Of the seven candidate genes identified in Chinese Spring with resistance gene-like domains, three PK-LRR genes and the two LRR domain-containing genes were absent in CDC Landmark, thus eliminating them as candidate genes (Figure 4.6). The NLR and PK-LRR domain containing genes *TraesCS1A03G0017700* and *TraesCS1A03G0018400* aligned to CDC Landmark genes *TraesLDM1A03G00003370* and *TraesLDM1A03G00003410*. Because *Tsc1* is dominant and CDC Landmark likely carries a functional *Tsc1* allele, these two genes were the only remaining candidates.

Alignments of the predicted amino acid sequences of the two candidate genes in common between CDC Landmark and Chinese Spring identified nonsynonymous substitutions relative to CDC Landmark in both candidate genes. The NLR gene, *TraesLDM1A03G00003370* was spliced differently than *TraesCS1A03G0017700*, resulting in a peptide of 1024 and 1005 amino acids, respectively. Due to the differences in splicing, only the first half of the amino acid sequences aligned with 85% identity (415/486). The PK-LRR genes, *TraesLDM1A03G00003410* and *TraesCS1A03G0018400* were more similar with just one nonsynonymous SNP and one synonymous SNP identified between the two sequences. It is possible that the PK domain of the PK-LRR is a protein tyrosine and serine/threonine kinase as an alignment with Pfam accession PF07714.20 had an e-value of 9×10^{-41}. However, the alignment with the protein kinase Pfam

accession PF00069.28 had a more significant e-value (8.6×10^{-48}), so the PK domain designation is used here.

4.4.6. Validation of *Tsc1*

Inoculation of 386 Prosper M_2 families and 576 LMPG-6 M_2 families yielded two and three independent families with completely insensitive M_3 progeny, respectively (Figure 4.7). TraesLDM1A03G00003410 was validated as *Tsc1* via comparative sequence analysis of mutant and wild type DNA. The reported structure of TraesLDM1A03G00003410 is 3632 bp long from transcriptional start to stop site with a single intron of 86 bp long, yielding a peptide with a length of 1181 amino acids. A 272 bp long 3' UTR is reported as part of the second exon. DeepTMHMM predicted a signal peptide of 35 amino acids in length. Amino acids 36-827, corresponding to the LRRs, are predicted to be outside, with amino acids 828-848 and 849-1181 being transmembrane and inside, respectively (Figure 4.6).

Three of the mutants, LMPG-6_ems1620, Prosper_ems53, and Prosper_ems260 have nonsense mutations resulting in premature stop codons and truncated peptide sequences of 871, 788, and 75 amino acids in length (Table 4.3). LMPG_ems752 has a missense mutation resulting in a leucine to phenylalanine substitution at amino acid 575. The remaining mutant, LMPG-6_ems1052 has a G/A SNP in the intron at the splice site between exon 1 and intron 1, likely resulting in the retention of intron 1. Future sequencing of cDNA from LMPG-6_ems1052 will confirm how the intronic SNP affects transcription of mRNA. The primer in the 3' UTR region was designed too close to the transcription stop site and as a result, the last 34-80 bp of the gene are not sequenced from the mutants. However, it is unlikely that additional mutations would be identified in this region. Additional primers further away from the transcriptional stop site will be designed to amplify the complete *Tsc1* coding sequence

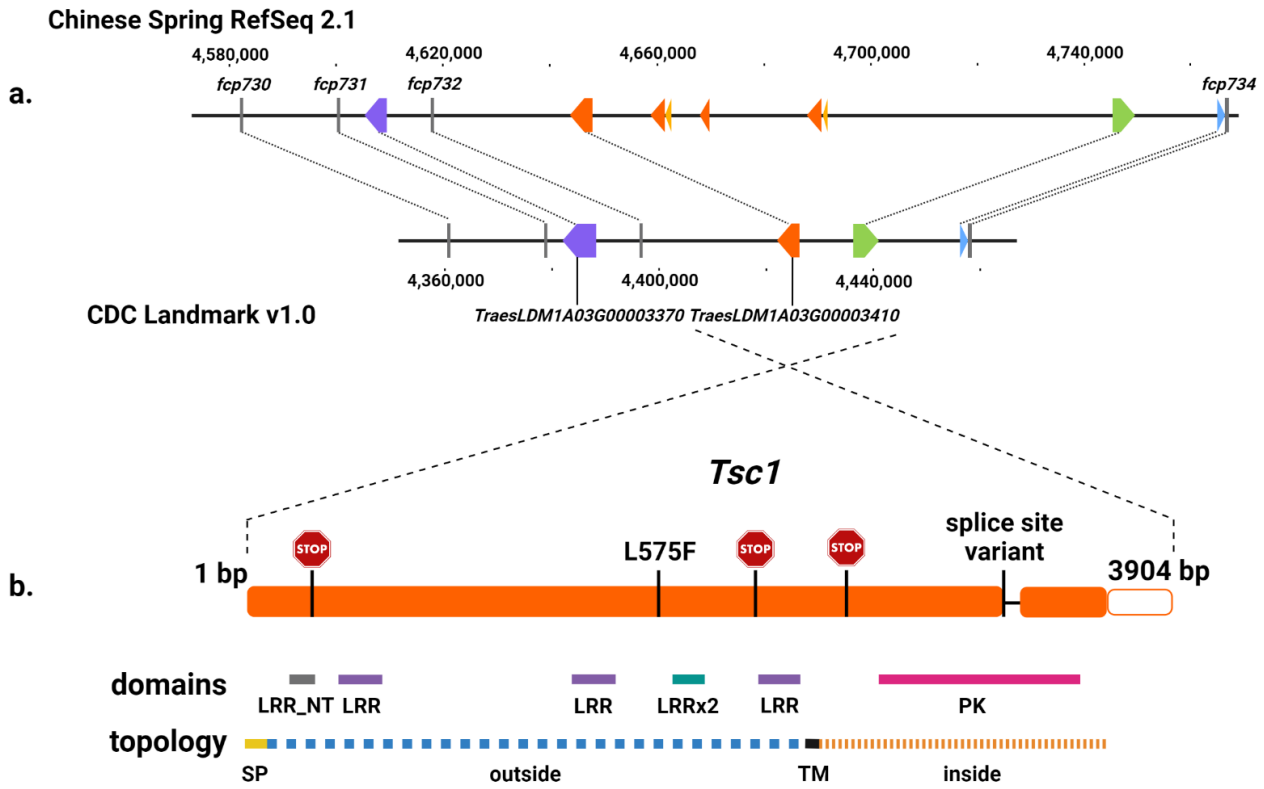

Figure 4.6. The *Tsc1* region.
a. Comparison of the candidate genes identified in Chinese Spring RefSeq 2.1(top) and CDC Landmark v1.0 (bottom) assemblies. The scale is in base pairs, representing the physical position on chromosome 1A in each of the assemblies. Genetic markers are displayed as vertical gray bars. Purple, orange, yellow, green, and blue arrows represent genes with nucleotide binding and ARC (NB-ARC), protein kinase (PK) and leucine rich repeat (LRR), LRR, retinal pigment epithelial membrane, and pseudo-gliadin domains, respectively. Dashed lines connect common markers and genes between the two assemblies. B. The structure of Tsc1 is shown with orange rectangles and orange outlined rectangle corresponding to the reported exons and 3' UTR. The vertical black lines in Tsc1 represent the position of the identified *Tsc1* mutants, with the mutation type above the gene. Immediately below the gene, the position of the LRR N-terminal (LRR_NT), LRR, two copies of LRRs, and the PK domain displayed as horizontal grey, lavender, teal, and pink bars, respectively. On the bottom, the physical positions of the most likely topological features are shown. The horizontal yellow, dashed blue, black, and dashed orange bars represent the physical positions of the most likely topological features, corresponding to the signal peptide, region outside, transmembrane, and region inside, respectively.

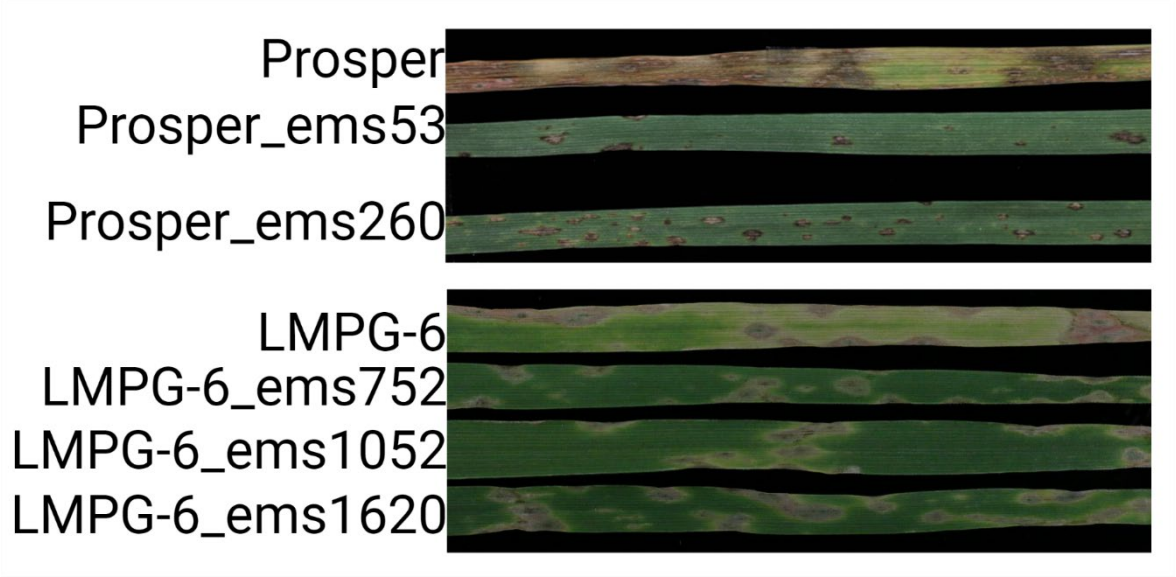

Figure 4.7. Inoculation of *Tsc1* mutants.
The leaves of Prosper and Prosper *Tsc1* mutants inoculated with Pti2 are shown on top. The leaves of LMPG-6 and LMPG-6 *Tsc1* mutants inoculated with Asc1 on bottom, photographed by Dr. Aliya Momotaz.

Table 4.3. *Tsc1* mutants and their amino acid changes.

Mutant Line	Location	Type	Amino acid change	Domain
Prosper_ems260	Exon1	Nonsense	W76STOP	LRR-N terminal domain
LMPG-6_ems752	Exon 1	Missense	L575F	LRR
Prosper_ems53	Exon 1	Nonsense	Q789STOP	LRR
LMPG-6_1620	Exon1	Nonsense	W872STOP	PK
LMPG-6_	Intron 1	Splice site variant	-	-

4.5. Discussion

Here, I report the cloning of *Tsc1*, which contains PK and LRR domains. *Tsc1* also contains a signal peptide and a transmembrane domain, indicating it likely acts as a cell surface receptor-like kinase (RLK). RLKs typically have extracellular ligand binding domains, a transmembrane domain, and an intracellular kinase domain. RLKs can act as pattern recognition receptors (PRRs), detecting pathogen-associated molecular patterns (PAMPs) and damage-associated molecular patterns (DAMPs) (reviewed by Wu and Zhou 2013). Arabidopsis RLK FLS2, with PK and LRR domains, acts as a PRR, detecting bacterial flagellin fragment flg22

(Gómez-Gómez and Boller, 2000). Binding of flg22 by *Fls2* triggers the recruitment of another RLK, BAK1, forming a RLK complex (Chinchilla et al. 2007). Recognition of flg22 triggers common PAMP-triggered immunity responses, including the production of reactive oxygen species, stomatal closure, and an increase in phytohormone levels (Bigeard et al. 2015). In addition to recognizing PAMPs and DAMPs, RLKs can recognize pathogen effectors. The rice R gene *Xa21* recognizes the *Xanthomonas oryzae* effector RaxX (Pruitt et al. 2015). The recognition of flg22 and RaxX by the host induces defense responses, restricting pathogen growth resulting in immunity. It is likely that *Tsc1* acts similarly to *Fls2* and *Xa21*, with the extracellular LRR domain detecting Ptr ToxC and the intracellular PK domain initiating immune signaling. However, because *P. tritici-repentis* is a necrotrophic pathogen, the resulting immune response and ultimate cell death is beneficial to the necrotrophic pathogen, whereas cell death restricts the growth of a biotrophic pathogen.

Comparative analysis of gene content and alleles between CDC Landmark and Chinese Spring reduced the number of candidate genes, effectively eliminating the need for high resolution mapping. However, the difference in gene content between CDC Landmark and Chinese Spring is evidence of presence/absence variation in the *Tsc1* region, which may challenge the development of codominant markers for marker-assisted removal of *Tsc1*. In fact, preliminary analysis indicates that many of the sequenced wheat genotypes are null for *Tsc1*. The absence of *Tsc1* in these lines is beneficial, but it also indicates that markers designed based on the *Tsc1* gene sequence itself will not be codominant when applied to diverse panels.

Analysis of markers closely linked to *Tsc1* on a set of genotypes with known sensitivity statuses revealed multiple alleles for each marker as well as multiple haplotypes, suggesting that *Tsc1* lies within a region of high recombination in natural populations. For example, marker

fcp731, which cosegregated with *Tsc1*, had four alleles within the susceptible lines and five alleles within the resistant lines. This diversity in marker alleles was likely helpful in finding polymorphic markers to use in genetic mapping, but it is less useful in MAS. As such, it is not recommended that these markers be used to select resistant genotypes in a natural population. The markers may be suitable for selection within a breeding population where the susceptibility status of the parents is known and can be associated with a particular marker allele.

Rearrangements on the proximal and distal sides of *Tsc1* relative to the Chinese Spring v2.1 reference genome is further evidence that the *Tsc1* region is a high recombination region, resulting in highly polymorphic markers, and increasing the difficulty in finding a marker that cosegregates with *Tsc1* in a natural population. Future characterization of the *Tsc1* region and alleles in diverse genotypes is required to identified SNPs correlated with the presence of *Tsc1* that can be targeted for marker development.

The *Tsc1*-Ptr ToxC interaction plays a significant role in tan spot development in both hexaploid and tetraploid backgrounds (Liu et al. 2020, Galagedara et al. 2020). Identification of *Tsc1* allows further characterization of the *Tsc1*-ToxC interaction, including the molecular mechanisms underlying the interaction. Although the structure of *Tsc1* indicates it could be capable of interacting directly with Ptr ToxC, this interaction is not confirmed. The identity of Ptr ToxC is not yet known, but it is likely a secondary metabolite (Effertz et al. 2002).

4.6. Literature Cited

Avni R, Nave M, Barad O, et al (2017) Wild emmer genome architecture and diversity elucidate wheat evolution and domestication. Science 357:93–97. https://doi.org/10.1126/science.aan0032

Ballance GM, Lamari L, Bernier CC (1989) Purification and characterization of a host selective toxin from *Pyrenophora tritici-repentis*. Physiol Mol Plant P 35:203–213

Ballance GM, Lamari L, Kowatsch R, Bernier CC (1996) Cloning, expression and occurrence of the gene encoding the Ptr necrosis toxin from *Pyrenophora tritici-repentis*. Mol Plant Pathol http://w.bspp.org.uk/mppol/1996/1209ballance/

Bigeard J, Colcombet J, Hirt H (2015) Signaling mechanisms in Pattern-Triggered Immunity (PTI). Mol Plant 8:521–539. https://doi.org/10.1016/j.molp.2014.12.022

Carter AH, Chen XM, Garland-Campbell K, Kidwell KK (2009) Identifying QTL for high-temperature adult-plant resistance to stripe rust (*Puccinia striiformis f. sp. tritici*) in the spring wheat (*Triticum aestivum L.*) cultivar 'Louise.' Theor Appl Genet 119:1119–1128. https://doi.org/10.1007/s00122-009-1114-2

Carter AH, Kidwell KK, DeMacon VL, et al (2020) Registration of the Louise-Penawawa spring wheat recombinant inbred line mapping population. J plant regist 14:474–480. https://doi.org/10.1002/plr2.20077

Cavanagh CR, Chao S, Wang S, et al (2013) Genome-wide comparative diversity uncovers multiple targets of selection for improvement in hexaploid wheat landraces and cultivars. PNAS 110:8057–8062. https://doi.org/10.1073/pnas.1217133110

Chinchilla D, Zipfel C, Robatzek S, et al (2007) A flagellin-induced complex of the receptor FLS2 and BAK1 initiates plant defence. Nature 448:497–500. https://doi.org/10.1038/nature05999

Chu CG, Friesen TL, Faris JD, Xu SS (2008) Evaluation of seedling resistance to tan spot and Stagonospora nodorum blotch in tetraploid wheat. Crop Sci 48:1107. https://doi.org/10.2135/cropsci2007.09.0516

Ciuffetti LM, Tuori RP, Gaventa JM (1997) A single gene encodes a selective toxin causal to the development of tan spot of wheat. Plant Cell 9:135–144. https://doi.org/10.1105/tpc.9.2.135

Effertz RJ, Anderson JA, Francl LJ (2001) Restriction fragment length polymorphism mapping of resistance to two races of *Pyrenophora tritici-repentis* in adult and seedling wheat. Phytopathology 91:572–578. https://doi.org/10.1094/PHYTO.2001.91.6.572

Effertz RJ, Meinhardt SW, Anderson JA, et al (2002) Identification of a chlorosis-inducing toxin from *Pyrenophora tritici-repentis* and the chromosomal location of an insensitivity locus in wheat. Phytopathology 92:527–533. https://doi.org/10.1094/PHYTO.2002.92.5.527

Faris JD, Anderson JA, Francl LJ, Jordahl JG (1997) RFLP mapping of resistance to chlorosis induction by *Pyrenophora tritici-repentis* in wheat. Theor Appl Genet 94:98–103. https://doi.org/10.1007/s001220050387

Faris JD, Liu Z, Xu SS (2013) Genetics of tan spot resistance in wheat. Theor Appl Genet 126:2197–2217. https://doi.org/10.1007/s00122-013-2157-y

Faris JD, Overlander ME, Kariyawasam GK, et al (2020) Identification of a major dominant gene for race-nonspecific tan spot resistance in wild emmer wheat. Theor Appl Genet 133:829–841. https://doi.org/10.1007/s00122-019-03509-8

Faris JD, Zhang Q, Chao S, et al (2014) Analysis of agronomic and domestication traits in a durum × cultivated emmer wheat population using a high-density single nucleotide polymorphism-based linkage map. Theor Appl Genet 127:2333–2348. https://doi.org/10.1007/s00122-014-2380-1

Faris JD, Zhang Z, Lu H, et al (2010) A unique wheat disease resistance-like gene governs effector-triggered susceptibility to necrotrophic pathogens. PNAS 107:13544–13549

Friesen TL, Faris JD (2010) Characterization of the wheat- Stagonospora nodorum disease system: what is the molecular basis of this quantitative necrotrophic disease interaction? Can J of Plant Pathol 32:20–28. https://doi.org/10.1080/07060661003620896

Galagedara N, Liu Y, Fiedler J, et al (2020) Genome-wide association mapping of tan spot resistance in a worldwide collection of durum wheat. Theor Appl Genet 133:2227–2237. https://doi.org/10.1007/s00122-020-03593-1

Gómez-Gómez L, Boller T (2000) FLS2. Molecular Cell 5:1003–1011. https://doi.org/10.1016/S1097-2765(00)80265-8

Hallgren J, Tsirigos KD, Pedersen MD, et al (2022) DeepTMHMM predicts alpha and beta transmembrane proteins using deep neural networks. Bioinformatics

Heffelfinger C, Fragoso CA, Lorieux M (2017) Constructing linkage maps in the genomics era with MapDisto 2.0. Bioinformatics 33:2224–2225. https://doi.org/10.1093/bioinformatics/btx177

Hosford, R.M. Jr. (1982). Tan spot—developing knowledge 1902–1981, virulent races and differentials, methodology, rating systems, other leaf diseases, literature. In: Hosford, RM Jr (ed) Tan spot of wheat and related diseases workshop. North Dakota Agric Exp Station, Fargo, 1–24.

International Wheat Genome Sequencing Consortium (IWGSC) (2014) A chromosome-based draft sequence of the hexaploid bread wheat (*Triticum aestivum*) genome. Science 345:1251788. https://doi.org/10.1126/science.1251788

International Wheat Genome Sequencing Consortium (IWGSC), IWGSC RefSeq principal investigators:, Appels R, et al (2018) Shifting the limits in wheat research and breeding

using a fully annotated reference genome. Science 361:eaar7191. https://doi.org/10.1126/science.aar7191

Kalia B, Bockus WW, Singh S, et al (2018) Mapping of quantitative trait loci for resistance to race 1 of *Pyrenophora tritici-repentis* in synthetic hexaploid wheat. Plant Breed 137:313–319. https://doi.org/10.1111/pbr.12586

Kariyawasam GK, Carter AH, Rasmussen JB, et al (2016) Genetic relationships between race-nonspecific and race-specific interactions in the wheat–*Pyrenophora tritici-repentis* pathosystem. Theor Appl Genet 129:897–908. https://doi.org/10.1007/s00122-016-2670-x

Lamari L, Bernier CC (1989) Virulence of isolates of *Pyrenophora tritici-repentis* on 11 wheat cultivars and cytology of the differential host reactions. Can J of Plant Pathol 11:284–290. https://doi.org/10.1080/07060668909501114

Lamari L, Sayoud R, Boulif M, Bernier CC (1995) Identification of a new race in *Pyrenophora tritici-repentis*: implications for the current pathotype classification system. Can J of Plant Pathol 17:312–318. https://doi.org/10.1080/07060669509500668

Li HB, Yan W, Liu GR, et al (2011) Identification and validation of quantitative trait loci conferring tan spot resistance in the bread wheat variety Ernie. Theor Appl Genet 122:395–403. https://doi.org/10.1007/s00122-010-1455-x

Liu Y, Salsman E, Wang R, et al (2020) Meta-QTL analysis of tan spot resistance in wheat. Theor Appl Genet 133:2363–2375. https://doi.org/10.1007/s00122-020-03604-1

Liu Z, Faris JD, Oliver RP, et al (2009) SnTox3 acts in effector triggered susceptibility to induce disease on wheat carrying the *Snn3* gene. PLoS Pathog 5:e1000581. https://doi.org/10.1371/journal.ppat.1000581

Liu Z, Zurn JD, Kariyawasam G, et al (2017) Inverse gene-for-gene interactions contribute additively to tan spot susceptibility in wheat. Theor Appl Genet 130:1267–1276. https://doi.org/10.1007/s00122-017-2886-4

Long YM, Chao WS, Ma GJ, et al (2017) An innovative SNP genotyping method adapting to multiple platforms and throughputs. Theor Appl Genet 130:597–607. https://doi.org/10.1007/s00122-016-2838-4

Martinez JP, Ottum SA, Ali S, et al (2001) Characterization of the ToxB Gene from *Pyrenophora tritici-repentis*. MPMI 14:675–677. https://doi.org/10.1094/MPMI.2001.14.5.675

Pruitt RN, Schwessinger B, Joe A, et al (2015) The rice immune receptor XA21 recognizes a tyrosine-sulfated protein from a Gram-negative bacterium. Sci Adv 1:e1500245. https://doi.org/10.1126/sciadv.1500245

Rozen S, Skaletsky H (1999) Primer3 on the WWW for general users and for biologist programmers. In: Bioinformatics Methods and Protocols. Humana Press, New Jersey, pp 365–386

Shabeer A, Bockus WW (1988) Tan spot effects on yield and yield components relative to growth stage in winter wheat. Plant Dis 72:599–602. https://doi.org/10.1094/PD-72-0599

Shankar M, Jorgensen D, Taylor J, et al (2017) Loci on chromosomes 1A and 2A affect resistance to tan (yellow) spot in wheat populations not segregating for tsn1. Theor Appl Genet 130:2637–2654. https://doi.org/10.1007/s00122-017-2981-6

Singh PK, Gonzalez-Hernandez JL, Mergoum M, et al (2006) Identification and molecular mapping of a gene conferring resistance to *Pyrenophora tritici-repentis* Race 3 in tetraploid wheat. Phytopathology 96:885–889. https://doi.org/10.1094/PHYTO-96-0885

Singh PK, Hughes GR (2006) Inheritance of resistance to the chlorosis component of tan spot of wheat caused by *Pyrenophora tritici-repentis*, races 1 and 3. Euphytica 152:413–420. https://doi.org/10.1007/s10681-006-9229-x

Singh PK, Mergoum M, Gonzalez-Hernandez JL, et al (2008) Genetics and molecular mapping of resistance to necrosis inducing race 5 of *Pyrenophora tritici-repentis* in tetraploid wheat. Mol Breeding 21:293–304. https://doi.org/10.1007/s11032-007-9129-3

Stadlmeier M, Jørgensen LN, Corsi B, et al (2019) Genetic dissection of resistance to the three fungal plant pathogens *Blumeria graminis* , *Zymoseptoria tritici* , and *Pyrenophora tritici-repentis* using a multiparental winter wheat population. G3: 1745–1757. https://doi.org/10.1534/g3.119.400068

Sun X-C, Bockus W, Bai G (2010) Quantitative trait loci for resistance to *Pyrenophora tritici-repentis* race 1 in a Chinese wheat. Phytopathology 100:468–473. https://doi.org/10.1094/PHYTO-100-5-0468

Tadesse W, Hsam SLK, Wenzel G, Zeller FJ (2006a). Identification and monosomic analysis of tan spot resistance genes in synthetic wheat lines (*Triticum turgidum* L. × *Aegilops tauschii* Coss.). Crop Sci 46:1212–1217. https://doi.org/10.2135/cropsci2005.10-0396

Tadesse W, Hsam SLK, Zeller FJ (2006b) Evaluation of common wheat cultivars for tan spot resistance and chromosomal location of a resistance gene in the cultivar "Salamouni." Plant Breed 125:318–322. https://doi.org/10.1111/j.1439-0523.2006.01243.x

Tadesse W, Reents HJ, Hsam SLK, Zeller FJ (2009) Monosomic analysis of tan spot resistance gene in the winter wheat cultivar 'Arina.' Plant Breed. https://doi.org/10.1111/j.1439-0523.2009.01729.x

Voorrips RE (2002) MapChart: Software for the graphical presentation of linkage maps and QTLs. J Hered 93:77–78. https://doi.org/10.1093/jhered/93.1.77

Williams ND, Miller JD, Klindworth DL (1992) Induced mutations of a genetic suppressor of resistance to wheat stem rust. Crop Sci 32: 612-616

Wu Y, Zhou J-M (2013) Receptor-like kinases in plant innate immunity: RLKs in plant innate immunity. J Integr Plant Biol 55:1271–1286. https://doi.org/10.1111/jipb.12123

Zhang Z, Running KLD, Seneviratne S, et al (2021) A protein kinase–major sperm protein gene hijacked by a necrotrophic fungal pathogen triggers disease susceptibility in wheat. Plant J 106:720–732. https://doi.org/10.1111/tpj.15194

Zurn JD, Newcomb M, Rouse MN, et al (2014) High-density mapping of a resistance gene to Ug99 from the Iranian landrace PI 626573. Mol Breeding 34:871–881. https://doi.org/10.1007/s11032-014-0081-8

5. CLONING OF SUSCEPTIBILITY GENE *Snn5-B1* AND MAPPING OF *Snn5-B2*

5.1. Abstract

The necrotrophic fungal pathogen *Parastagonospora nodorum* produces necrotrophic effectors (NEs) that interact with susceptibility genes in wheat to cause the disease septoria nodorum blotch (SNB). The interaction between the NE SnTox5 and the dominant host susceptibility gene *Snn5* plays a significant role in the development of SNB. *Snn5* was previously mapped to the long arm of chromosome 4B using a doubled haploid (DH) population derived from the SnTox5-insensitive *T. turgidum* ssp. *carthlicum* accession PI 94749 and SnTox5-sensitive durum variety Lebsock. Here, I combined forward and reverse genetics approaches to clone *Snn5* and map an additional SnTox5 sensitivity gene to chromosome 2B using a recombinant inbred line (RIL) population derived from a cross between two durum cultivars, Kronos and Gredho. Given the presence of multiple SnTox5 sensitivity genes, I propose that the original sensitivity gene mapped to chromosome 4B be termed *Snn5-B1* and the second sensitivity gene mapped to the B subgenome be termed *Snn5-B2*. *Snn5-B1* contains both protein kinase and major sperm protein domains, both of which were found to be necessary for function based on analysis of *Snn5-B1* mutant sequences. *Snn5-B2* was delineated to a 8.54 cM interval and explained 53.6% of the variation in sensitivity scores. This research will extend our knowledge of the wheat-*P. nodorum* system and aid in the development of SNB-resistant wheat via genomic selection and/or gene editing.

5.2. Introduction

An estimated 8.8 million metric tons of grain were lost in 2019 due to SNB, enough to bake 12.3 billion loaves of bread (Savary et al. 2019; Wulf and Krattinger 2022). It is likely that this is an underestimation as the estimated yield losses do not account for yield losses due to SNB in Australia, where SNB is prevalent. SNB is caused by the devastating necrotrophic fungal pathogen *P.*

nodorum that infects wheat worldwide. *P. nodorum* produces many NEs that are recognized by wheat genes in an inverse gene-for-gene manner (reviewed by Peters Haugrud et al. 2022). This interaction triggers typical host defense responses, ultimately leading to cell death, which is beneficial to the necrotrophic pathogen that derives nutrients from dying tissue (Liu et al. 2012).

Multiple host-pathogen interactions have been identified in the wheat-*P. nodorum* pathosystem, each contributing significantly to the development of SNB (reviewed by Peters Haugrud et al. 2022). The sixth interaction characterized was the *Snn5-B1*-SnTox5 interaction, formerly the *Snn5*-SnTox5 interaction. Wheat lines carrying the SnTox5 sensitivity gene *Snn5-B1* exhibit necrosis when infected with SnTox5-producing *P. nodorum* isolates and are therefore susceptible (Friesen et al. 2012). *Snn5-B1* was mapped in a DH population, LP749, derived from a cross between Lebsock, a durum wheat, and *T. turgidum* ssp. *carthlicum* accession PI 94749. *Snn5-B1* was mapped to the long arm of chromosome 4B and the *Snn5-B1*-SnTox5 interaction accounted for 37-63% of the variation in disease scores in LP749.

Lebsock has sensitivity genes to NEs SnTox5 (*Snn5-B1*), SnToxA (*Tsn1*) and SnTox3 (likely *Snn3-B1*). As the population would segregate for three sensitivity genes, an isolate, Sn2000KO6-1, which did not produce SnToxA or SnTox3 was used to inoculate the population, isolating the *Snn5-B1*-SnTox5 reaction. When Sn2000KO6-1 was used, the *Snn5-B1*-SnTox5 interaction explained 63% of the variation (Friesen et al. 2012). When the isolate Sn2000, which produces SnToxA and SnTox5, was used, the *Snn5-B1*-SnTox5 interaction explained 37% of the variation. However, the average population disease scores were higher when isolate Sn2000 was used, demonstrating the additive nature of the *Snn5-B1*-SnTox5 and *Tsn1*-SnToxA interactions.

The LP749 population was also inoculated with isolate Sn1501, which produces SnTox5 and SnTox3, and isolate Sn1501ΔTox3, which produces SnTox5, but not SnTox3. The *Snn5-B1*

locus explained 53% of the variation when Sn1501 was used for the inoculations and 51% of the variation when Sn1501ΔTox3 was used (Friesen et al. 2012). The *Snn3-B1* locus only explained 3% of the variation caused by Sn1501. Additionally, disease scores were not significantly different for each genotype class between isolates. However, disease scores and lesion size were more severe when both *Snn5-B1*-SnTox5 and *Snn3-B1*-SnTox3 reactions were present. Inoculations of LP749 with Sn2000 and Sn1501 demonstrate that the *Snn5-B1*-SnTox5 interaction plays a significant role in the development of SNB, even when the isolate produces multiple NEs.

Saturation mapping was previously conducted in the LP7499 population (Sharma unpublished). Twenty-four new STARP, SSR, and indel markers that detected loci near the *Snn5-B1* locus were developed. The map now contains a total of 62 molecular markers with a density of 1.6 cM/marker. *Snn5-B1* was delineated to a 2.9 cM interval corresponding to 1.38 Mb in the Chinese Spring reference v1.0 genome (IWGSC 2018).

Recently, Kariyawasam et al. (2022) conducted a GWAS evaluating the virulence of 197 *P. nodorum* isolates on the SnTox5 differential line, LP29. The marker with the most significant marker-trait association resided inside the candidate gene Sn2000_06735. When Sn2000_06735 was disrupted via CRISPR-Cas9-mediated gene disruption, the isolate was no longer virulent on LP29, thus validating Sn2000_06735 as SnTox5. Gain-of-function transformants of SnTox5 into the avirulent isolate Sn79-1087, Sn79+Tox5-3 further validated the gene. SnTox5 is a 16.26 kDa protein with signal peptide and pro-sequences. Notably, it contains six cysteine residues predicted to form three disulfide bridges in the same position as the previously cloned SnTox3. Although SnTox5 and SnTox3 had only 45.13% homology at the amino acid level, their predicted secondary structures were remarkably similar with the predicted SnTox5 structure and

the crystal structure of SnTox3 having an α-helix and eleven β-strands. Eight of the β-strands form a β-barrel.

The cloning of SnTox5 and production of the gain-of-function transformant Sn79+Tox5-3 allowed the isolation of host sensitivity gene-SnTox5 interactions. Two GWAS evaluating SnTox5 sensitivity have been conducted using Sn79+Tox5-3 culture filtrates. The first study evaluated SnTox5 sensitivity in 510 *Triticum turgidum* ssp. *durum* landraces and cultivars selected from the Global Durum Panel (GDP) (Mazzucotelli et al. 2020). 67% of the GDP was sensitive to SnTox5 and three significant marker-trait associations were identified on the short arm of chromosome 2B, the long arm of chromosome 4B, and the short arm of chromosome 7B with $-\log_{10}(p)$ values of 6.59, 4.90, and 4.81, respectively (Agnes Szabo-Hever personal communication). While the associations on chromosomes 2B and 7B are novel, the association on chromosome 4B corresponds to *Snn5-B1*. This was the first indication of the presence of multiple SnTox5 sensitivity genes in durum wheat.

The second study evaluated SnTox5 sensitivity in a winter wheat panel, consisting of 264 lines from the National Small Grains Collection core global hexaploid winter wheat germplasm collection. 75.6% of the winter wheat panel was sensitive to SnTox5, but no significant marker-trait associations were identified (Peters Haugrud 2021). However, the marker with the highest $-\log_{10}(p)$ value was in the reported *Snn5-B1* region.

My long-term goal is to clone the SnTox5 sensitivity genes to better characterize the interactions between the Tox5 sensitivity genes and SnTox5. Towards this goal, the objectives of the current research were to: 1) identify *Snn5-B1* candidate genes in a wheat reference genome sequence, 2) develop SnTox5 insensitive mutants for candidate gene validation, 3) validate the *Snn5-B1* candidate gene via comparative sequence analysis of SnTox5-insensitive mutants and

wild type sequences, 4) assess SnTox5 sensitivity in the Langdon-*Triticum turgidum* ssp. *dicoccoides* substitution lines to validate the SnTox5 sensitivity loci on chromosomes 2B and 7B in durum wheat, 5) map the SnTox5 sensitivity gene *Snn5-B2* on chromosome 2B in a durum population, and 6) identify candidate genes for *Snn5-B2* in the durum reference genome. Achievement of these goals will further the understanding of *Snn5-B1*-SnTox5 interaction on a molecular level and provides a strong foundation for cloning *Snn5-B2*. Cloning the SnTox5 sensitivity genes would allow us to conduct allelic diversity studies to identify causal mutations that can be targeted for the development of diagnostic molecular markers that can be used for marker-assisted elimination of SnTox5 sensitivity genes, aiding in the development of *P. nodorum* genetically resistant wheat.

5.3. Materials and methods

5.3.1. Plant materials

Previously, saturation mapping of the *Snn5-B1* locus was conducted in a doubled haploid (DH) population (LP749) derived from the SnTox5-insensitive *T. turgidum* ssp. *carthlicum* accession PI 94749 and SnTox5-sensitive durum variety Lebsock (Sharma et al. 2019). Twenty-four previously sequenced *Triticum* genotypes were assessed for SnTox5 sensitivity. The panel of sequenced *Triticum* genotypes included sixteen hexaploid *Triticum aestivum*, one synthetic hexaploid, one *Triticum turgidum* ssp. *dicoccoides*, and four *Triticum turgidum* ssp. *durum* accessions (Table 5.1).

To validate *Snn5-B1*, loss of function mutants were generated and/or identified in three genotypes. First, the *Snn5-B1* differential line, LP29, which carries the *Snn5-B1* allele from Lebsock, was used for ethyl methanesulfonate (EMS) based mutagenesis. Second, TILLING mutants of SnTox5-sensitive bread wheat cultivar Cadenza were ordered from

www.seedstor.ac.uk (Krasileva et al. 2017). Lastly, the SnTox5 sensitivity bread wheat cultivar Fielder was used to generate Cas9-RNP mediated gene knockouts.

Four chromosome substitution lines developed in the durum cultivar Langdon were evaluated to investigate the SnTox5 sensitivity loci identified in the GDP GWAS. The Langdon - *T. turgidum* ssp. *dicoccoides* (LDN-DIC) 2B and 7B substitution lines developed by Dr. Steven Xu and Dr. Leonard R. Joppa which used the *T. turgidum* ssp. *dicoccoides* accessions Israel-A and PI 481521 as the chromosome donors were infiltrated with SnTox5-containing culture filtrates (CFs) (Joppa and Cantrell 1990; Xu et al. 2004; Dr. Steven Xu personal communication).

A *T. turgidum* ssp. *durum* recombinant inbred line (RIL) mapping population (KG) consisting of 149 lines derived from a cross between cultivars Kronos and Gredho was used to map *Snn5-B2*. The KG population was obtained from Dr. Jorge Dubcovsky. Five F_1 plants from Svevo × PI 94749 and Kronos × Gredho were evaluated for SnTox5 sensitivity to determine the dominance of the *Snn5-B2* SnTox5 sensitivity.

Table 5.1. Accessions with published genomic sequences used in this study.

Accession	SnTox5-sensitivity	Species	Reference	doi
ArinaLrFor	I	*T. aestivum*	Walkowiak et al. 2020	10.1038/s41586-020-2961-x
Cadenza	S	*T. aestivum*	Walkowiak et al. 2020	10.1038/s41586-020-2961-x
Cappelli	I	*T. turgidum* ssp. *durum*	IWGSC 2014	10.1126/science.1251788
CDC Landmark	I	*T. aestivum*	Walkowiak et al. 2020	10.1038/s41586-020-2961-x
CDC Stanley	I	*T. aestivum*	Walkowiak et al. 2020	10.1038/s41586-020-2961-x
Chinese Spring	S	*T. aestivum*	IWGSC et al. 2018	10.1126/science.aar7191
Claire	I	*T. aestivum*	Walkowiak et al. 2020	10.1038/s41586-020-2961-x
Fielder	S	*T. aestivum*	Sato et al. 2021	10.1093/dnares/dsab008
Jagger	S	*T. aestivum*	Walkowiak et al. 2020	10.1038/s41586-020-2961-x
Julius	I	*T. aestivum*	Walkowiak et al. 2020	10.1038/s41586-020-2961-x
Kronos*	I	*T. turgidum* ssp. *durum*	-	-
LongReach Lancer	I	*T. aestivum*	Walkowiak et al. 2020	10.1038/s41586-020-2961-x
Mace	S	*T. aestivum*	Walkowiak et al. 2020	10.1038/s41586-020-2961-x
Norin 61	I	*T. aestivum*	Walkowiak et al. 2020	10.1038/s41586-020-2961-x
Paragon	I	*T. aestivum*	Walkowiak et al. 2020	10.1038/s41586-020-2961-x
PI 190962	I	*T. aestivum* ssp. *spelta*	Walkowiak et al. 2020	10.1038/s41586-020-2961-x
Renan	MS	*T. aestivum*	Aury et al. 2022	10.1093/gigascience/giac034
Robigus	I	*T. aestivum*	Walkowiak et al. 2020	10.1038/s41586-020-2961-x
Strongfield	S	*T. turgidum* ssp. *durum*	IWGSC 2014	10.1126/science.1251788
Svevo	S	*T. turgidum* ssp. *durum*	Maccaferri et al. 2019	10.1038/s41588-019-0381-3
SY Mattis	MS	*T. aestivum*	Walkowiak et al. 2020	10.1038/s41586-020-2961-x
W7984	I	Synthetic hexaploid	Chapman et al. 2015	10.1186/s13059-015-0582-8
Weebill 1	S	*T. aestivum*	Walkowiak et al. 2020	10.1038/s41586-020-2961-x
Zavitan	I	*T. aestivum* ssp. *dicoccoides*	Zhu et al. 2019	10.1534/g3.118.200902

*The Kronos genome was assembled by Dr. Jorge Dubcovksy's lab and is available under the Toronto license and can be downloaded from https://opendata.earlham.ac.uk/opendata/data/Triticum_turgidum/EI/v1.1.

5.3.2. SnTox5 infiltrations and *P. nodorum* inoculations

LP29 M_2 families were infiltrated with CFs of *P. nodorum* isolate Sn2000K06-1. CFs were prepared according to Friesen and Faris (2010). Briefly, the isolate was grown on V8-

potato dextrose agar medium for 1 week. Ten milliliters of sterile distilled water were poured over the plate and gently swirled to release the pycnidia into the water. Five hundred microliters of spore suspension were used to inoculate 60 ml of liquid Fries medium. Cultures were grown on an orbital shaker at 100 rpm for a week prior to two weeks of stationary growth under dark conditions at room temperature. Culture filtrates were filtered through a layer of Miracloth (EMD Millipore Corp, MA, USA) and then filtered through .45 µm pore size membrane using vacuum filtration (EMD Millipore Corp, MA, USA).

Recently, *P. nodorum* strain Sn79+Tox5-3 was generated by transforming SnTox5 into the avirulent *P. nodorum* strain Sn79-1087 (Kariyawasam et al. 2022). CFs of strain Sn79+Tox5-3 were used for all further infiltrations. Sn79+Tox5-3 CFs were prepared the same as Sn2000K06-1 CF. However, Sn79+Tox5-3 CFs were concentrated using Amicon Ultracel – 3K centrifugal filters (Merk Millipore Ltd., Cork, Ireland).

In all infiltrations, the differential line LP29 was infiltrated to ensure SnTox5 production and BR34 or PI 94749 were included as SnTox5-insensitive checks. A 1 ml-needleless syringe was used to infiltrate approximately 25-50 µL of CF into the most recently fully expanded leaf of plants during Feekes stage 2, at approximately 2 weeks post planting. Infiltration boundaries were marked with a felt tipped permanent marker. The LP29 M_2 and the Svevo × PI 94749 and Kronos × Gredho F_1 were grown in the greenhouse post infiltration. All other plants were grown in a growth chamber post infiltration. In both the greenhouse and growth chamber, plants were grown at 21˚C with a 16-hour photoperiod.

LP29 M_2 were scored as sensitive or insensitive five days post infiltration with Sn2000K06-1 CF based on the presence or absence of necrosis. All other infiltrations were scored on 0-3 scale, modified from Zhang et al. 2011 by Dr. Sudeshi Seneviratne that includes

intermediate scores between whole numbers where 0 is no disease and 3 is completely necrotic (Sudeshi Seneviratne 2019). The expanded scale allows more accurate scoring of the spectrum of sensitivity reactions. Scores were recorded 5 days post infiltration.

The SnTox5-insensitive LP29, Cadenza, and Fielder mutants were evaluated for susceptibility to SnTox5 producing isolate Sn79+Tox5. Wildtype LP29, Cadenza, and Fielder were included as positive controls and PI 94749 was included as a negative control. Three seeds of each genotype were planted in a single cone. To prepare inoculum, the isolate was grown on V-8 potato dextrose agar for 1 week under 24 hr fluorescent light. Distilled water was poured over the agar plate, releasing spores. 200µL of spore suspension was restreaked onto a new agar plate. Spores were grown under the same conditions as prior for 7 days. Spores were collected and diluted to 10^6 spores/mL. Tween20 was added to the inoculum at a rate of one drop/50 mL of spore suspension. When the second leaf was fully expanded, around two weeks after planting, the plants were inoculated until runoff was observed. An airflow of 17 psi was used. Then plants were put in a misting chamber at 21 °C with constant light. After 24 hours, the plants were moved to a growth chamber at 21 °C and a 12 hr photoperiod. Plants were scored at 7 days post inoculation using the scale described by Liu et al. 2004.

Phenotypic data from the GDP SnTox5 sensitivity GWAS and LP749 saturation mapping project were obtained from Dr. Agnes Szabo-Hever and Sapna Sharma, respectively.

5.3.3. Genotyping

Genotypic data from the GDP SnTox5 sensitivity GWAS and LP749 saturation mapping project were obtained from Dr. Agnes Szabo-Hever and Sapna Sharma, respectively. The KG population was genotyped with the 90K iSelect SNP genotyping array (Wang et al., 2014) at the USDA ARS small grains genotyping laboratory, Fargo, ND, USA, and the whole genome map

was assembled by Gurminder Singh. Exome capture data generated by the WheatCAP project are viewable on the Chinese Spring RefSeq 1.0 Jbrowse and available in the Wheat T3 database (https://wheat.triticeaetoolbox.org/). Reported SNPs in the exome capture data were used to infer *Snn5-B1* alleles.

5.3.4. *Snn5-B1* candidate gene identification

The saturated genetic map of the *Snn5-B1* region in the LP749 population was obtained from Sapna Sharma. The primer sequences of the markers cosegregating with and flanking *Snn5-B1* were used in a BLASTn search against the Chinese Spring genome assembly RefSeq 1.0 to obtain the physical position of each marker. The physical order of the markers was compared to the genetic order of the markers to identify rearrangements. Then, markers outside rearrangements were selected to delineate the candidate gene region.

The nucleotide and protein sequences of the high confidence annotated genes in the candidate gene region of Chinese Spring RefSeq Annotation v1.1 were obtained from Ensembl. Hmmscan was used to identify Pfam protein domains in the protein sequences (https://www.ebi.ac.uk/Tools/hmmer/search/hmmscan). Pfam domains with e-values of at least 1×10^{-5} were considered significant. SnTox5 was found to show structural similarity to SnTox3 (Kariyawasam et al. 2022). Given the possibility that the corresponding host-sensitivity genes also showed structural similarity, the protein sequence of *Snn3-D1* (Zhang et al. 2021) was used in a tBLASTn search of the candidate gene region in the Chinese Spring RefSeq v1.0 assembly to identify homologs. The reported peptide sequence of the *Snn3-D1* homologs were aligned to the *Snn3-D1* peptide sequence to assess sequence coverage and the level of identity and similarity.

5.3.5. Generation and identification of *Snn5-B1* mutants

5.3.5.1. LP29 Mutagenesis

The line LP29, selected from the LP749 population, carries the functional *Snn5-B1* allele inherited from Lebsock. LP29 seeds were treated with 0.25% ethyl methanesulfonate in 0.05 M phosophate buffer as described in Williams et al. 1992. Fourteen LP29 M_2 seeds were planted per M_2 family and the second emerged leaf was infiltrated with Sn2000K06-1 CF. Reactions were scored 5 days post infiltration. Insensitive plants were transplanted, infiltrated a second time to confirm insensitivity, and self-pollinated. LP29 M_3 and M_4 were infiltrated with Sn79+Tox5-3 and scored at 3 days.

5.3.5.2. Selection of Cadenza TILLING mutants

The nucleotide sequences of TraesCS4B02G343100 and TraesCS4B02G343200 were used in a BLASTn search of a scaffold level assembly of bread wheat Cadenza, which was available through the Toronto agreement on the Earlham Institute's Grassroots Infrastructure website. The Cadenza assembly was later published (Walkowiak et al. 2020). TILLING mutants were selected with mutations in TraesCS4B02G343100 and TraesCS4B02G343200 genes on Ensembl. Stop mutations, splice-site variants, and missense mutations with predicted deleterious effects were prioritized for selection. Fifteen mutants were ordered with reported mutations in TraesCS4B02G343100 and twenty mutants were ordered with reported mutants in TraesCS4B02G343200. One mutant ordered had reported mutations in both genes.

5.3.5.3. Cas9-RNP mediated gene knockouts

Additionally, Cas9-RNP mediated gene knockouts in the cultivar Fielder were generated by Snigdha Poddar (Poddar et al. 2022). Two guide RNA were designed, each targeting a 20 bp sequence in exon 2 of TraesCS4B02G343100. Cas9 and the gRNA were delivered as pre-

assembled ribonucleoproteins via particle bombardment. T_0 plants were infiltrated with CF of Sn79+Tox5-3 and assessed for sensitivity to validate the *Snn5-B1* candidate gene. In this study, T_1 plants from six independent T_0 plants with bialleleic or homozygous mutations were infiltrated with CF of Sn79+Tox5-3.

5.3.6. *Snn5-B1* sequencing

Snn5-B1 was amplified in three overlapping fragments via PCR and sequenced with 5 primers (Table 5.2). Primers were designed from the Chinese Spring RefSeq v1.0 genome assembly (IWGSC 2018) to amplify TraesCS4B02G343100 using NCBI Primer 3 (Rozen and Skaletsky 1999). TraesCS4B02G343100 was amplified from SnTox5-insensitive LP29 mutants, LP29, Fielder, Cadenza, LP749 population parents, and nine durum cultivars selected from the GDP. Sensitive sister lines of the segregating TraesCS4B02G343100 Cadenza TILLING mutant families were also sequenced. A minimum of two biological replicates and two technical replicates per amplicon were sequenced from the LP29ems and Cadenza TILLING lines. One biological replicate was sequenced for all other accessions. All sequencing reactions were 20 µL and consisted of 400 ng of template DNA, 1× PCR buffer, 1.5 mM $MgCl_2$, 0.125 mM dNTPs, 8 nmol of each primer, and 2 units of Taq polymerase. A touchdown PCR program was used with an initial denaturation at 94°C for 5 min, followed by 35 cycles of 94°C for 30 s, an annealing temperature starting at 61°C that decreased by 0.2°C each cycle for 30 seconds, and a 72°C extension for 2 min, followed by a final extension at 72°C for 7 min. 7µL of each PCR produce was electrophoresed on a 1% agarose gel to confirm amplification. The remaining PCR product was purified with ExoSAP IT (Thermo Fisher Scientific, Waltham, Massachusetts, USA). PCR products were sequenced with primers reported in Table 5.2 via Sanger sequencing (Eurofins Genomics, Louisville, KY, USA). TraesCS4B02G343100 was assembled for each sample in

CodonCode Aligner 7.1.2 and point mutations were identified by comparative sequence analysis (CodonCode Corporation, Centerville, Massachusetts, USA, http://www.codoncode.com/aligner/). Fielder knockout mutants were sequenced in Podder et al. (2022).

To determine gene structure, mRNA was extracted from Cadenza using the RNeasy Mini Kit (Qiagen, Hilden, Germany) and *Snn5-B1* cDNA was synthesized using SuperScript™ III One-Step RT-PCR System with Platinum™ Taq DNA Polymerase (Thermo Fisher Scientific, Waltham, Massachusetts, USA) following the manufacturer's protocol. Each 50 ul reaction mixture contains 2 μg of the RNA template, 1 μL of 10uM Snn5 gene specific primers Snn5.cDNA.42F and Snn5.3UTR.R1, 2 μL of SuperScript™ III One-Step RT-PCR System with Platinum™ Taq DNA Polymerase, and 25 μL of 2X reaction mix. The cDNA synthesis and PCR amplification were performed in a single tube with the following program: Starting with incubation at 55°C for 30 min followed by 95°C for 2 min for cDNA synthesis and denature, then proceed with 40 cycles of denaturing at 95 °C for 15", annealing at 60°C for 30", and extension at 68°C for 3 min. The program ended with a final extension step at 68 for 5 min.

To achieve *Snn5-B1* gene specific amplification, the above PCR products were used for an 80-fold dilution. A nested PCR was performed using 2 ul of the diluted products and gene specific nested primers Snn5cDNA.69F and Snn5.stopR. The rest of PCR ingredients in the total volume of 50 μl reaction include 1X PCR buffer, 1.5 mM MgCl2, 0.125 mM dNTPs, 0.4 uM of each primer and 5 unit of Taq DNA polymerase. A touchdown PCR program was used for the nested PCR: starting with denaturing at 94 °C for 5 min, followed by 35 cycles of 94 °C for 30 s, an initial annealing temperature 61°C with a temperature decrement of 0.2 °C each cycle for 30 s, and 72 °C extension for 3 min, followed by a final extension of 72 °C for 7 min. The PCR

products were separated on a 2% agarose gel and stained with ethidium bromide (Sigma-Aldrich, St. Louis, Missouri, USA). The PCR products were visualized and extracted from the gel using Promega Wizard™ SV Gel and PCR Clean-Up System (Fisher Scientific, Waltham, Massachusetts, USA) and sent to Eurofins Genomics (Louisville, KY, USA) for Sanger sequencing.

Table 5.2. Primers used for amplification and sequencing of *Snn5-B1* genomic DNA and cDNA

Purpose	Forward	Reverse
Genomic DNA amplification	*Snn5-B1_gDNA_F1 CTTTTGCTGAGAAAGAAAAAGCA	*Snn5-B1_gDNA_R1 TCAGGAACAGTTCACTAAGCATGT
	*Snn5-B1_gDNA_F2 ATGTCGTTTTGGTGTGATGAATAC	*Snn5-B1_gDNA_R2 TACAGGGGTTGTATAATGGAAAGG
	*Snn5-B1_gDNA_F3 CTAGTTCTCCATTGTATGGAACGA	Snn5-B1_gDNA_R3 TTGATAGACCTCCTTTATCTGGTG
cDNA amplification	Snn5.B1.cDNA.42F TTTGCAGATAAGGTTGGCAGTG	Snn5.B1.3UTR.R1 CTCAACAAGGCCTAACCGTCTT
	Snn5.B1.cDNA.69F* GTATGGTGAAGTTTACAAG	Snn5.B1.stopR* CTATCAGCCTAGAACTTGGTC

The asterisk indicates primers that were used for sequencing.

5.3.7. *Snn5-B1* allele identification and haplotype analysis

The coding sequence and nucleotide sequences of *Snn5-B1* in Cadenza were aligned to the nucleotide sequences of *Snn5-B1* in 35 other accessions to identify nucleotide polymorphisms that could alter the peptide sequence. Of these 36 accessions, 24 have available genome sequences (Table 5.1). *Snn5-B1* alleles in the accessions with available genome sequences were identified using BLASTn searches on Ensembl plants (https://plants.ensembl.org/), Graingenes (https://wheat.pw.usda.gov/blast/), URGI (https://urgi.versailles.inrae.fr/blast/), or the CerealsDB (https://www.cerealsdb.uk.net/cerealgenomics/CerealsDB/blast_WGS.php). The assembly of Renan was downloaded from http://www.genoscope.cns.fr/plants/ (Aury et al. 2021) and a local

BLAST database was constructed using BLAST+ (Camacho et al. 2009). The *Snn5-B1* sequences of the remaining accessions were amplified and sequenced in this study. Amino acid substitutions and deletions were identified by translating the inferred coding sequences using the Expasy translate tool (https://web.expasy.org/translate/) and aligning the peptide sequences to the translated Cadenza Snn5-B1 peptide sequence using Clustal Omega (https://www.ebi.ac.uk/Tools/msa/clustalo/). The 36 accessions were all evaluated for SnTox5 sensitivity and designated insensitive, moderately sensitive, or sensitive corresponding to sensitivity scores 0 to ≤1, 1 to ≤2, and 2 to ≤3.

5.3.8. Evaluation of SnTox5 sensitivity marker-trait association haplotypes in the Global Durum Panel

Accessions in the GDP were assigned an MTA haplotype based on the presence of the alleles associated with sensitivity for each of the peak SnTox5 sensitivity markers on chromosomes 2B, 4B, and 7B. Counts were calculated for each MTA and MTA haplotype to assess how common MTA or particular combinations of MTA were in the GDP. A box and whisker plot was constructed displaying the distribution of the average SnTox5 sensitivity scores across six experimental replicates within each MTA haplotype in Excel using the inclusive method to calculate interquartile ranges. To determine if the mean sensitivity scores for each MTA haplotype were significantly different from one another, a means separation analysis was determined using Fisher's protected LSD at $\alpha=0.05$ using SPSS 28. Becasue a different number of accessions belong to each MTA haplotype, the LSD was specific to the pair of haplotypes being compared.

5.3.9. Mapping of *Snn3-B2* in the Kronos × Gredho population

SnTox5 reaction scores from the three replicates were tested for homogeneity with Barlett's Chi-Squared test in JMP Pro 15. Homogenous replicates were combined to calculate mean sensitivity scores for each RIL. QTL detection used the genetic map constructed by Gurminder Singh. Genomic regions associated with SnTox5 sensitivity in the KG population were identified by regressing the mean sensitivity scores against the genotypic data. QTL analysis was performed using the computer program Qgene v 4.4.0 (Joehanes and Nelson 2008). Single-Trait Multiple Interval Mapping (STMIM) was used to identify QTL associated with sensitivity. The forward cofactor selection method and an interval of 2 cM were used. A permutation test of 1000 iterations was used to identify the critical LOD threshold at the 0.01 level of probability. The coefficient of determination (R^2) was used to indicate the amount of variation in sensitivity scores explained by the QTL. Single-marker regression was used to identify the marker with the strongest association with SnTox5 sensitivity.

5.3.10. *Snn5-B2* candidate gene identification

The probe sequences of the markers flanking and within the SnTox5 sensitivity loci identified in the KG population were used in a BLASTn search of the Svevo Rel 1.0 genome assembly to identify the physical position of the markers (Maccaferri et al. 2019). The positions of the markers significantly associated with SnTox5 sensitivity on chromosome 2B in the KG population and the GDP GWAS were compared. The markers flanking the *Snn5-B2* peak in the KG QTL analysis (IWB7661 and IWB10434) were selected to define the candidate gene region. As the previous SnTox5 sensitivity gene had both protein kinase (PK) and major sperm protein (MSP) domains, genes in the candidate gene region with the same protein domains were considered strong candidates. PK-MSP genes within the candidate gene region were extracted

from the Svevo Rel 1.0 genome assembly by filtering the annotated genes based on physical position and the MSP protein domain ID, IPR000535, using BioMart (https://plants.ensembl.org/biomart). Unspliced transcript, coding sequences, and protein sequences for each of the PK-MSP transcripts within the candidate gene region were also extracted using BioMart.

Transcripts with no overlap among coding sequences were treated as separate genes, rather than alternate transcripts for further analysis. Candidate gene sequences were compared between sequenced durum accessions Svevo and Kronos.

5.4. Results

5.4.1. SnTox5 sensitivity in sequenced wheat genotypes

Phenotyping of sequenced lines was conducted in two stages. Initially, bread wheats Chinese Spring and Cadenza and *T. turgidum* spp. *durum* cultivar Kronos were evaluated for SnTox5 sensitivity to determine if they carried functional SnTox5 sensitivity genes. These cultivars were selected for their genetic and genomic resources. In 2017, Krasileva et al. published TILLING populations of Cadenza and Kronos, and in 2018 and genome assemblies were available for Cadenza and Chinese Spring. Both Cadenza and Chinese Spring infiltrations were necrotic by three days post infiltration, indicating that both carried a functional SnTox5 sensitivity gene (Figure 5.1). Later, an additional twenty-one sequenced lines were evaluated for sensitivity to SnTox5 (Table 5.1). Thirteen sequenced accessions were insensitive to SnTox5. Eight sequenced accessions showed sensitivity and three showed moderate sensitivity.

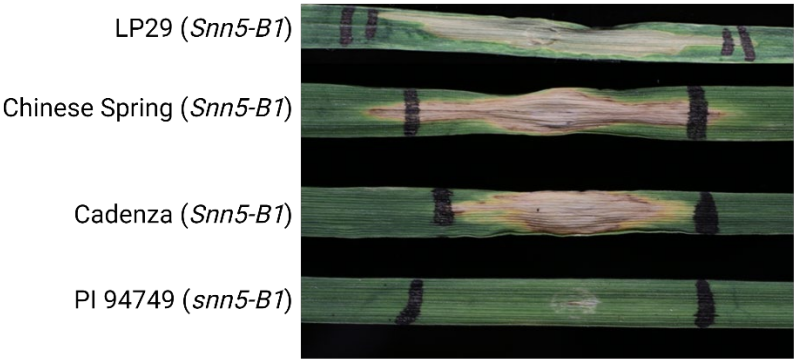

Figure 5.1. Evaluation of SnTox5 sensitivity in Chinese Spring and Cadenza.
Infiltration of Chinese Spring and Cadenza with CF of Sn79+Tox5-3 indicated that both were sensitive to SnTox5.

5.4.2. Identification of *Snn5-B1* candidate genes

Snn5-B1 was previously mapped to the long arm of chromosome 4B in LP749 (Friesen et al. 2012). Sapna Sharma developed a saturated genetic map consisting of 62 molecular markers and delineated *Snn5-B1* to a 2.9 cM interval (Sharma 2019). A comparison of the genetic order and physical order of the markers cosegregating and flanking *Snn5-B1* revealed an inversion between markers *fcp760* and *fcp761* (Figure 5.2). The closest markers flanking *Snn5-B1* and outside this inversion, *fcp759* and *fcp764*, were selected to delineate the candidate gene region.

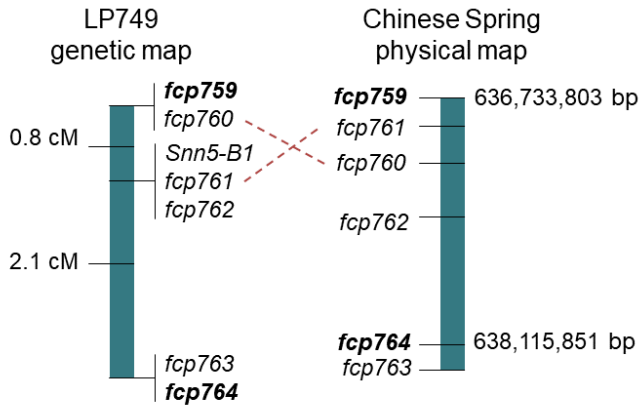

Figure 5.2. Comparison of genetic and physical order of markers cosegregating and flanking *Snn5-B1*.
The genetic order of markers in LP749 is shown on the left, while the physical order of the markers in Chinese Spring RefSeq v1.0 is shown on the right. Dashed lines connect markers that are inverted between the genetic and physical maps. Bold markers are the physically closest flanking markers delineating the candidate gene region.

Within the 1.38 Mb candidate gene region, a total of 20 high confidence genes were identified in the RefSeq Annotation v1.1 (Table 5.3). A BLASTn search of the *Snn3-D1* nucleotide sequence against the candidate gene region in the Chinese Spring assembly identified two homologs, TraesCS4B02G343100 and TraesCS4B02G343200 (Figure 5.3). Both genes contained MSP and protein kinase PK domains, but TraesCS4B02G343200 contained additional Rx N-terminal and NB-ARC domains. TraesCS4B02G343100 and TraesCS4B02G343200 had predicted peptide sequences of 452 and 1409 amino acid, respectively. An alignment of the peptide sequences of TraesCS4B02G343100 and TraesCS4B02G343200 to the peptide sequence of *Snn3-D1* revealed higher coverage and identity between TraesCS4B02G343100 and *Snn3-D1* compared to the alignment of TraesCS4B02G343200 and *Snn3-D1*. Query coverage was 98% with 47% amino acid identity and 64% amino acid positives in the TraesCS4B02G343100 and *Snn3-D1* alignment. Query coverage in the TraesCS4B02G343200 and *Snn3-D1* alignment was 29% and amino acid

Table 5.3. *Snn5-B1* candidate genes in Chinese Spring.

Gene	Transcription start site	Transcription stop site	Pfam accessions	Pfam descriptions
TraesCS4B02G342800	636737253	636738575	PF03514.17	GRAS domain family
TraesCS4B02G342900	636781857	636783655	none	
TraesCS4B02G343000	636799150	636802057	PF00999.24	Sodium/hydrogen exchanger family
TraesCS4B02G343100	636916138	636918886	PF00069.28, PF07714.20, PF00635.29	Protein kinase domain, Protein tyrosine and serine/threonine kinase,
TraesCS4B02G343200	636921012	636932262	PF00069.28, PF07714.20, PF00931.25, PF18052.4, PF00635.29	Protein kinase domain, Protein tyrosine and serine/threonine kinase, NB-ARC domain, Rx N-terminal domain, MSP (Major sperm protein) domain
TraesCS4B02G343285	636969901	636970569	PF13041.9, PF12854.10, PF01535.23, PF13812.9, PF17177.7	PPR repeat family, PPR repeat, Pentatricopeptide repeat domain, Pentacotripeptide-repeat region of PRORP
TraesCS4B02G343287	636970983	636971456	PF12854.10, PF13041.9, PF01535.23, PF13812.9,	PPR repeat, PPR repeat family, Pentatricopeptide repeat domain
TraesCS4B02G343307	636980768	636981553	PF13041.9, PF12854.10, PF17177.7, PF13812.9	PPR repeat family, PPR repeat, Pentacotripeptide-repeat region of PRORP, Pentatricopeptide repeat domain
TraesCS4B02G343309	636981647	636982072	PF12854.10, PF13041.9, PF01535.23, PF13812.9, PF17177.7	PPR repeat, PPR repeat family, Pentatricopeptide repeat domain, Pentracotripeptide-repeat region of PRORP
TraesCS4B02G343300	636982115	636984919	PF12854.10, PF13041.9, PF01535.23, PF13812.9, PF17177.7	PPR repeat, PPR repeat family, Pentatricopeptide repeat domain, Pentracotripeptide-repeat region of PRORP
TraesCS4B02G343500	637333392	637337190	none	
TraesCS4B02G343600	637345811	637346289	PF04727.16	ELMO/CED-12 family
TraesCS4B02G343700	637385777	637388761	PF06101.14	Vacuolar protein sorting-associated protein 62
TraesCS4B02G343800	637389539	637396491	PF00005.30, PF00664.26	ABC transporter, ABC transporter transmembrane region
TraesCS4B02G344000	637621554	637622958	PF00249.34, PF13921.9	Myb-like DNA-binding domain
TraesCS4B02G344100	637623712	637628173	PF00092.31, PF13768.9, PF13519.9, PF14624.9, PF05762.17, PF17123.8, PF13639.9, PF00097.28	von Willebrand factor type A domain, VWA / Hh protein intein-like, VWA domain containing CoxE-like protein, RING-like zinc finger, Ring finger domain, Zinc finger, C3HC4 type (RING finger)
TraesCS4B02G344200	637722285	637725028	PF00092.31, PF13768.9, PF14624.9, PF13519.9, PF05762.17, PF17123.8, PF13639.9, PF00097.28	von Willebrand factor type A domain, VWA / Hh protein intein-like, VWA domain containing CoxE-like protein, RING-like zinc finger, Ring finger domain, Zinc finger, C3HC4 type (RING finger)
TraesCS4B02G344300	637736691	637739835	PF01373.20	Glycosyl hydrolase family 14
TraesCS4B02G344400	637979318	637981133	PF01157.21	Ribosomal protein L21e
TraesCS4B02G344500	638115620	638120497	PF08242.15, PF13649.9, PF13489.9, PF10294.12, PF13847.9, PF08241.15	Methyltransferase domain, Lysine methyltransferase

identity and positives were 33% and 51%, respectively. The lower query coverage in the TraesCS4B02G343200 and *Snn3-D1* alignment was expected as the additional Rx N-terminal and NB-ARC domains present in TraesCS4B02G343200 are absent in *Snn3-D1*.

The shared PK and MSP domains between TraesCS4B02G343100, TraesCS4B02G343200, and *Snn3-D1* made TraesCS4B02G343100 and TraesCS4B02G343200 highly attractive candidate genes. Additionally, the previously cloned SNB susceptibility genes *Snn1*, *Tsn1*, and *Snn3-D1* all contained PK domains and TraesCS4B02G343100 and TraesCS4B02G343200 were the only candidate genes with PK domains. Thus, these genes were the primary candidates.

5.4.3. Validation of *Snn5-B1* candidates

Five hundred eighty-five LP29 M_2 families were infiltrated with CF of SnTox5-producing *P. nodorum* isolate Sn2000K06-1, and five independent families segregating for sensitivity were identified (Table 5.4). Evaluation of M_3 generations with Sn79+Tox5-3 CF confirmed insensitivity to SnTox5. Sequencing of TraesCS4B02G343100 from SnTox5 insensitive mutants revealed all mutants had a single nonsynonymous SNP in the gene. All mutations identified in LP29 SnTox5-insensitive mutant lines were missense mutations with three being in the PK domain and two in the MSP domain.

A total of 34 Cadenza TILLING lines were evaluated for sensitivity to SnTox5 with 14 of the lines having reported mutations in the first PK-MSP gene, TraesCS4B02G343100, but not in TraesCS4B02G343200. 19 of the lines had mutations in the second PK-MSP gene, TraesCS4B02G343200, but not in TraesCS4B02G343100, and one line had mutations in both genes. Fourteen seeds of each TILLING line were planted for evaluation, but two lines displayed very poor germination and only three plants were infiltrated. Both of these lines had mutations in

TraesCS4B02G343200, but not in TraesCS4B02G343100. Of the remaining 17 TILLING lines with mutations in TraesCS4B02G343200, but not in TraesCS4B02G343100, all were sensitive to SnTox5. Notably, eight of these sensitive families were reported to have nonsense mutations.

Within the 14 TILLING lines with mutations in TraesCS4B02G343100, but not in TraesCS4B02G343200, eight were completely sensitive. Five of the remaining families were completely insensitive or segregating for sensitivity. Three of these mutants had nonsense mutations, one had a missense mutation, and one had a predicted splice acceptor mutation (Table 5.4). Lines that were completely insensitive or segregating for sensitivity had mutations in both the PK and MSP domains. One line, Cadenza0024, had a missense mutation that caused a predicted splice acceptor mutation. Some individuals in this family had reduced sensitivity but were not completely insensitive. The single line with missense mutations in both candidate genes segregated for reduced sensitivity, but no plants were completely insensitive.

Snn5-B1 candidate TraesCS4B02G343100 was knocked out via Cas9-RNP mediated gene knockout in Podder et al. (2022). A total of 10 M_0 plants were generated with homozygous or biallelic mutations. Six of these M_0 plants were infiltrated with Sn79+Tox5 to confirm that disrupting *Snn5-B1* resulted in insensitivity to SnTox5. Seed was obtained from six independent M_0 plants. All M_1 were insensitive to Sn79+Tox5-3 CF (Table 5.4).

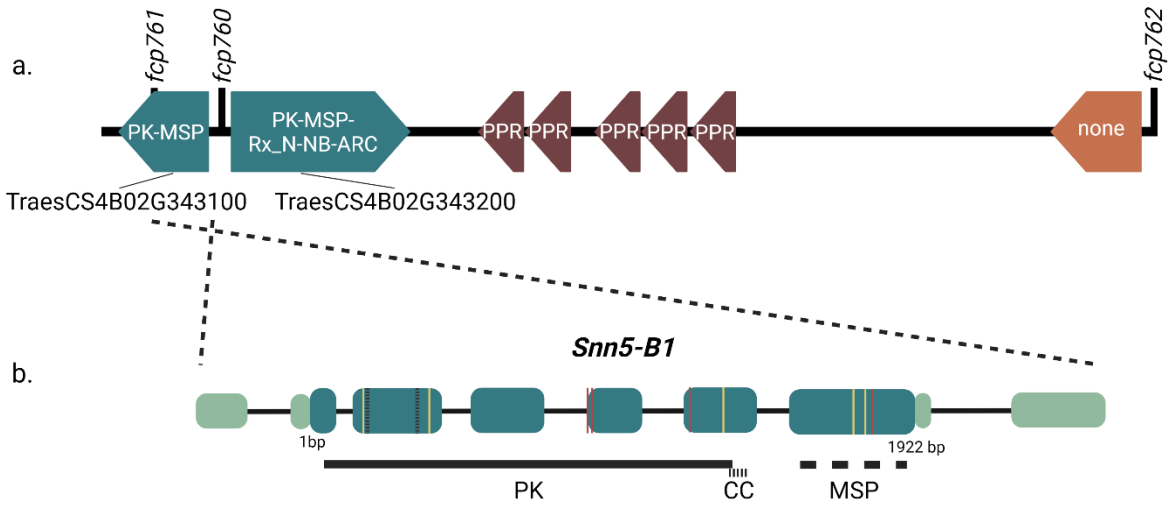

Figure 5.3. *Snn5-B1* candidate genes.
a. High-confidence genes and markers cosegregating with the *Snn5-B1* locus in the LP749 population. PK, MSP, Rx_N, NB-ARC, and PRR corresponds to protein kinase, major sperm protein, Rx N-terminal domain, NB-ARC, and Pentatricopeptide repeat domains, respectively. b. Structure of *Snn5-B1*. Yellow and red vertical bars represent the locations of mutants in SnTox5-insensitive LP29ems and Cadenza TILLING lines, respectively. The purple dashed vertical line in exon 2 represents the location gRNA targeted in Cas9-RNP mediated gene knockout of *Snn5-B1*.

Table 5.4. SnTox5-insensitive *Snn5-B1*-disrupted mutants and their amino acid changes

Source	Mutant Line	Location	Type	Amino acid change	Domain
Cas9-RNP mediated gene knockout	Fielder 6.1-3	Exon 2	Biallelic frameshift (-5 bp, -1 bp)		PK
	Fielder 2.4-4	Exon 2	homozygous frameshift (-10 bp, -10 bp)		PK
	Fielder 3.3-2	Exon 2	Biallelic frameshift (+1 bp, -2 bp)		PK
	Fielder 6.3-4	Exon 2	Biallelic frameshift (-11 bp, -6 bp)		PK
	Fielder 2.4-2	Exon 2	Biallelic frameshift (-2 bp, -8 bp) + substitutions		PK
	Fielder 6.1-4	Exon 2	Biallelic frameshift (-8 bp, -3 bp)		PK
TILLING mutants	Cadenza0300	Intron 3	Splice acceptor variant*	-	-
	Cadenza1733	Exon 4	Missense	P198S	PK
	Cadenza0610	Exon 5	Stop gained	W249STOP	PK
	Cadenza1531	Exon 5	Stop gained	W249STOP	PK
	Cadenza1470	Exon 6	Stop gained	Q403STOP	MSP
EMS population	LP29ems509	Exon 2	Missense	L48F	PK
	LP29ems464	Exon 2	Missense	L99F	PK
	LP29ems459	Exon 5	Missense	V269M	PK
	LP29ems438	Exon 6	Missense	G378R	MSP
	LP29ems399	Exon 6	Missense	A394V	MSP

The LP29, Cadenza, and Fielder SnTox5-insensitive mutants were inoculated with Sn79+Tox5-3 to evaluate susceptibility to an SnTox5-producing isolate. Unfortunately, only three of the LP29 mutants grew. No plants of LP29ems459 or LP29ems438 grew. All mutants saw a reduction in susceptibility compared to their corresponding wild types (Figure 5.4). Of the wild type genotypes, LP29 was the most susceptible with a score of 4. Cadenza and Fielder had scores of 3 and 2, respectively. Cadenza0300, the Cadenza TILLING line with a predicted splice-site mutation, had a score of 2. This was higher than the other Cadenza TILLING mutants, but still less than wild type Cadenza. As evident in Figure 5.4, Cadenza0300 produces very narrow leaves. This abnormal leave architecture could interfere with disease reactions.

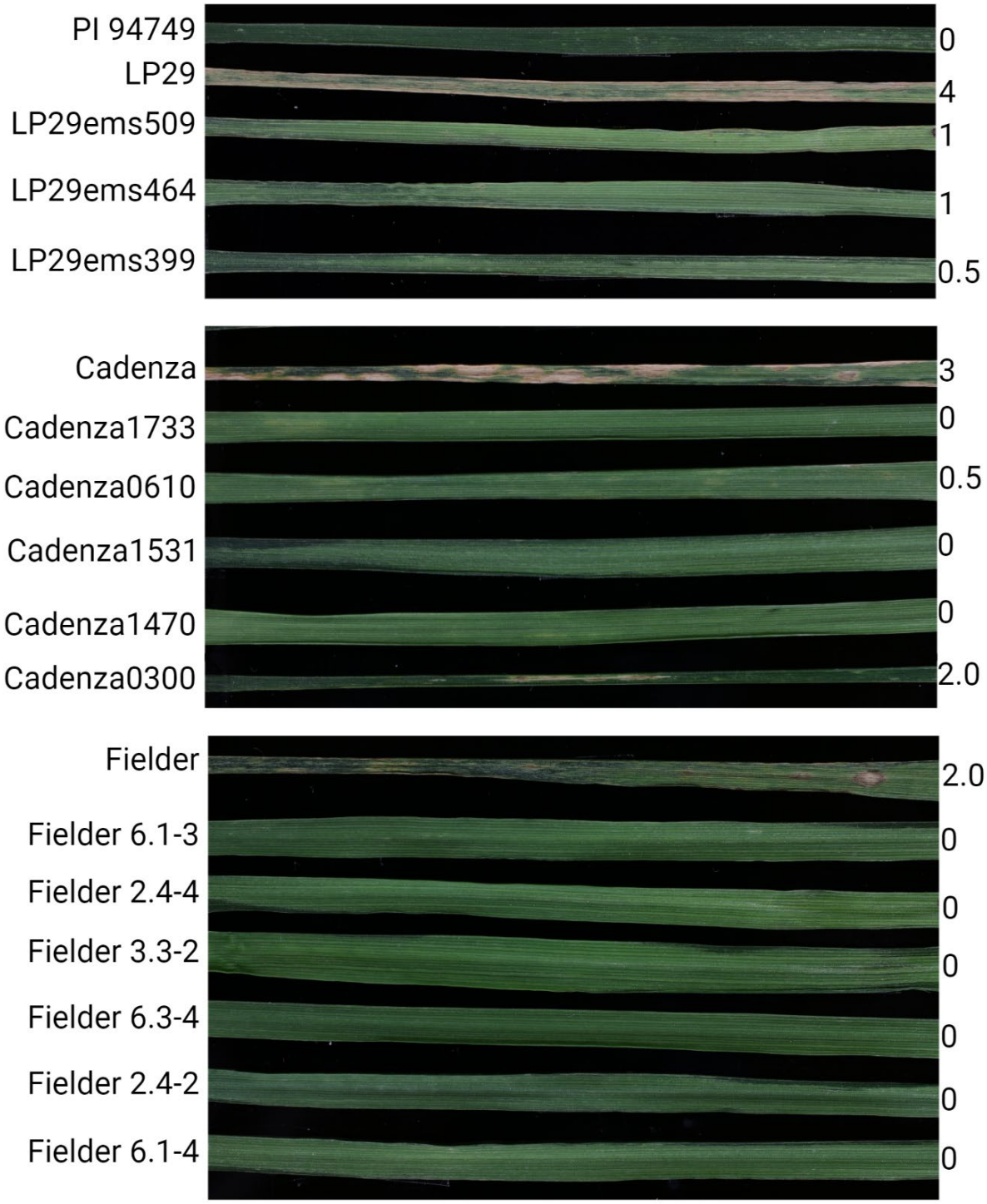

Figure 5.4. Inoculation of SnTox5-insensitive mutants.
Genotypes are labeled to the left of the leave photographs. The disease score for each genotype is right of the leaves.

5.4.4. Haplotype analysis

The *Snn5-B1* coding sequences from 36 accessions were compared to identify polymorphisms between the accessions. Five nonsynonymous SNPs were identified within the predicted coding sequences including a nonsynonymous SNP in exon 1 resulting in a glycine to glutamate substitution (G23E). A nonsynonymous SNP in exon 3 results in an alanine to valine substitution (A188V). Two SNPs in exon 5 result in alanine to glycine and alanine to aspartate substitutions (A251G and A283D). One nonsynonymous SNP in exon 6 results in an arginine to cysteine substitution (R419C). The substitutions in exons 1, 3, and 5 are within the predicted PK domain whereas the substitution in exon 6 is within the predicted MSP domain.

In addition to the nonsynonymous SNPs identified, a large deletion of 283 bp spanning part of intron 5 and exon 6 was identified in PI 94749. Forty-eight bases of the deletion are in the intron, and the remaining 235 bases of the deletion are in exon 6. The deletion disrupts the splice site and introduces a frameshift mutation resulting in a premature stop codon. In absence of sequencing cDNA of *Snn5-B1* from PI 94749, an alignment of the haplotype 1 amino acid sequence and the PI 94749 sequence assuming the unlikely event that despite the disruption of the splice site, part of exon 6 is included in the coding sequence (Figure 5.5). Despite the assumption that part of exon 6 is still transcribed, exon 6 of PI 94749 contains only two of the 133 amino acids in exon 6 of the functional allele of *Snn5-B1*. Consequently, the entire MSP domain is deleted in PI 94749. As such, this polymorphism, identified only in PI 94749 will be referred to as -MSP.

```
PI94749         MDIEFHLLETITNKFADKVGSGGYGEVYKGLYNGKEIAVKRLHPLQGLDDKAFDSEFRNL 60
Haplotype1      MDIEFHLLETITNKFADKVGSGGYGEVYKGLYNGKEIAVKRLHPLQGLDDKAFDSEFRNL 60
                ************************************************************

PI94749         SKVKHKNVVQLLGYCYQIVKKFVPYNGELVMAMEMERILCFEYMEGGSLDKHIGDESCGL 120
Haplotype1      SKVKHKNVVQLLGYCYQIVKKFVPYNGELVMAMEMERILCFEYMEGGSLDKHIGDESCGL 120
                ************************************************************

PI94749         DWQSCYQIIKGTCDGLNHLHGAHEKPIFHLDLKPSNILLDKNSRTAKIADLGLSRLVAST 180
Haplotype1      DWQSCYQIIKGTCDGLNHLHGAHEKPIFHLDLKPSNILLDKNSRTAKIADLGLSRLVAST 180
                ************************************************************

PI94749         ETHKTQMANVKGTIGYMPPEYIDGGYISKKYDVFSLGVIILKIMTGNKGHSRCYEMPQEQ 240
Haplotype1      ETHKTQMANVKGTIGYMPPEYIDGGYISKKYDVFSLGVIILKIMTGNKGHSRCYEMPQEQ 240
                ************************************************************

PI94749         FTKHVIENWEARLQGTSGYSSHQNDILQVKKCIEIAVECVEKARYKRPLIKDIVHQLEEL 300
Haplotype1      FTKHVIENWEARLQGTSGYSSHQNDILQVKKCIEIAVECVEKARYKRPLIKDIVHQLEEL 300
                ************************************************************

PI94749         EAKIKEMSLYSDMPIDLTGQR---------------------------------------- 321
Haplotype1      EAKIKEMSLYSDMPIDLTGQTSSNYNILAVDPAIELRFLFEPRKDISTCMQLTNQTDGSV 360
                ********************

PI94749         ------------------------------------------------------------ 321
Haplotype1      AFRVITNQAKYSVQPTKGIMAPCSKRYIYVTLRAQDAAPLNMQCNDMFVVQSTRVNDGRT 420


PI94749         --------------------------------   321
Haplotype1      SDGIADDEVMAGTAVGMVRLPIVYVGCDQVLG   452
```

Figure 5.5. Alignment of PI 94749 and Haplotype 1 *Snn5-B1* amino acid sequences. The highlighted portion indicates the 133 amino acids translated from exon 6 of *Snn5-B1*.

Five amino acid haplotypes were identified, with Haplotype 1 being the functional *Snn5-B1* allele identified and validated in LP29, Cadenza, and Fielder (Table 5.5). Haplotype 1 was found in 15 accessions, 12 of which were *T. aestivum* cultivars. Two *T. turgidum* ssp. *durum* cultivars, Lebsock and CBW_09034, an Argentinian cultivar, and the SnTox5 differential line LP29, which inherited *Snn5-B1* from Lebsock, also had Haplotype 1. Within Haplotype 1, five cultivars (Paragon, LongReach Lancer, Claire, Renan, and CBW_09034) were insensitive to SnTox5. The remaining 10 accessions were moderately sensitive or sensitive.

Haplotype 2, containing polymorphism G23E, was only present in bread wheat cultivar Norin 61, which was insensitive to SnTox5. Haplotype 3, containing substitution A283D, was not present in any bread wheat accessions but was found in nine durum cultivars and the

synthetic hexaploid line W7984 and the spelt wheat line PI 190961. As W7984 is a synthetic hexaploid, it inherited its *Snn5-B1* allele from a durum accession (Altar84). Haplotype 3 included six insensitive and five sensitive accessions. Eight accessions belong to haplotype 4, which has polymorphisms A188V, A251G, A283D, and R419C. Of these eight accessions, four were bread wheat cultivars, one was a wild emmer accession, and three were durum cultivars. The last haplotype, Haplotype 5, contains the -MSP polymorphism where the entire MSP domain is deleted. The only accession in Haplotype 5 was PI 94749, the insensitive parent in the LP749 population.

The only sensitive bread wheats had Haplotype 1, but not every bread wheat with Haplotype 1 was sensitive. Sensitive durum cultivars had Haplotypes 1 and 3. No single SNP within the coding sequence was predictive of SnTox5 insensitivity.

Table 5.5. Inferred *Snn5-B1* amino acid haplotypes.

haplotype	Accession	Species	SnTox5 sensitivity*	G23E	A188V	A251G	A283D	R419C	-MSP
				Exon 1	Exon 3	Exon 5		Exon 6	
1	Paragon	*T. aestivum*	I	-	-	-	-	-	-
	LongReach Lancer	*T. aestivum*	I	-	-	-	-	-	-
	Claire	*T. aestivum*	I	-	-	-	-	-	-
	Julius	*T. aestivum*	I	-	-	-	-	-	-
	CBW_09034	*T. turgidum* ssp. *durum*	I	-	-	-	-	-	-
	Renan	*T. aestivum*	MS	-	-	-	-	-	-
	SY Mattis	*T. aestivum*	MS	-	-	-	-	-	-
	Chinese Spring	*T. aestivum*	S	-	-	-	-	-	-
	Cadenza	*T. aestivum*	S	-	-	-	-	-	-
	Jagger	*T. aestivum*	S	-	-	-	-	-	-
	Mace	*T. aestivum*	S	-	-	-	-	-	-
	Weebill 1	*T. aestivum*	S	-	-	-	-	-	-
	Fielder	*T. aestivum*	S	-	-	-	-	-	-
	LP29	*T. turgidum ssp carthicum* × *T. turgidum* ssp. *durum*	S	-	-	-	-	-	-
	Lebsock	*T. turgidum* ssp. *durum*	S	-	-	-	-	-	-
2	Norin 61	*T. aestivum*	I	+	-	-	-	-	-
3	W7984	synthetic hexaploid	I	-	-	-	+	-	-
	Kronos	*T. turgidum* ssp. *durum*	I	-	-	-	+	-	-
	WID_802	*T. turgidum* ssp. *durum*	I	-	-	-	+	-	-
	Olimpik	*T. turgidum* ssp. *durum*	I	-	-	-	+	-	-
	Cappelli	*T. turgidum* ssp. *durum*	I	-	-	-	+	-	-
	PI 190961	*T. spelta*	I	-	-	-	+	-	-
	Svevo	*T. turgidum* ssp. *durum*	S	-	-	-	+	-	-
	Lahn	*T. turgidum* ssp. *durum*	S	-	-	-	+	-	-
	Arcobaleno	*T. turgidum* ssp. *durum*	S	-	-	-	+	-	-
	IDSN46-7013	*T. turgidum* ssp. *durum*	S	-	-	-	+	-	-
	Strongfield	*T. turgidum* ssp. *durum*	S	-	-	-	+	-	-
4	CDC Landmark	*T. aestivum*	I	-	+	+	+	+	-
	Robigus	*T. aestivum*	I	-	+	+	+	+	-
	CDC Stanley	*T. aestivum*	I	-	+	+	+	+	-
	Zavitan	*T. aestivum* ssp. *dicoccoides*	I	-	+	+	+	+	-
	Sohag4	*T. turgidum* ssp. *durum*	I	-	+	+	+	+	-
	ESDCB-2015/2016-31	*T. turgidum* ssp. *durum*	I	-	+	+	+	+	-
	JUPARE_C2001	*T. turgidum* ssp. *durum*	I	-	+	+	+	+	-
	Arina*LrFor*	*T. aestivum*	I	-	+	+	+	+	-
5	PI 94749	*T. turgidum* ssp. *carthicum*	I	-	-	-	-	-	+

*I, MS, and S indicate insensitive, moderately sensitive, and sensitive, respectively.

5.4.5. SnTox5 sensitivity in the Global Durum Panel

Three significant associations with SnTox5 sensitivity were identified previously in the GDP in a GWAS conducted by Dr. Agnes Szabo-Hever. Of the 510 accessions included in the study, 322, 247, and 80 accessions had the marker alleles associated with sensitivity for the peak associations on chromosomes 7B, 2B, and 4B, respectively. Each accession was assigned an MTA haplotype based on the presence of the peak markers associated with SnTox5 sensitivity. The range of phenotypic scores within each haplotype was very similar, with all haplotypes having individuals with SnTox5 sensitivity scores less than 0.2 and greater than 2.5 (Figure 5.6). Despite the similar ranges of phenotypic scores, the distributions of the phenotypic scores were different, demonstrated by the different sized interquartile ranges for the haplotypes. The 4B/7B haplotype, in particular, had a larger interquartile range, with 50% of the accessions having scores between 0.29 and 3. Haplotype 2B/4B/7B had the smallest interquartile range with 50% of the accessions having scores between 2.83 and 3.

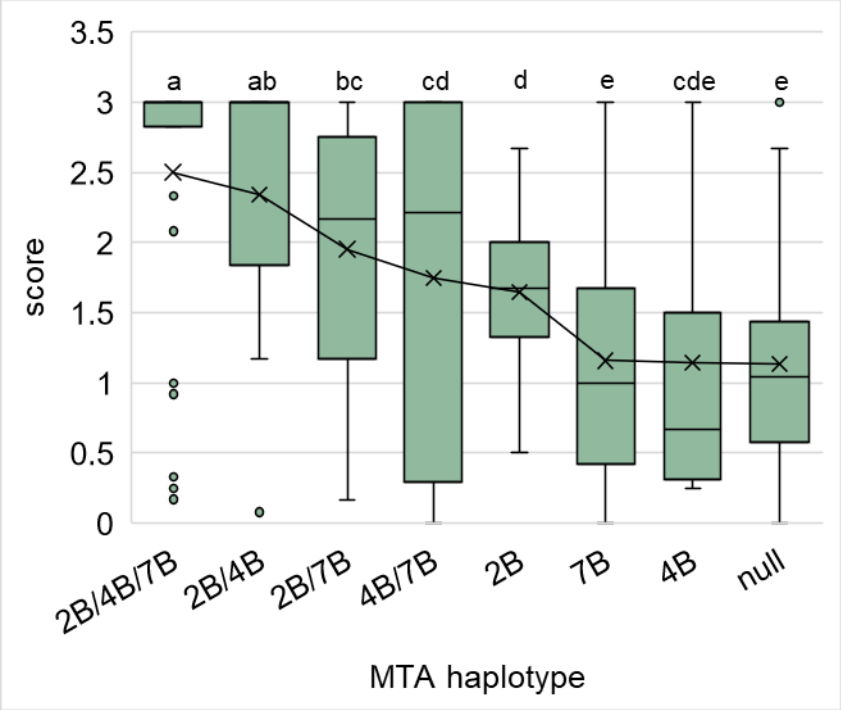

Figure 5.6. Distribution of SnTox5 sensitivity scores within the GDP.
The box represents the range of the middle 50% of the data for each haplotype. Lines extending from the boxes represent the full range of phenotypic scores for a haplotype. Outliers are denoted as a single dot. Phenotypic means are marked with an "X". Haplotypes with the same lowercase letter at the top of the chart are not significantly different at the 0.05 level of probability.

To identify significant differences among phenotypic means between MTA haplotypes, Fisher's protected LSD was calculated at an α level of 0.05 (Table 5.6). Because each haplotype had a unique number of accessions, an LSD value was calculated for each comparison of means. In general, the more MTAs in the haplotype, the higher the average SnTox5 sensitivity score, suggesting that the MTAs may be additive. The only single MTA with a mean SnTox5 sensitivity significantly different than the mean of the null haplotype was the 2B haplotype. The mean score for 7B and 4B haplotypes were not significantly different from each other or the null haplotype, which did not have the 2B, 4B, or 7B MTA, indicating that alone, neither significantly contributes to sensitivity to SnTox5 in the GDP. However, the 4B haplotype was incredibly rare with just four genotypes having only the 4B MTA. Additionally, the null

haplotype had a mean score of 1.14, with 15 individuals having a sensitivity score greater than 1.5. The presence of strong sensitivity in some lines with the null haplotype suggests that these individuals have SnTox5 sensitivity loci not detected in the GDP GWAS, potentially due to their relative rarity.

Table 5.6. MTA haplotypes and mean SnTox5 sensitivity scores in the GDP

MTA haplotype	N[+]	Mean[*]
2B, 4B, 7B	29	2.5a
2B, 4B	11	2.31ab
2B, 7B	103	1.95bc
4B, 7B	36	1.75cd
2B	113	1.65d
7B	154	1.16e
4B	4	1.15cde
none	60	1.14e

[+]Number of accessions with the GDP with a particular MTA haplotype
*Means followed the same letter are not significantly different at the 0.05 level of probability. The error term is Mean Square(Error) = 0.718.

The SnTox5-insensitive *T. turgidum* ssp *durum* cultivar Svevo, which has the 2B/7B haplotype, was crossed to the SnTox5-insensitive *Triticum turgidum* ssp. *carthlicum* accession PI 94749 to assess the dominance of the SnTox5 sensitivity loci. F_1 plants were sensitive when infiltrated with CF of Sn79+Tox5, indicating that sensitivity to SnTox5 is dominant. However, due to the presence of two sensitivity loci in the sensitive parent, I cannot conclude whether sensitivity is the dominant trait conferred by one or both of the sensitivity loci.

5.4.6. Evaluation of SnTox5 sensitivity in Langdon- *Triticum turgidum* ssp *dicoccoides* substitution lines

The North Dakota durum cultivar Langdon (*T. turgidum* ssp. *durum*) was included in the GDP. Its marker alleles at the three significant associations indicated that Langdon had the 2B/7B haplotype, and therefore lacked the 4B association with SnTox5. To test if SnTox5

sensitivity was conferred by the 2B or 7B association or both, Langdon-*T. dicoccoides* (Israel A) and Langdon-*T. dicoccoides* (PI 48521) substitution lines were evaluated for SnTox5 sensitivity. When infiltrated, Langdon developed necrosis while the two *Triticum turgidum* ssp. *dicoccoides* accessions were completely insensitive (Figure 5.7). Both Langdon-DIC2B(Israel A) and Langdon-DIC2B(PI 481521) were less sensitive than Langdon or the 7B substitution lines, indicating the presence of a major SnTox5 sensitivity locus on chromosome 2B. Given the confirmation of the SnTox5 sensitivity locus on chromosome 2B, this locus was given the gene designation *Snn5-B2*, referring to the second SnTox5 sensitivity locus identified in the B subgenome of wheat.

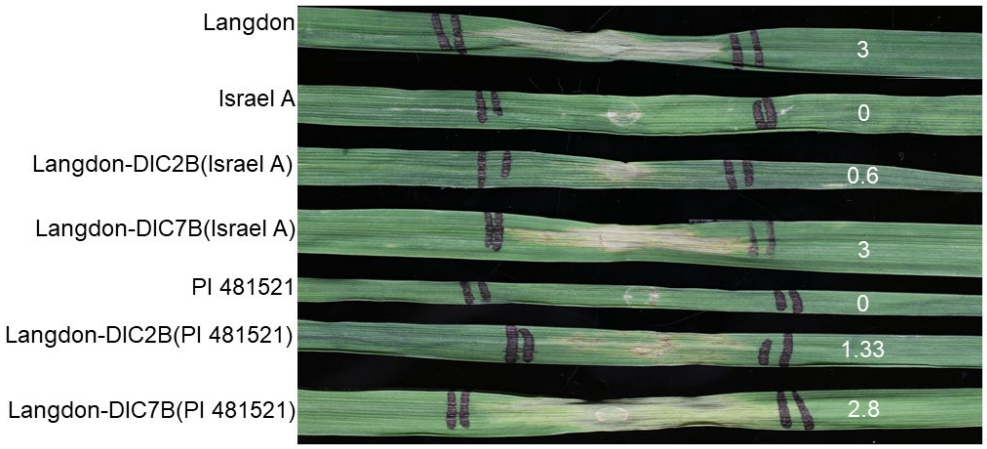

Figure 5.7. Evaluation of SnTox5 sensitivity in Langdon-*Triticum turgidum* ssp. *dicoccoides* substitution lines.
Genotypes are displayed to the left of the leaf photographs. The average sensitivity score corresponding to each genotype is displayed on the leaf to the right of the infiltration site.

5.4.7. SnTox5 sensitivity in the Kronos × Gredho population

When infiltrated with Sn79-Tox5-3 culture filtrate, Kronos had a very light sensitivity, with only light chlorosis developing, whereas Gredho developed strong necrosis (Figure 5.8). Kronos × Gredho F_1 plants were sensitive to SnTox5, indicating that sensitivity is conferred by a dominant gene.

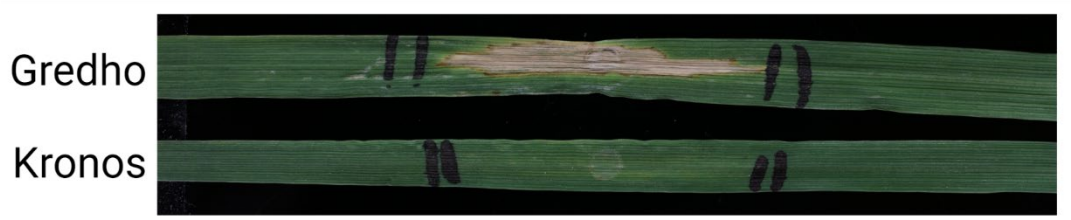

Figure 5.8. Evaluation of SnTox5 sensitivity in durum cultivars Gredho and Kronos. Gredho, top, developed necrosis when infiltrated with Sn79-Tox5-3 CF, while Kronos, bottom, did not.

Three replicates of the KG population were infiltrated with Sn79+Tox5-3. Bartlett's Chi-squared test for homogeneity of variance among the three replicates indicates the replicates were not significantly different (P=0.2026). Therefore, the sensitivity scores from the replicates were combined to calculate a mean score for each line, which was used for QTL mapping. For STMIM, the LOD significance threshold, $\alpha_{0.01} = 5.845$, was determined using a permutation test with 1000 iterations. A single QTL was identified at 6 cM on the short arm of chromosome 2B with a LOD of 24.84 that explained 53.6% of the variation in sensitivity scores (Figure 5.9). The QTL was just 4 cM, ranging from 4-8 cM using STMIM. However, the closest flanking markers were at 3.66 and 12.20 cM, spaning 8.54 cM.

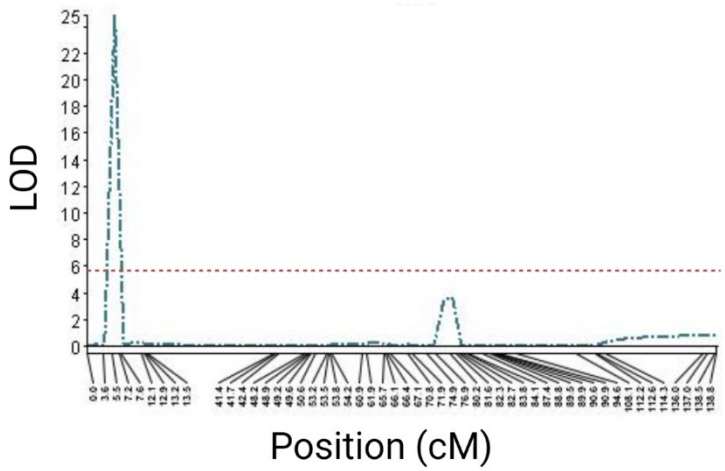

Figure 5.9. Single-trait multiple interval regression maps of chromosome 2B associated with sensitivity to SnTox5 sensitivity in Kronos × Gredho.
The dashed red line represents the significant LOD threshold of 5.845. The teal dashed line represents the LOD of the markers at each position.

5.4.8. Identification of *Snn5-B2* candidate genes

The probe sequences of the markers flanking and inside the 2B QTL identified in the KG QTL analysis were used in a BLASTn search of the Svevo Rel 1.0 genome assembly to determine the physical location of the markers (Maccafferi et al. 2019). No rearrangements were detected in the candidate gene region between the KG genetic map and the physical map, indicating the closest marker physically at the flanking marker genetic positions could be used to define the candidate gene region (Table 5.7). Distal to the QTL, two markers cosegregated at 3.66 cM, IWB7661 and IWB8365. The IWB8365 marker detected a SNP at 8.63 Mb. The IWB7661 probe sequence aligns to two positions, 8.64 and 9.08 Mb. To be cautious, the 8.64 Mb position was selected as the distal flanking marker position as it yielded the larger candidate gene region. IWB10434 at 23.87 Mb flanked the QTL on the proximal side, yielding a QTL spanning 15.23 Mb. Three peak markers, IWB72374, IWA2304, and IWA2303 cosegregated at 5.52 cM. IWA2304 and IWA2303 both detected SNPs at 15.71 Mb. IWB72374 detected SNPs at 15.69 and 16.46 Mb. All peak marker positions resided within the MTA region identified on

chromosome 2B in the GDP GWAS, which was at physical position 12.13-16.95 Mb. Therefore, both analyses likely detected the same SnTox5 sensitivity gene, *Snn5-B2*.

Table 5.7. Genetic and physical locations of markers near the *Snn5-B2* candidate gene region.

Marker	Genetic position (cM)	Physical position (bp)
IWB26054	0.00	5,376,052
IWB50555	0.00	5,376,216
IWB7669	0.00	5,443,355
IWB8365	3.66	8,627,591
IWB7661	3.66	8,642,366/9,081,690
IWB72374	**5.52**	**15,685,641/ 16,455,054**
IWA2304	**5.52**	**15,711,334**
IWA2303	**5.52**	**15,711,695**
IWB60877	7.30	17,825,520
SNPIDX227	7.64	18,336,769
IWB8851	7.64	19,752,176
IWB24437	7.64	21,592,167
IWB10434	12.20	23,873,757
IWB10512	12.90	24,313,794
IWB9352	12.90	24,748,387

Physical positions refer to the position on chromosome 2B in the Svevo Rel 1.0 genome assembly (Maccaferri et al. 2019). The peak markers identified by STMIM QTL analysis and their position in the KG genetic map and physical positions are bolded. The flanking makers, their genetic positions, and the physical position used to define the candidate gene region are underlined.

The candidate gene region contained 232 genes in the Svevo annotation. Given the evidence that *Snn5-B1* contained PK and MSP domains, further analysis focused on candidate genes with those domains. Four genes were found within the candidate gene region that contained PK and MSP domains with a total of 24 reported splice variants (Table 5.8). The third gene in the region, TRITD2Bv1G007390, was 176,042 bp long, much longer than the other PK-MSP genes. Analysis of the splice variants of this gene indicated there may be three separate PK-

MSP genes. TRITD2Bv1G007370, TRITD2Bv1G007400, and TRITD2Bv1G007700 each had only one PK and MSP domain.

Table 5.8. *Snn5-B2* candidate genes.

Gene ID	Position	Gene length (bp)
TRITD2Bv1G007370	15,585,810-15,587,738	1,928
TRITD2Bv1G007390	15,630,524-15,806,566	176,042
TRITD2Bv1G007400	15,630,833-15,632,470	1,637
TRITD2Bv1G007700	16,234,121-16,236,263	2,141

The candidate genes identified in Svevo Rel 1.0 were used in a BLASTn search of the Kronos scaffold level assembly, available under the Toronto license (Maccaferri et al. 2019, https://opendata.earlham.ac.uk/opendata/data/Triticum_turgidum/EI/v1.1.). All genes were either null or significantly diverged in Kronos. TRITD2Bv1G007370 and the 2nd and 3rd potential gene within TRITD2Bv1G007390 are likely null in Kronos as no BLASTn hit was found with sequence identity greater than 90%. TRITD2Bv1G007400, the first gene within TRITD2Bv1G007390, and TRITD2Bv1G007700 are potentially present, but significantly diverged, as the best hits for these genes were between 97 and 98%. All six PK-MSP genes remain candidates and require further analysis.

5.5. Discussion

The SnTox5 sensitivity gene, *Snn5-B1* on chromosome 4B, was cloned in this study. *Snn5-B1* was found to contain PK and MSP domains, which is the same set of protein domains as were found in *Snn3-D1* (Zhang et al. 2022). Three mutants, Cadenza1470, LP29ems438, and LP29ems399, with mutations in the MSP domain of *Snn5-B1* were insensitive to SnTox5, indicating that the MSP domain is required for *Snn5-B1* function. *Snn5-B1* and *Snn3-D1* are the only PK-MSP susceptibility genes cloned so far. However, an orange wheat blossom midge

resistance gene, *Sm1*, was found to contain an MSP domain, in addition to NLR and kinase domains (Walkowiak et al. 2020). The function of the MSP domain is unknown in *Snn5-B1*, *Snn3-D1*, and *Sm1*. The MSP domain has been found to mediate motility in nematode sperm, form immunoglobulin-like folds and symmetric dimers, and play a role in mediating protein-protein interactions (Tarr and Scott 2005; Kaiser et al. 2005). In plants, MSP domains have been identified in vesicle-associated membrane protein association proteins (VAPs). VAPs confer the formation of membrane contact sites between the endoplasmic reticulum and other organelles or the plasma membrane by mediating protein-protein interactions (reviewed by James and Kehlenbach et al. 2021). Indeed, fluorescent tagging of VAP genes identified in *Arabidopsis* and expressed in *Nicotiana benthamiana* revealed the localization of VAP to the endoplasmic reticulum, plasma membrane, and the contact sites between them (Wang et al. 2016). The *Nicotiana benthamiana* VAP gene VAP27 was found to interact with the tomato Cf9 protein, which recognized the effector Avr9 to confer resistance to *Cladosporium fulvum* in a gene-for-gene manner (Laurent et al. 2000). Like other VAP genes, VAP27 had an N-terminal MSP, central coiled coil, and C-terminal transmembrane domain.

Snn5-B1 does not have the transmembrane domain, but it does have coiled-coil and MSP domains. Although *Snn5-B1* is likely not membrane bound, it is possible that it mediates protein-protein interactions like the VAP and MSP genes. However, at this time the alternate possibility that *Snn5-B1* interacts indirectly with SnTox5, possibly as a guard, cannot be discounted. Further characterization of the function of the MSP domain in *Snn5-B1* is required to understand the molecular mechanisms by which *Snn5-B1* confers sensitivity to SnTox5.

Inoculation of the *Snn5-B1* mutant Cadenza TILLING, LP29 EMS, and Fielder Cas9-RNP mediated gene knockout lines demonstrated a reduction in disease compared to non-

mutagenized Cadenza, LP29, and Fielder. The reduction of disease in *Snn5-B1* mutants suggests that the mutants interfered with the ability of SnTox5 to use *Snn5-B1* to cause disease, further demonstrating that necrotrophs use NE to target host-sensitivity gene to cause disease and induce cell death, which is required for the growth of necrotrophic pathogens. Repeated inoculations would allow quantification of the reduction in disease.

A previous GWAS of SnTox5 sensitivity in the GDP determined that 67% of the panel was sensitive to SnTox5. Sequencing of *Snn5-B1* alleles from eight accessions included in the GDP indicated that the *Snn5-B1* allele was not predictive of sensitivity to SnTox5. GWAS identified three peaks on chromosomes 2B, 4B (*Snn5-B1*), and 7B. Analysis of the phenotypic means for accessions with different MTA haplotypes identified significant differences in phenotypic means. Interestingly, of the haplotypes with only a single MTA, the 2B haplotype was the only haplotype with a single MTA with a phenotypic mean significantly different than the phenotypic mean of the haplotype with no MTA. *Snn5-B1* was first mapped in durum cultivar Lebsock, where it was the only significant SnTox5 sensitivity locus identified. So, it was surprising that only 4/510 durum accessions had the 4B haplotype. Previously, it was suspected that SnTox5 sensitivity in durum was likely due to *Snn5-B1*, as was observed in Lebsock.

Haplotype analysis did not identify an individual SNP in *Snn5-B1* that was solely predictive of SnTox5 insensitivity. In fact, some bread and durum wheat with the *Snn5-B1* functional allele were insensitive. As such, no diagnostic marker for SnTox5 sensitivity was developed in this study. Sequence analysis of a greater number of *Snn5-B1* alleles from durum and bread wheat may inform how different polymorphisms affect sensitivity to SnTox5. However, given the relative rarity of the 4B MTA in durum, it is likely that *Snn5-B1* markers alone would be inadequate at predicting SnTox5 sensitivity.

Work is ongoing to develop a population segregating for all three sensitivity loci to better quantify the affect each locus has on sensitivity to SnTox5. Additional populations are being developed to map SnTox5 sensitivity in cultivars that do not have the 2B, 4B, or 7B associations and to map the 7B association. The frequency of SnTox5 sensitivity is not yet evaluated in hard red spring wheat, but work is initiated.

The cloning of *Snn5-B1* allows for the sequencing and identification of alleles associated with insensitivity that can be targeted for the development of diagnostic molecular markers. The cloning of *Snn5-B1* and mapping of *Snn5-B2* add to the understanding of SnTox5 sensitivity in wheat.

5.6. Literature cited

Aury J-M, Engelen S, Istace B, et al (2022) Long-read and chromosome-scale assembly of the hexaploid wheat genome achieves high resolution for research and breeding. GigaScience 11:giac034. https://doi.org/10.1093/gigascience/giac034

Camacho C, Coulouris G, Avagyan V, et al (2009) BLAST+: architecture and applications. BMC Bioinformatics 10:421. https://doi.org/10.1186/1471-2105-10-421

Chapman JA, Mascher M, Buluç A, et al (2015) A whole-genome shotgun approach for assembling and anchoring the hexaploid bread wheat genome. Genome Biol 16:26. https://doi.org/10.1186/s13059-015-0582-8

Friesen TL., Chu C, Xu SS, Faris JD (2012) SnTox5- *Snn5*: a novel *Stagonospora nodorum* effector-wheat gene interaction and its relationship with the SnToxA- *Tsn1* and SnTox3- *Snn3* - *B1* interactions: Characterization of the SnTox5- Snn5 interaction. Molecular Plant Pathology 13:1101–1109. https://doi.org/10.1111/j.1364-3703.2012.00819.x

James C, Kehlenbach RH (2021) The interactome of the VAP family of proteins: an overview. Cells 10:1780. https://doi.org/10.3390/cells10071780

Joppa, L. R., and Cantrell, R. G. 1990. Chromosomal location of genes for grain protein content of wild tetraploid wheat. Crop Sci. 30:1059-1064

Kaiser SE, Brickner JH, Reilein AR, et al (2005) Structural basis of FFAT motif-mediated ER targeting. Structure 13:1035–1045. https://doi.org/10.1016/j.str.2005.04.010

Kariyawasam GK, Richards JK, Wyatt NA, et al (2022) The *Parastagonospora nodorum* necrotrophic effector SnTox5 targets the wheat gene *Snn5* and facilitates entry into the leaf mesophyll. New Phytologist 233:409–426. https://doi.org/10.1111/nph.17602

Krasileva KV, Vasquez-Gross HA, Howell T, et al (2017) Uncovering hidden variation in polyploid wheat. Proc Natl Acad Sci USA 114(6): 913-921. https://doi.org/10.1073/pnas.1619268114

Laurent F, Labesse G, de Wit P (2000) Molecular cloning and partial characterization of a plant VAP33 homologue with a major sperm protein domain. Biochem. Biophys. Res. Commun. 270:286–292. https://doi.org/10.1006/bbrc.2000.2387

Maccaferri M, Harris NS, Twardziok SO, et al (2019) Durum wheat genome highlights past domestication signatures and future improvement targets. Nat Genet 51:885–895. https://doi.org/10.1038/s41588-019-0381-3

Peters Haugrud, A (2021). Mapping and characterization of yield component traits and Septoria nodorum blotch susceptibility in wheat. North Dakota State University

Peters Haugrud AR, Zhang Z, Friesen TL, Faris JD (2022) Genetics of resistance to septoria nodorum blotch in wheat. Theor Appl Genet. https://doi.org/10.1007/s00122-022-04036-9

Sato K, Abe F, Mascher M, et al (2021) Chromosome-scale genome assembly of the transformation-amenable common wheat cultivar 'Fielder.' DNA Research 28:dsab008. https://doi.org/10.1093/dnares/dsab008

Savary S, Willocquet L, Pethybridge SJ, et al (2019) The global burden of pathogens and pests on major food crops. Nat Ecol Evol 3:430–439. https://doi.org/10.1038/s41559-018-0793-y

Seneviratne, S (2019). Genomic analysis of septoria nodorum blotch susceptibility genes *Snn1* and *Snn2* in wheat. North Dakota State University

Sharma, S (2019) *Genetics of Wheat Domestication and Septoria Nodorum Blotch Susceptibility in Wheat*. North Dakota State University

Tarr D, Scott A (2005) MSP domain proteins. Trends in Parasitology 21:224–231. https://doi.org/10.1016/j.pt.2005.03.00

The International Wheat Genome Sequencing Consortium (IWGSC), Appels R, Eversole K, et al (2018) Shifting the limits in wheat research and breeding using a fully annotated reference genome. Science 361:eaar7191. https://doi.org/10.1126/science.aar7191

The International Wheat Genome Sequencing Consortium (IWGSC), Mayer KFX, Rogers J, et al (2014) A chromosome-based draft sequence of the hexaploid bread wheat (*Triticum aestivum*) genome. Science 345:1251788. https://doi.org/10.1126/science.1251788

Walkowiak S, Gao L, Monat C, et al (2020) Multiple wheat genomes reveal global variation in modern breeding. Nature 588:277–283. https://doi.org/10.1038/s41586-020-2961-x

Wang P, Richardson C, Hawkins TJ, et al (2016) Plant VAP 27 proteins: domain characterization, intracellular localization and role in plant development. New Phytol 210:1311–1326. https://doi.org/10.1111/nph.13857

Williams ND, Miller JD, Klindworth DL (1992) Induced mutations of a genetic suppressor of resistance to wheat stem rust. Crop Sci 32: 612-616

Wulff BB, Krattinger SG (2022) The long road to engineering durable disease resistance in wheat. Curr Opin in Biotechnol 73:270–275. https://doi.org/10.1016/j.copbio.2021.09.002

Xu SS, Khan K, Klindworth DL, et al (2004) Chromosomal location of genes for novel glutenin subunits and gliadins in wild emmer wheat (*Triticum turgidum* L. var. *dicoccoides*). Theor Appl Genet 108:1221–1228. https://doi.org/10.1007/s00122-003-1555-y

Zhang Z, Running KLD, Seneviratne S, et al (2021) A protein kinase–major sperm protein gene hijacked by a necrotrophic fungal pathogen triggers disease susceptibility in wheat. Plant J 106:720–732. https://doi.org/10.1111/tpj.15194

Zhu T, Wang L, Rodriguez JC, et al (2019) Improved Genome Sequence of Wild Emmer Wheat Zavitan with the Aid of Optical Maps. Genes Genom Genet 9:619–624. https://doi.org/10.1534/g3.118.200902

6. GENOMIC STRUCTURE OF THE *Tsn1* REGION IN SEQUENCED WHEAT CULTIVARS AND DEVELOPMENT OF DIAGNOSTIC MOLECULAR MARKERS

6.1. Abstract

The *Tsn1* gene confers sensitivity to the necrotrophic effector ToxA, which is produced by four necrotrophic fungal pathogens, including those that cause the foliar diseases tan spot, septoria nodorum blotch, and spot blotch. Codominant simple sequence repeat (SSR) markers that delineate *Tsn1* to 351 kb were developed previously, but they are not amenable to high throughput genotyping (HGT), and their efficacy in predicting the allelic state of *Tsn1* among natural populations was not previously determined. Here, the published genome assemblies of fifteen bread wheat, two durum wheat, and one wild emmer wheat accessions were used in a structural comparison of gene and transposable element content in *Tsn1*- and *Tsn1*+ lines, revealing two conserved haplotypes. Because *Tsn1* is almost always null in insensitive cultivars, conserved single nucleotide polymorphisms KASP markers suitable for HGT were designed in the closest syntenic region between *Tsn1*- and *Tsn1*+ assemblies. The KASP markers delineated *Tsn1* to 135 kb in the ToxA-sensitive consensus sequence and were validated on over 1,500 lines from diverse hard red spring wheat, durum, and winter wheat panels. Phenotyping of the panels revealed that the markers correctly predicted a ToxA insensitive phenotype in 99.13-100% of the accessions. The markers presented here could be used for reliable and robust marker-assisted elimination of *Tsn1*, furthering the development of wheat genetically resistant to multiple pathogens.

6.2. Introduction

The *Tsn1* gene interacts with ToxA in an inverse gene-for-gene manner where the compatible interaction between the dominant host susceptibility gene *Tsn1* and the necrotrophic

effector (NE) ToxA induces programed cell death, which allows necrotrophs to obtain nutrients and complete their life cycles, ultimately leading to susceptibility. The necrotic lesions ultimately reduce the photosynthetic area of leaves and lower yields (Shabeer and Bockus 1988). In wheat-necrotrophic pathogen interactions, the *Tsn1*-ToxA interaction is unique in that *ToxA* has been identified in four pathogens, *Pyrenophora tritici-repentis* (Tomas and Bockus 1987; Ballance et al. 1989), *Parastagonospora nodorum* (Friesen et al. 2006), *Phaeosphaeria avenaria* f. *tritici 1* (*Pat1*, McDonald et al. 2013), and *Bipolaris sorokiniana* (McDonald et al. 2018). Susceptibility to pathogens that produce ToxA is conferred by the dominant host susceptibility gene *Tsn1*, characterized by the production of necrotic lesions along the leaves. The *Tsn1*-ToxA interaction significantly impacts the level of disease, explaining up to 95% of the disease symptoms in the *P. nodorum* pathosystem (Faris and Friesen 2009).

ToxA was first identified in *P. tritici-repentis* where it was found to play a role in the development of the disease tan spot (TS, Tomas and Bockus 1987, Ballance et al. 1989). *PtrToxA* encodes a 23 amino acid pre- domain and a 4.3 kDa pro- domain, which are cleaved prior to secretion of the 13.2 kDa Ptr ToxA protein (reviewed by Ciuffetti et al. 2010). *PtrToxA* is found in about 83-100% of isolates, depending on the region the isolates are collected (Lamari et al. 1998, Antoni et al. 2010, Moreno et al. 2015; Abdullah et al. 2017). The gene encoding ToxA was later identified in *P. nodorum*, the causal agent of septoria nodorum blotch (SNB) in wheat, with 99.7% similarity to *PtrToxA* (Friesen et al. 2006). *SnToxA* was present in 40% of *P. nodorum* isolates in a global panel, ranging from 6% in isolates collected in China to 97% in isolates collected in Australia (McDonald et al. 2013). Haplotype analysis of ToxA in diversity panels of *P. nodorum* and *P. tritici-repentis* revealed higher nucleotide diversity in the *P. nodorum* isolates, suggesting that ToxA was transferred from *P. nodorum* to *P. tritici-repentis*

(Friesen et al. 2006). Ptr ToxA and SnToxA were found to be functionally identical in terms of conferring sensitivity in wheat plants containing *Tsn1* (Liu et al. 2006).

Additionally, the *ToxA* gene has been identified in *Pat1*, a subgroup of *P. avenaria* that is non-pathogenic on oats but infects wheat and barley (McDonald et al. 2013; Shaw 1957). Within *Pat1,* the *ToxA* gene was present in 43% of isolates collected in the US, Canada, and Iran (McDonald et al. 2013). The *ToxA* gene has also been identified in isolates of *B. sorokinina,* the causal agent of spot blotch (SB), collected in Australia (McDonald et al. 2018), the Unites States (Friesen et al. 2018), India (Navanthe et al. 2020), and most recently, Mexico (Wu et al. 2021) where *BsToxA* was present in 34%, 86.6%, 70%, and 10.2% of isolates, respectively. The lower prevalence of *BsToxA* in Mexican isolates is possibly due to less conducive environmental conditions. In the Mexican state Veracruz, which has environmental conditions more amenable to *B. sorokinina* growth and dispersion, *BsToxA* was present in 34.5% of isolates.

Tsn1 contains nucleotide binding (NB), leucine rich repeats (LRR), and protein kinase (PK) domains (Faris et al. 2010). Amplification of the *Tsn1* specific marker from 386 *Triticum* accessions revealed that the gene was only present in ToxA-sensitive cultivars and nearly all the ToxA-insensitive cultivars were in the null state. The presence/absence variation of *Tsn1* rendered all gene-specific markers dominant. Codominant markers flanking *Tsn1* and 351 kb apart were designed based on the sequenced bacterial artificial chromosome (BAC) contig developed in the durum cultivar Langdon (Faris et al. 2010). The *Tsn1* region has been identified as a recombination hot spot (Faris et al. 2000), which may result in a high rate of linkage disequilibrium decay and reduce marker-trait associations in natural populations. Additionally, these codominant markers targeted simple sequence repeats (SSRs) and were therefore not as

amenable to high throughput genotyping platforms as digital single nucleotide polymorphism (SNP) assays such as Kompetitive allele specific PCR (KASP) markers.

Given that *Tsn1* confers susceptibility to four wheat pathogens it is imperative *Tsn1* be selectively removed from wheat breeding lines. Here, I conducted a thorough structural analysis of the *Tsn1* genomic region, characterizing gene and transposable element (TE) content, and identified syntenic regions in *Tsn1*+ and *Tsn1*- accessions. I designed high throughput diagnostic SNP markers and validated them on hard red spring wheat, durum, and winter wheat panels, demonstrating their usefulness in marker-assisted elimination of *Tsn1*.

6.3. Materials and methods

6.3.1. Plant materials

Fifteen sequenced hexaploid and three sequenced tetraploid wheat lines were evaluated for ToxA sensitivity (Table 6.1) and used for synteny analysis and/or marker development. Three panels, the Global Durum Panel (GDP), a winter wheat panel (WWP), and a hard red spring wheat panel (HRSWP) were evaluated for ToxA sensitivity and genotyped with the designed markers to assess the diagnostic capability of the markers (Supplementary Table 2). The GDP consists of 1,011 tetraploid genotypes, selected to represent the global diversity of tetraploid wheat (Mazzucotelli et al. 2020). Here, a reduced set of 513 genotypes from the GDP selected based on growth habit and seed production were evaluated. The GDP genotypes evaluated in this study were originally reported as *Triticum turgidum* ssp. *durum* landraces and cultivars. Five genotypes have since been reported as other *Triticum turgidum* subspecies including three rivet wheat landraces (*Triticum turgidum* ssp. *turgidum*), one cultivated emmer wheat (*Triticum turgidum* ssp. *dicoccum*), and one Khorasan wheat (*Triticum turgidum* ssp. *turanicum*) (Mazzucotelli et al. 2020). In this chapter, GDP refers to the set of 513 genotypes evaluated in

this study. The WWP consists of 264 *Triticum aestivum* lines selected from the USDA-ARS National Small Grains Collection core global hexaploid winter wheat germplasm collection, a diverse collection in terms of origin and market class. Originally, the set consisted of 300 accessions and was used to map stem and stripe rust resistance (Bulli et al. 2016; Muleta et al. 2020; Mihalyov et al. 2017). The whole set was obtained and increased by single-seed decent, but after two rounds of increase only 264 lines had seed production adequate for disease evaluations (Peters Haugrud 2021). The HRSWP evaluated here consists of 812 lines with more consistent germination selected from a panel of 875 hard red spring wheat lines from the USDA-ARS National Small Grains Collection and was originally used for a stripe rust resistance GWAS (Maccaferri et al. 2015).

Table 6.1. Sequenced wheat genotypes evaluated for ToxA sensitivity and used to characterize the *Tsn1* genomic region

						Analysis assembly was used in[a]		
Genotype	Ploidy level	Species	Assembly type	Assembly version	ToxA sensitivity	Synteny	Marker development	Gene-based haplotype
ArinaLrFor	6x	*Triticum aestivum*	pseudomolecule	3.0	-	+	+	+
CDC Stanley	6x	*Triticum aestivum*	pseudomolecule	1.2	-	+	+	+
Chinese Spring	6x	*Triticum aestivum*	pseudomolecule	1.0	-	+	+	+
Julius	6x	*Triticum aestivum*	pseudomolecule	1.0	-	+	+	+
Mace	6x	*Triticum aestivum*	pseudomolecule	1.0	-	+	+	+
SY Mattis	6x	*Triticum aestivum*	pseudomolecule	1.0	-	+	+	+
CDC Landmark	6x	*Triticum aestivum*	pseudomolecule	1.0	+	+	+	+
Jagger	6x	*Triticum aestivum*	pseudomolecule	1.1	+	+	+	+
LongReach Lancer	6x	*Triticum aestivum*	pseudomolecule	1.0	+	+	+	+
Norin61	6x	*Triticum aestivum*	pseudomolecule	1.1	+	+	+	+
Claire	6x	*Triticum aestivum*	scaffold	1.1	-	-	+	-
Robigus	6x	*Triticum aestivum*	scaffold	1.1	-	-	+	-
Weebil	6x	*Triticum aestivum*	scaffold	1.0	-	-	+	-
Kronos	4x	*Triticum turgidum* ssp. *durum*	scaffold	1.0	-	-	+	-
Svevo	4x	*Triticum turgidum* ssp. *durum*	pseudomolecule	1.0	-	-	+	+
Zavitan	4x	*Triticum turgidum* ssp. *dicoccoides*	pseudomolecule	1.0	-	-	+	+
Cadenza	6x	*Triticum aestivum*	scaffold	1.1	+	-	+	-
Paragon	6x	*Triticum aestivum*	scaffold	1.1	+	-	+	-

[a] Plus (+) and minus (-)indicate that a particular assembly was included or excluded from an analysis.
[b] Plus (+) and minus (-) indicate sensitive and insensitive to ToxA, respectively.

6.3.2. ToxA production and infiltration

GDP and WWP phenotypic data were obtained from Agnes Szabo-Hever and Amanda Peters Haugrud who led the ToxA-infiltration experiments on the two panels, respectively. Gurminder Singh and I led the ToxA infiltration experiments for the HRSWP and the sequenced wheat genotypes in Table 6.1 for this study as described below.

Cultures containing ToxA expressed in *Pichia pastoris* were obtained from Dr. Timothy Friesen at the USDA-ARS Cereal Crops Research Unit in Fargo, ND. A toothpick was dipped into frozen yeast culture and streaked onto a YPDS plate with 100µg/mL Zeocin (10 g yeast extract, 20 g peptone, 182.2 g sorbitol, distilled H_20 to 900 mL, 20 g agar, autoclaved, then 100 mL 20% dextrose, and 1 mL 100 mg/mL Zeocin). The plate was placed upside down in a 30 °C incubator for 3 days. A single colony was selected from the plate and streaked onto a fresh YPDS plate, and again incubated upside down at 30 °C for 3 days. A toothpick was used to select a single colony from the second plate and was placed into 2 mL YPD broth (10 g yeast extract, 20 g peptone, distilled H_20 to 900 mL, autoclaved, then 100 mL 20% dextrose). This starter culture grew while shaking at 30 °C for 48 hours. The starter culture was diluted 1:1000 into 1000 mL flasks containing 500 mL YPD. The expression cultures were grown in a 30 °C orbital shaker at 100 RPM for 48 hours. The cultures were then transferred to 50 mL culture tubes and spun at 3000 G for 10 min to precipitate the yeast. The supernatant was filtered through a .45µm pore size filter membrane via vacuum filtration.

Plants were grown in 164 mL plastic cones (Stuewe and Sons, Inc., Corvallis, OR, USA) with 3 seeds planted per cone. Two plants per cone were infiltrated with ToxA culture filtrate on the second leaf using a 1 mL needless syringe. The boundaries of the infiltration site were marked with a permanent marker. After infiltration, plants grew in a growth chamber at 21 °C

with a 12-h photoperiod. Plants were scored on a 0-3 scale at 5 days after infiltration according to Zhang et al. (2011). Three replications of a two-plant experimental unit were evaluated per line.

6.3.3. DNA extraction

Approximately 15 cm of young leaf tissue was clipped from each plant and was placed inside a 2 mL microcentrifuge tube with a single 3.96875 mm. stainless steel bearing ball (Thomson, Radford, VA). The tubes were kept in the -80 °C freezer for at least two hours prior to grinding on a Retsch Mixer Mill MM 400 (Retsch GmbH, Hann, Germany). The frozen tissue was ground for 60 seconds at 24 Hz. Then the adapter was rotated 180°, and tissue was ground again. DNA was extracted from the ground plant tissue as described by Faris et al. (2000) with minor modifications. The extracted DNA pellet was dissolved in 60 µL TE buffer, quantified using a Nanodrop spectrophotometer ND-8000 (ThermoFisher Scientific, Waltham, MA), and diluted to approximately 100 ng/µL for polymerase chain reactions (PCR).

DNA was extracted from the panels in deep-well plates using the SDS-based extraction protocol reported by Pallotta et al. (2003) at the USDA ARS small grains genotyping laboratory, Fargo, ND, USA. Samples were quantified using PicoGreen dsDNA Quantification Reagent (Manufacturer) and read on the Synergy Neo2 (BioTek, Santa Clara, CA). The PicoGreen concentrations were used to normalize the DNA on either a QIAgility (Qiagen, Germantown, MD) or Fluent (Tecan, Männedorf, Switzerland) liquid handling robot.

6.3.4. Synteny analysis

Synteny analysis focused on the area between the previously reported flanking markers, *fcp620* and *fcp394*. Ten hexaploid genotypes with complete pseudomolecule assemblies were included in synteny analysis (Table 4.1) (IWGSC 2018; Walkowiak et al. 2020).

Pseudomolecule assemblies were acquired from the Leibniz Institute of Plant Genetics and Crop Plant Research (https://wheat.ipk-gatersleben.de/). The positions of *fcp620* and *fcp394* were identified by conducting BLASTn searches of the amplified marker sequences in the Chinese Spring reference genome v1.0 (IWGSC 2018) against the genotype assemblies. The region between *fcp620* and *fcp394* was extracted from chromosome 5B of each assembly using samtools (Li et al. 2009). Genotypes SY Mattis and ArinaLrFor have a 5B:7B chromosomal translocation (Walkowiak et al. 2020), therefore the *Tsn1* region was extracted from chromosome 7B of these two genotypes.

Synteny within the extracted genomic region of ToxA-sensitive and ToxA-insensitive genotypes was identified with Smash ++ (Hosseini et al. 2020) to determine the plausibility of constructing consensus ToxA-sensitive and -insensitive sequences. The parameters used were k-mer size = 14, number of substitutions in substitution-tolerant Markov model (STMM) = 5, and a minimum segment size of 300 bp. Multiple sequence alignments of the ToxA-sensitive and ToxA-insensitive sequences were generated using K-align 3 (Lassmann 2020), and consensus sensitive and insensitive sequences (*Tsn1*+Cons and *Tsn1*-Cons) were generated using Emboss Cons 6.6.0.0 (Rice et al. 2000). Release 19 of the nonredundant Transposable Element Platform (TREP) nucleotide sequence database was used to mask the consensus sequences with RepeatMasker v 4.1.0 (Wicker et al. 2002; Smit et al. 2013-2015). Transposable element (TE) content and distribution was assessed in the consensus sequences by TE class as defined by Wicker et al. (2007), with the percentage of each class being the ratio of the length of the sequences that matched to a TE class and the total length of the consensus sequence (Table 4.2). Synteny between the masked consensus sequences was identified with Smash ++ using the same parameters as were used for initial synteny analysis. GFF files were constructed for genes,

markers, TE, and syntenic regions in *Tsn1*+Cons and *Tsn1*-Cons and visualized in Geneious Prime 2021.0.3 (https://www.geneious.com) to visualize syntenic low copy DNA regions that could be targeted for marker development.

6.3.5. Marker development

To identify diagnostic markers for *Tsn1*, the alignment of the repeat masked consensus sensitive and insensitive sequences was used to identify SNPs that could be targeted for marker development. Contextual SNP sequences were used in BLASTn searches against additional hexaploid scaffold level assemblies and *Triticum turgidum* assemblies to determine their SNP alleles (Avni et al. 2017; Maccaferri et al. 2019; http://opendata.earlham.ac.uk/Triticum_turgidum/; Walkowiak et al. 2020).

The hexaploid assemblies were hosted at the Leibniz Institute of Plant Genetics and Crop Plant Research (https://wheat.ipk-gatersleben.de/). BLASTn searches of the assembly of the durum cultivar Svevo and the wild emmer accession Zavitan were conducted at Ensembl plants (http://plants.ensembl.org/). BLASTn searches of the durum cultivar Kronos assembly were conducted at Grassroots Infrastructure (https://grassroots.tools/service/blast-blastn). SNPs that did not consistently differentiate ToxA-sensitive from ToxA-insensitive lines were eliminated as target SNP.

Nine semi-thermal asymmetric reverse PCR (STARP) markers were designed according to the recommended parameters reported in Long et al. (2017), with six targeting the distal side of *Tsn1* and three targeting the proximal side. The STARP markers were first amplified via PCR from sequenced lines with known *Tsn1* alleles as described in Long et al. (2017) and electrophoresed on 6% nondenaturing polyacrylamide gels. Gels were stained with Gelred™ nucleic acid stain (Biotium Corporate, Hayward, CA) and scanned with a Typhoon 9500 variable

mode imager (GE healthcare Biosciences, Waukesha, WI). This procedure was also used to evaluate STARP on the WWP and GDP.

Selected STARP markers were converted to KASP by dropping the induced mutation in the STARP forward primer and replacing the STARP tails with KASP fluorescent tails. No adjustments were made to the reverse primer. STARP and KASP markers were run as digital assays by the North Central Small Grains Genotyping Lab in Fargo, ND. Due to the size of the panel, only the digital KASP assays were run on the HRSWP. Primer sequences for all four markers are reported in Table 6.2. For each marker, the accuracy of the phenotypic prediction was calculated using all lines with homozygous alleles for that marker. Prediction accuracies were calculated separately for each marker in the three panels.

Table 6.2. *Tsn1* marker primers

Marker type	Marker name	Forward primers[a]	Reverse primer	Position of SNP[b]
KASP	*fcp991*	GAAGGTGACCAAGTTCATGCTTCTTGTATGGAGCAGCGACTAGGT	ACTTCCTACTGGTTATGGAATGGTTC	546766568
		GAAGGTCGGAGTCAACGGATTTCTTGTATGGAGCAGCGACTAGGG		
KASP	*fcp992*	GAAGGTGACCAAGTTCATGCTCTAGTGCCATCTACCAATCCCC	TACAGATGTCCAGAACCTTTGAC	546806925
		GAAGGTCGGAGTCAACGGATTCTAGTGCCATCTACCAATCCCT		
STARP	*fcp993*	GACGCAAGTGAGCAGTATGACTCTTGTATGGAGCAGCGACTAAGT	ACTTCCTACTGGTTATGGAATGGTTC	546766568
		GCAACAGGAACCAGCTATGACTCTTGTATGGAGCAGCGACTCGGG		
STARP	*fcp994*	GCAACAGGAACCAGCTATGACCTAGTGCCATCTACCAATTCCC	TACAGATGTCCAGAACCTTTGAC	546806925
		GACGCAAGTGAGCAGTATGACCTAGTGCCATCTACCAATCTCT		

[a] For each marker, the primer targeting the insensitive allele is listed first and the SNP associated with the insensitive allele is underlined.

[b]SNP positions are based on the IWGSC RefSeq v.1.0

6.3.6. Gene-based haplotype analysis

Because the genomic region between markers *fcp620* and *fcp394* was too large (351 kb) to reasonably conduct a nucleotide-based haplotype analysis, a gene-based comparison was conducted to assess structural haplotypes in the *Tsn1* region in the sequenced hexaploid lines with pseudomolecule level assemblies. Given the level of sequence conservation in the *Tsn1* region in hexaploid *Tsn1*+ and *Tsn1*- lines (see results), genes were identified in a representative insensitive sequenced line (Chinese Spring) and a sensitive sequenced line (CDC Landmark). Because Chinese Spring does not have *Tsn1* and may be missing additional genes in the *Tsn1* region, genes were annotated in the *Tsn1* region of the ToxA-sensitive genotype CDC Landmark using the TriAnott pipeline (Leroy et al. 2012). Protein domains were identified using Pfam (http://pfam.xfam.org/, accessed April 20th, 2020). Genes smaller than 500 bp or without Pfam matches with an e-value of at least $1x10^{-5}$ were considered pseudogenes. Predicted open reading frames with homology to the polypeptide of LTR copia-type domain were considered TEs. The annotated genes in the *Tsn1* region of the durum reference genome Svevo v.1 and the wild emmer reference genome Zavitan v.1 were identified on Ensembl plants in case there were tetraploid-specific genes that did not show up in the Chinese Spring or CDC Landmark annotations (Maccaferri et al 2019; Avni et al. 2017; IWGSC 2018; Walkowiak et al. 2020). In December 2021, a *de novo* annotation of CDC Landmark by Plant Genomes and System Biology and the Earlham Institute was published on Ensembl plants (release 52). The genes annotated in CDC Landmark using the TriAnnott pipeline were compared to those in the *de novo* annotation (PGSBv2.1). The presence and position of the annotated genes were identified in the genome assemblies of eight ToxA-sensitive and four ToxA-insensitive wheat lines by conducting BLASTn searches of all the identified annotations against the pseudomolecule level assemblies

(Table 6.3). While the presence of these genes could be confirmed in scaffold level assemblies, the presence of other potential genes not identified in the set of annotated genes could not be ruled out. Therefore, lines with scaffold level assemblies were excluded from gene-based haplotype analysis.

6.3.7. Assessing recombination events

Apparent crossovers were identified in the panels using lines with homozygous marker alleles. For the purpose of identifying apparent double crossovers, the reaction to ToxA of lines was used to infer the allelic state of *Tsn1*, i.e. sensitive to ToxA = dominant *Tsn1* allele; insensitive to ToxA = recessive or null *Tsn1* allele. Genotypes from the WWP and GDP with apparent double crossover events were further evaluated to determine if the lines were heterogenous or if they had true double crossover events (Supplementary Table 2). First, six plants from each genotype were planted. Each plant was infiltrated with ToxA and scored independently. If the phenotype of the line was homogenous among the plants, DNA was extracted from three plants as described above. If the phenotype was heterogenous among the plants, DNA was extracted from six plants. Markers *fcp793* and *fcp794* were run on the extracted DNA allowing detection of crossovers for individuals. Heterogenous lines were removed from further analysis. The dominant gene-specific *Tsn1* marker *fcp623* (Faris et al. 2010) was also evaluated on lines with apparent double crossovers to further confirm the presence/absence of a *Tsn1* DNA sequence.

6.4. Results

6.4.1. Prevalence of ToxA sensitivity

Among the eighteen sequenced wheat genotypes, six (33%) were sensitive and 12 (66%) were insensitive to ToxA. The six ToxA-sensitive genotypes were all hexaploid and consisted of

CDC Landmark, Jagger, LongReach Lancer, Norin61, Cadenza, and Paragon (Table 6.1). In the HRSWP, GDP, and WWP, 51.7%, 27.7%, and 38.4% of the genotypes were sensitive to ToxA (Figure 4.1, Supplementary Table 2). The distribution of phenotypic scores was bimodal in both the panels and the sequenced lines, with most of the genotypes having a score of 0-.49 or 2.5-3.

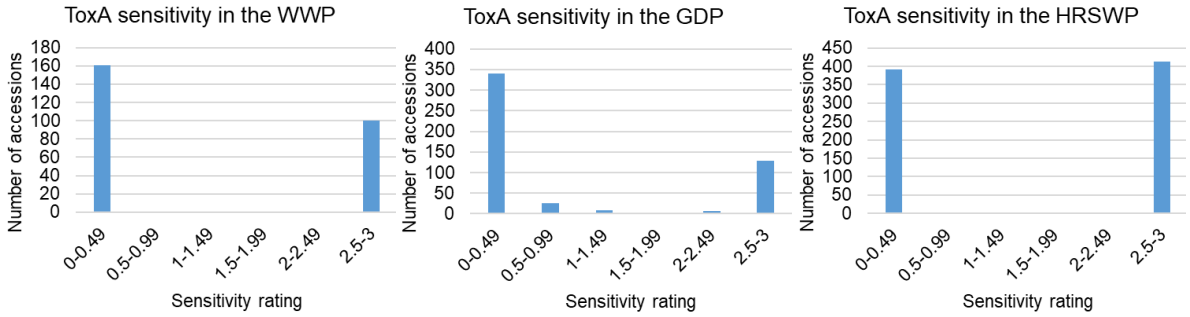

Figure 6.1. ToxA sensitivity distributions in the HRSWP, GDP, and WWP.

6.4.2. Development and comparison of *Tsn1*+ and *Tsn1*- sequences

The *Tsn1* region was defined as the sequence flanked by markers *fcp620* and *fcp394*. Within the ToxA insensitive hexaploid genotypes, the length of the *Tsn1* region ranged from 281.7 to 298.4 kb with an average length of 288.4 kb. The *Tsn1* region was larger in the ToxA-sensitive hexaploid genotypes where it ranged from 328.6 to 448.4 kb. The ToxA-sensitive hexaploid genotype Jagger had a smaller *Tsn1* region (328.6 kb) than the other five ToxA-sensitive genotypes with pseudomolecule level assemblies, which had *Tsn1* regions ranging from 444.9 to 448.4 kb, varying by just 3.5 kb. The smaller *Tsn1* region in Jagger reduced the average *Tsn1* region to 416.8 kb for the ToxA-sensitive lines, which was approximately 128 kb larger than the average *Tsn1* region in the insensitive hexaploid genotypes. The size of the *Tsn1* region in the ToxA-insensitive durum cultivar Svevo was 290.8 kb, which was within the range identified in the ToxA-insensitive hexaploid genotypes. The length of the *Tsn1* region in the ToxA-insensitive wild emmer Zavitan genome was slightly smaller at 275.7 kb. Therefore, there

was a substantial difference in the size of the *Tsn1* region between sensitive and insensitive genotypes with the *Tsn1* region being larger in the sensitive genotypes.

To assess the feasibility of making consensus ToxA-insensitive and -sensitive sequences, the program Smash++ was used to identify syntenic regions between sequences flanked by SSR markers *fcp620* and *fcp394* (Hosseini et al. 2020). A single syntenic block between the sequences of ToxA-insensitive genotypes was identified. Similarly, a single syntenic block between the sequences of ToxA-sensitive genotypes was also identified. No structural rearrangements were identified within or among either the sensitive or insensitive groups. Given this finding, consensus sequences were created for each of the two sensitivity classes, and they are hereafter referred to as *Tsn1*+Cons and *Tsn1*-Cons.

Ten syntenic regions ranging in length from approximately 2.5 kb to 15.5 kb were identified in *Tsn1*+Cons and *Tsn1*-Cons, representing low copy DNA that did not display presence absence variation between sequences. STARP (*fcp993* and *fcp994*) and KASP (*fcp991* and *fcp992*) markers were designed flanking *Tsn1* in the syntenic regions nearest the gene (Figure 6.2). The region between *fcp991* and *fcp992* is 40.4 kb and 41.5 kb in the Chinese Spring RefSeq v1.0 assembly (IWGSC 2018) and *Tsn1*-Cons, respectively. In *Tsn1*+Cons, *fcp991* and *fcp992* are 134.8 kb apart from each other and 77.2 kb and 57.5 kb away from the start of *Tsn1*, respectively.

Tsn1-Cons was 305.5 kb and 45.44% was identified as repetitive elements. *Tsn1*+Cons was larger with a length of 332.7 kb and 46.30% repetitive elements. In both *Tsn1*+Cons and *Tsn1*-Cons, gypsy retrotransposons were the largest TE superfamily, representing 30.72% and 25.38% of the total length respectively (Table 6.3). There were less Copia elements in the *Tsn1*-

Cons compared to the *Tsn1*+Cons. However, in general, the TE makeup between *fcp620* and *fcp394* was relatively similar in *Tsn1*+Cons and *Tsn1*-Cons.

Table 6.3. TE content and distribution in the *Tsn1* region

		fcp620-fcp394			
Classification		Sensitive		Insensitive	
Order	Superfamily	Length (bp)	%	Length (bp)	%
Class I elements (Retrotransposons)					
LTR	Copia (RLC)	51970	15.62	28937	9.47
	Gypsy (RLG)	102193	30.72	77540	25.38
	Unknown (RLX)	24026	7.22	26702	8.74
LINE	Unknown (RIX)	14252	4.28	8616	2.82
SINE	Unknown (RSX)	1370	0.41	1003	0.33
Class II elements (DNA Transposons)					
	Unknown (DXX)	119	0.04	0	0.00
Subclass 1					
TIR	Tc1-*Mariner* (DTT)	982	0.30	1653	0.54
	hAT (DTA)	159	0.05	0	0.00
	Mutator (DTM)	436	0.13	3271	1.07
	PIF-Harbinger (DTH)	1110	0.33	3681	1.20
	CACTA (DTC)	69162	20.79	66043	21.62
	Unknown (DTX)	46	0.01	0	0.00
Subclass 2					
	Helitron (DHH)	1890	0.57	945	0.31
Others	Unknown (XXX)	333	0.10	60	0.02
	SSRs	2210	0.66	2542	0.83

Only two gene-based haplotypes were identified in the hexaploid pseudomolecule level assemblies. Haplotype 1 was common among ToxA-insensitive cultivars and haplotype 2 was common among ToxA-sensitive cultivars (Table 6.3). Therefore, the consensus sequences *Tsn1*-Cons and *Tsn1*+Cons represent the two gene-based haplotypes, and the positions of the genes in the consensus sequences are displayed in Figure 6.2. No tetraploid-specific genes were identified.

Four genes were common among the sensitive and insensitive pseudomolecule level assemblies (Table 6.4.). One of these was a wall-associated kinase (TraesCS5B02G368200),

which contains the sequence for marker *fcp620* and resides at the very proximal end of genomic region under investigation. The other three genes in common to both haplotypes were in the distal region of the segment between *fcp992* and *fcp394* and consisted of genes that encode an RNA recognition motif domain (TraesCS5B02G368400), a potassium transporter (TraesCS5B02G368500) and a palmitoyltransferase (TraesCS5B02G368600). Within Haplotype 1, a gene encoding cathepsin propeptide inhibitor and peptidase domains was identified between *fcp620* and *fcp991*. Two unique genes were identified in Haplotype 2. The first unique gene in Haplotype 2 encoded proteins with endonuclease/exonuclease/phosphatase family, DUF4283, and zinc knuckle protein domains according to the TriAnnot gene prediction. However, the PGSBv2.1 annotation of this gene (TraesLDM5B03G02955820) indicated that the sequence containing the endonuclease/exonuclease/phosphatase family protein domains was not part of the open reading frame that coded for the DUF4283 and zinc knuckle domains. The second unique gene to Haplotype 2 was *Tsn1*.

Table 6.4. Gene-based haplotypes between *fcp620* and *fcp991*.

Haplotype	ToxA sensitive	Accessions	TraesCS5B02G368200	TraesCS5B02G368300	TraesLDM5B03G02955820	Tsn1	TraesCS5B02G368400	TraesCS5B02G368500	TraesCS5B02G368600
1	-	ArinaLrFor, CDC Stanley, Chinese Spring, Julius, Mace, Svevo, SY Mattis, Zavitan	+	+	-	-	+	+	+
2	+	CDC Landmark, Jagger, Lancer, Norin61	+	-	+	+	+	+	+

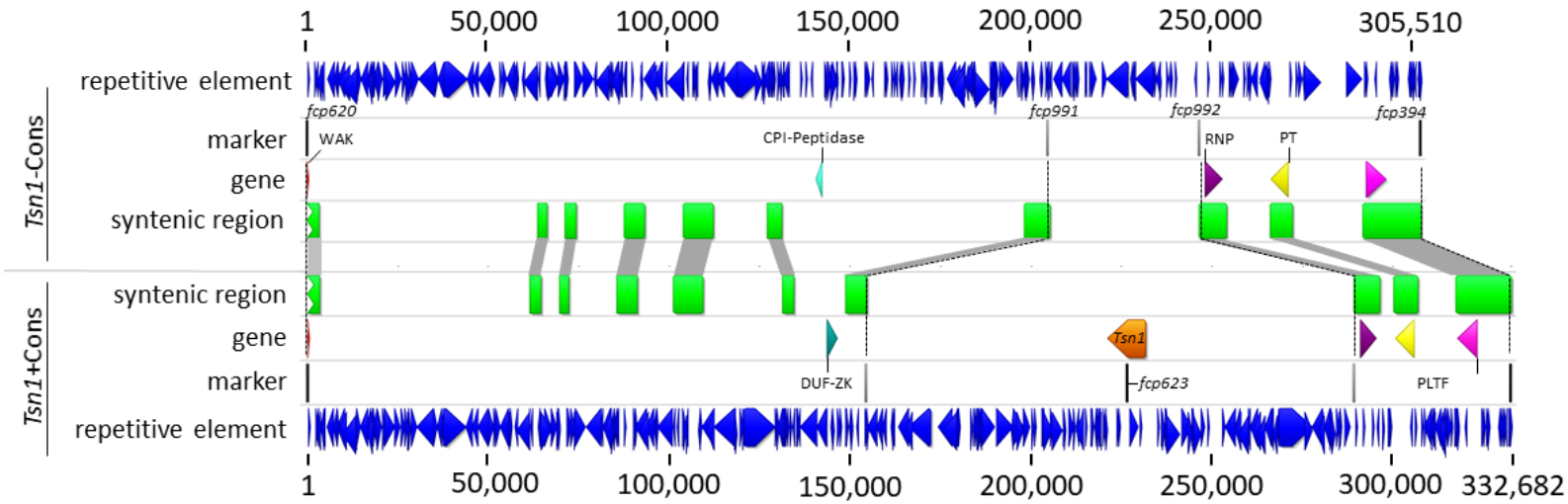

Figure 6.2. Structural comparison of *Tsn1* region in *Tsn1*+ and *Tsn1*- consensus sequences.
The bold horizontal line on the top and bottom of the figure represent the ToxA insensitive and ToxA sensitive consensus sequences, respectively. The top four tracks represent structural features in the *Tsn1*- consensus sequence, while the bottom four tracks represent structural features in the *Tsn1*+ sensitive consensus sequence. Tracks contain features as labeled in the figure. Markers are represented by vertical bars with black bars being the previously designed markers (*fcp620*, *fcp623*, and *fcp394*) and grey bars (*fcp991* and *fcp992*) being the KASP markers designed in this study. Within the gene tracks, the red, aqua, teal, purple, yellow, and pink genes contain wall associated receptor kinase (WAK), cathepsin propeptide inhibitor and peptidase (CPI-Peptidase), DUF4283 and zinc knuckle (DUF-ZK), RNA recognition motif (RNP), potassium transporter (PT), and palmitoyltransferase domains (PLTF), respectively. The orange gene is *Tsn1*. Positions are in base pairs and arrows on genes and repetitive elements demonstrate the directionality of the feature.

6.4.3. Marker validation

KASP markers *fcp991* and *fcp992* were used to genotype the WWP, GDP, and HRSWP (Figure 6.3). In all panels, clear clusters formed, representing the *Tsn1*+ and *Tsn1*- alleles. When the KASP markers *fcp991* and *fcp992* predicted a genotype would be insensitive, it was true in 99.13-100% of cases in all three panels (Table 6.5). In the three panels, there were genotypes where the marker alleles indicated the line would be sensitive to ToxA, but the line was experimentally found to be insensitive. Because of this, the accuracy predicting when a genotype would be sensitive to ToxA was lower (88.68-94.17%).

In total, 1523 accessions had homozygous alleles for both *fcp991* and *fcp992*. When ToxA sensitivity was treated as a marker for *Tsn1*, there was no recombination detected between the markers and *Tsn1* for 94.5% of those accessions. Of the remaining accessions, six had a single crossover detected between *fcp991* and *Tsn1*, nine had single crossovers between *fcp992* and *Tsn1*, and 69 had apparent double crossover events, with a crossover occurring between *Tsn1* and the markers on both sides of *Tsn1*. Given the preponderance of apparent double crossovers and that 94.2% of the apparent double crossovers were insensitive to ToxA, the marker *fcp623,* which targets *Tsn1* was used to confirm double crossover events. A double crossover event between *fcp993* and *fcp994* resulting in alleles predictive of sensitivity, but showing an insensitive phenotype, would mean that the line would be null for *Tsn1*, and therefore null for *fcp623*.

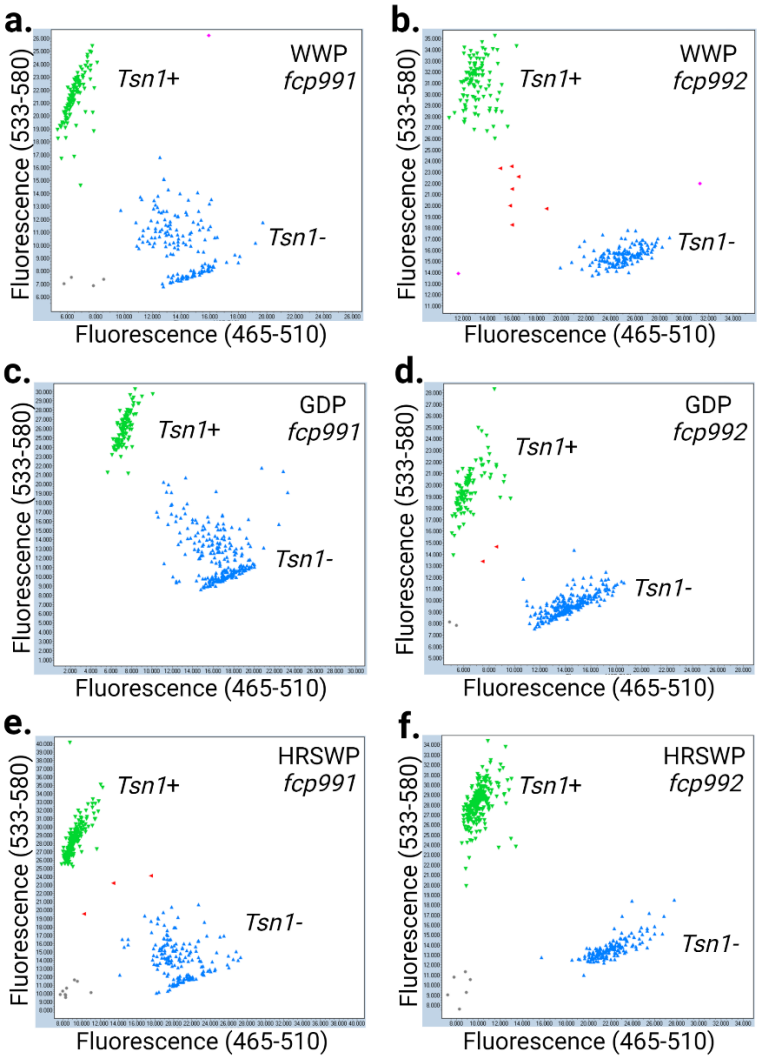

Figure 6.3. Endpoint fluorescence scatter plots for markers *fcp991* and *fcp992* on the WWP, GDP, and HRSWP.
Marker *fcp991* is shown in (a), (c), and (e) on the WWP, GDP, and HRSWP, respectively.
Marker *fcp992* is shown in (b), (d), and (f) on the WWP, GDP, and HRSWP, respectively.
Alleles are shown for all individuals of the WWP and a subset of the GDP and HRSWP.

In sixty-five accessions with apparent double crossovers, only seven were true double crossovers. Four accessions with apparent double crossovers still need to be evaluated for *fcp623*. Most of the apparent double crossovers actually carried *Tsn1*, indicating they were not true crossovers. Most importantly, there were only two cases where both flanking markers indicated that an accession would be insensitive and it was not.

Phenotyping of multiple individuals from 9 lines from the WWP and 19 lines from the GDP that were apparent single or double cross over lines confirmed the previously observed phenotypes. Two accessions in the GDP with apparent double crossovers with average phenotypic scores of 1.08 and 1.25 still need to be reevaluated for sensitivity to ToxA. Plants of the line Ankar II showed were heterogenous. Analysis of six plants for reactions to ToxA and marker of *fcp993* and *fcp994* indicated Ankar II did not contain a double crossover but was instead a seed mixture. Ankar II was therefore removed from the dataset. The marker alleles of *fcp993* and *fcp994* in the remaining lines were homogeneous for each line.

Table 6.5. Accuracies of correct phenotypic prediction given the marker prediction in three panels.

	Accuracy predicting insensitive phenotype (%)				Accuracy predicting sensitive phenotype (%)			
panel	*fcp991*	*fcp992*	*fcp993*	*fcp994*	*fcp991*	*fcp992*	*fcp993*	*fcp994*
HRSW	99.40	99.42	-	-	89.14	88.84	-	-
GDP	99.41	99.13	99.40	98.84	89.68	88.68	90.26	89.10
WW	100.00	99.33	100.00	100.00	93.69	93.64	93.40	94.17

6.5. Discussion

The *Tsn1* gene in wheat recognizes ToxA produced by four necrotrophic pathogens, *P. nodorum*, *P. tritici-repentis*, *B. sorokiniana*, and the *P. avenaria* subgroup *Pat1*, leading to cell death (Tomas and Bockus 1987; Balance et al. 1989; Friesen et al. 2006; McDonald et al. 2013; McDonald et al. 2018). *P. nodorum*, *P. tritici-repentis*, and *B. sorokiniana* cause the major wheat disease septoria nodorum blotch (SNB), tan spot (TS), and spot blotch (SB), respectively. In 2019, these pathogens were estimated to cause global yield loses of 0.9%, 1.64%, and 1.67% (Savary et al. 2019). These relatively small percentages translate to massive yield losses when applied to global wheat production. Tan spot, septoria nodorum blotch, and spot blotch infections

caused estimated yield losses of 8.8, 16.0, and 16.3 million tons, enough wheat to bake 69.4 billion loaves of bread (Wulff and Krattinger 2022).

In this study, approximately 50% of the cultivars and breeding lines (n=513) in the hard red spring wheat panel were sensitive to ToxA, indicating that sensitivity to ToxA is relatively common in cultivated wheats. While testing accessions in breeding programs for sensitivity to ToxA is possible, the infiltrations required to phenotype are laborious and require growing yeast cultures to produce ToxA. Additionally, as *Tsn1* confers dominant sensitivity to ToxA, both *Tsn1/Tsn1* lines and *Tsn1/tsn1* lines will be sensitive, so the selection of heterozygous lines is not possible. For efficient high throughput selection of lines insensitive to ToxA, marker-assisted selection is more user-friendly. The codominant KASP markers developed here, *fcp991* and *fcp992*, are 99.13-100% accurate when predicting the insensitive status of a plant.

There were very few single crossovers between the gene and either flanking marker, but a preponderance of apparent double crossover where the marker alleles indicated that the cultivar would be sensitive but infiltrations with ToxA showed that the cultivar was insensitive. Marker alleles for *fcp623*, which targets *Tsn1*, were evaluated to determine if these cultivars were true double crossovers. 10.6% of the apparent double crossover were not true double crossovers as they carried *Tsn1*. This implies that although *Tsn1* was present, it was nonfunctional either through the acquisition of mutations that rendered the protein nonfunctional or due to the lack of *Tsn1* expression. Sequencing and expression analysis of *Tsn1* from these lines will elucidate the nature of the ToxA insensitive status. It is possible that in the future additional markers could be added to select for nonfunctional *Tsn1* alleles, but the KASP markers developed here reliably select for *Tsn1* absent lines. Including these markers in marker-assisted selection arrays would

allow the efficient selection of lines insensitive to ToxA, and therefore less susceptible to *P. nodorum*, *P. tritici-repentis*, *B. sorokiniana*, and the *P. avenaria* subgroup *Pat*1.

6.6. Literature cited

Abdullah S, Sehgal SK, Ali S, Liatukas Z, Ittu M, Kaur N (2017) Characterization of *Pyrenophora tritici-repentis* (tan spot of wheat) races in Baltic states and Romania. Plant Pathol J 33:133–139

Antoni EA, Rybak K, Tucker MP, Hane JK, Solomon PS, Drenth A, Shankar M, Oliver RP (2010) Ubiquity of ToxA and absence of ToxB in Australian populations of *Pyrenophora tritici - repentis*. Austral Plant Pathol 39:63-68

Avni R, Nave M, Barad O, et al (2017) Wild emmer genome architecture and diversity elucidate wheat evolution and domestication. Science 357:93–97

Ballance GM, Lamari L, Bernier CC (1989) Purification and characterization of a host-selective necrosis toxin from *Pyrenophora tritici-repentis*. Physiol Mol Plant Pathol 35:203–213.

Bulli P, Zhang J, Chao S, Chen X, Pumphrey M (2016) Genetic architecture of resistance to stripe rust in a global winter wheat germplasm collection. G3-Genes Genom Genet 6: 2237-2253 doi:10.1534/g3.116.028407

Ciuffetti LM, Manning VA, Pandelova I, Betts MF, Martinez JP (2010) Host-selective toxins, Ptr ToxA and Ptr ToxB, as necrotrophic effectors in the *Pyrenophora tritici-repentis*-wheat interaction. New Phytol 187:911-919

Faris JD and Friesen TL (2009) Reevaluation of a tetraploid wheat population indicates that the *Tsn1*-ToxA interaction is the only factor governing Stagonospora nodorum blotch susceptibility. Phytopathology 99:906-912

Faris JD, Haen KM, Gill BS (2000) Saturation mapping of a gene-rich recombination hot spot region in wheat. Genetics 154:823–835.

Faris JD, Zhang Z, Lu H, Lu Z, Reddy L, Cloutier S, Fellers JP, Meinhardt SW, Rasmussen JB, Xu SS, Oliver RP, Simons KJ, Friesen TL (2010) A unique wheat disease resistance-like gene governs effector-triggered susceptibility to necrotrophic pathogens. Proc Natl Acad Sci 107:13544-13549

Friesen TL, Stukenbrock EH, Liu Z, Meinhardt S, Ling H, Faris JD, Rasmussen JB, Solomon PS, McDonald BA, Oliver RP (2006) Emergence of a new disease as a result of interspecific virulence gene transfer. Nat Genet 38:953-956

Friesen TL, Holmes DJ, Bowden RL, Faris JD (2018) *ToxA* is present in U.S. *Bipolaris sorokiniana* population and is a significant virulence factor on wheat harboring *Tsn1*. Plant Dis 102:2446-2452

Hosseini M, Pratas D, Morgenstern B, Pinho AJ (2020) Smash++: an alignment-free and memory-efficient tool to find genomic rearrangements. GigaScience 9:giaa048. https://doi.org/10.1093/gigascience/giaa048

International Wheat Genome Sequencing Consortium (IWGSC), IWGSC RefSeq principal investigators:, Appels R, et al (2018) Shifting the limits in wheat research and breeding using a fully annotated reference genome. Science 361:eaar7191.

Lamari L, and Bernier C C (1989) Evaluations of wheat lines and cultivars to tan spot [*Pyrenophora tritici-repentis*] based on lesion type. Can J Plant Pathol 11:49–56

Lassmann T (2019) Kalign 3: multiple sequence alignment of large datasets. Bioinformatics btz795. https://doi.org/10.1093/bioinformatics/btz795

Li H, Handsaker B, Wysoker A, Fennell T, Ruan J, Homer N, Marth G, Abecasis G, Durbin R, 1000 Genome Project Data (2009) The Sequence Alignment/Map format and SAMtools. Bioinformatics 25:2078–2079

Liu Z, Friesen TL, Ling H, Meinhardt SW, Oliver RP, Rasmussen JB, Faris JD (2006) The *Tsn1*-ToxA interaction in the wheat-*Stagonospora nodorum* pathosystem parallels that of the wheat-tan spot system. Genome 49:1265-1273

Long YM, Chao WS, Ma GJ, Xu SS, Qi LL (2017) An innovative SNP genotyping method adapting to multiple platforms and throughputs. Theor Appl Genet 130:597–607

Maccaferri M, Harris NS, Twardziok SO, et al (2019) Durum wheat genome highlights past domestication signatures and future improvement targets. Nat Genet 51:885–895.

Maccaferri M, Zhang J, Bulli P, Abate Z, Chao S, Cantu D, Bossolini E, Chen X, Pumphrey M, Dubcovsky J (2015) A genome-wide association study of resistance to stripe rust (*Puccinia striiformis* f. sp. *tritici*) in a worldwide collection of hexaploid spring wheat (*Triticum aestivum* L.). G3-Genes Genom Genet 5:449–465.

Mazzucotelli E, Sciara G, Mastrangelo AM, et al (2020) The Global Durum Wheat Panel (GDP): An international platform to identify and exchange beneficial alleles. Front Plant Sci 11:569905.

McDonald MC, Ahren D, Simpfendorfer S, Milgate A, Solomon PS (2018) The discovery of the virulence gene *ToxA* in the wheat and barley pathogen *Bipolaris sorokiniana*. Mol Plant Pathol. 19:432-439

McDonald MC, Oliver RP, Friesen TL, Brunner PC, McDonald BA (2013) Global diversity and distribution of three necrotrophic effectors in *Phaeosphaeria nodorum* and related species. New Phytol 199:241–251

Mihalyov PD, Nichols VA, Bulli P, Rouse MN, Pumphrey MO (2017) Multi-locus mixed model analysis of stem rust resistance in winter wheat. Plant Genome-US https://doi.org/10.3835/plantgenome2017.01.0001

Moreno MV, Stenglein S, Perelló AE (2015) Distribution of races and Tox genes in *Pyrenophora tritici-repentis* isolates from wheat in Argentina. Trop Plant Pathol 40:141–146.

Muleta KT, Chen X, Pumphrey M (2020) Genome-wide mapping of resistance to stripe rust caused by *Puccinia striiformis* f. sp. *tritici* in hexaploid wheat. Crop Sci 60:115-131

Navathe S, Yadav PS, Chand R, Mishra VK, Vasistha NK, Meher PK, Joshi AK, Gupta PK (2020) *ToxA – Tsn1* Interaction for spot blotch susceptibility in Indian wheat: An example of inverse gene-for-gene relationship. Plant Dis 104:71–81.

Pallotta, MA, P Warner, RL Fox, H Kuchel, SJ Jefferies and P Langridge (2003) Marker assisted wheat breeding in the southern region of Australia. Proceedings of the Tenth International Wheat Genetics Symposium (1-6 September 2003, Paestum, Italy) p.789-791.

Peters Haugrud AR, Zhang Z, Friesen TL, Faris JD (2022) Genetics of resistance to septoria nodorum blotch in wheat. Theor Appl Genet

Savary S, Willocquet L, Pethybridge SJ, et al (2019) The global burden of pathogens and pests on major food crops. Nat Ecol Evol 3:430–439. https://doi.org/10.1038/s41559-018-0793-y

Shabeer A and Bockus WW (1988). Tan spot effects on yield and yield components relative to growth stage in winter wheat. Plant Dis 72:599-602

Shaw DE (1957) Studies on *Leptosphaeria avenaria*. f. sp. *triticea* on cereals and grasses. Can J Bot 35:113-118

Smit AFA, Hubley R, Green P (2013-2015) RepeatMasker Open-4.0 <http://www.repeatmasker.org>

Tomas A and Bockus WW (1987) Cultivar-specific toxicity of culture filtrate of *Pyrenophora tritici-repentis*. Phytopathology 77:1337–1340

Virdi SK, Liu Z, Overlander ME, Zhang Z, Xu SS, Friesen TL, Faris JD (2016) New insights into the roles of host gene-necrotrophic effector interactions in governing susceptibility of durum wheat to tan spot and spetoria nodorum blotch. G3-Genes Genom Genet 6:4139-4150

Walkowiak S, Gao L, Monat C, Haberer G, Kassa MT, Brinton J, Ramirez-Gonzalez RH, Kolodziej MC, Delorean E, Thambugala D (2020) Multiple wheat genomes reveal global variation in modern breeding. Nature 588:277-283

Wicker T, Matthews DE, Keller B (2002) TREP: a database for Triticeae repetitive elements. Trends Plant Sci 7:561–562

Wicker T, Sabot F, Hua-Van A, et al (2007) A unified classification system for eukaryotic transposable elements. Nat Rev Genet 8:973–982.

Wu L, He X, Lozano N, Zhang X, Singh PK (2021) ToxA, a significant virulence factor involved in wheat spot blotch disease, exists in the Mexican population of *Bipolaris sorokiniana*. Trop Plant Pathol 46:201–206

Zhang Z, Friesen TL, Xu SS, Shi G, Liu Z, Rasmussen JB, Faris JD (2011) Two putatively homoeologous wheat genes mediate recognition of SnTox3 to confer effector-triggered susceptibility to *Stagnonospora nodorum*. Plant J 65:27-38

Wulff BB, Krattinger SG (2022) The long road to engineering durable disease resistance in wheat. Curr Opin Biotechnol 73:270–275. https://doi.org/10.1016/j.copbio.2021.09.002

7. GENERAL CONCLUSIONS

The work presented here furthers our understanding of host-necrotrophic pathogen interactions in wheat by identifying two host-sensitivity genes (*Tsc1* and *Snn5-B1*) and developing robust genetic markers to select lines null for a third (*Tsn1).* First, the nucleotide sequences of *Tsc1* and *Snn5-B1* were both identified using sequence comparison. Comparison of two genome sequences of accessions that differed in chlorosis production in response to inoculation with Ptr ToxC-producing isolates filtered candidate genes down to just two genes. To identify *Snn5-B1,* the sequence of *Snn3-D1* was used to identify candidates in a SnTox5 sensitive sequence with sequence homology to *Snn3-D1*, again reducing the list of candidates to just two genes. The cloning of *Tsc1* and *Snn5-B1* demonstrates the power of having a genome assembly of an accession carrying the trait of interest. The need for time intensive methods like high-resolution mapping or the producing of BAC libraries and subsequent chromosome walking were eliminated.

The successful use of homology based-candidate gene identification in the cloning of *Snn5-B1* indicates that in the *P. nodorum* necrotrophic effectors with structural similarities likely target host-sensitivity genes with structural similarity and knowledge about the structure of NE may inform the identification of host-sensitivity gene candidates. Additionally, the structure of *Snn5-B1* may allow identification of additional SnTox5-sensitivity loci using the same homology based-candidate gene identification method.

As was demonstrated in Chapter 6, knowing the nucleotide sequence of a gene is not the only requirement to develop robust genetic markers. Multiple *Tsn1*- and *Tsn1*+ sequenced were used to characterize the TE and gene content in the *Tsn1* region, allowing the identification of the closest low copy DNA segments common among all the analyzed assemblies to target for the

development of codominant markers tightly linked to *Tsn1*. Validation of the designed markers, *fcp991* and *fcp992*, demonstrate the success of this genomic structural analysis method with near perfect identification of *Tsn1*- accessions.

Based on the multiple *Snn5-B1* haplotypes and the allelic diversity observed in the markers closely linked to *Tsc1,* it is likely that the *Snn5-B1* and *Tsc1* gene regions have more haplotypes than the *Tsn1* gene region, which had just two conserved gene-based haplotypes. However, similar structural characterizations of the gene regions of *Snn5-B1* and *Tsc1* regions, as was done here in the development of *Tsn1* markers, combined with allelic diversity analysis, would inform the development of molecular markers to select insensitive alleles. Pending the development of *Tsc1* and *Snn5-B1* molecular markers, the gene sequences can be targeted using gene-editing methods to disrupt the gene, rendering them unable to recognize their corresponding NE, and therefore, preventing the NEs from using the host-sensitivity genes to induce cell death and disease.

The analyses in this dissertation were contingent on the publication of multiple wheat genome sequences and demonstrate some of the ways the sequences can be used in gene cloning projects. A sequenced wheat accession with your trait of interest is immensely powerful in marker development, candidate gene identification, and allelic comparisons, reducing the time required to clone a gene. I suspect the cloning of resistance and susceptibility genes will surge as more wheat genomes become available.